arXiv:1511.01448v2 [stat.ME] 5 Nov 2015

Stochastic Particle Flow for Nonlinear High-Dimensional Filtering Problems

Flávio Eler de Melo*[1], Simon Maskell†[1], Matteo Fasiolo‡[2], and Fred Daum§[3]

[1]Department of Electrical Engineering and Electronics, University of Liverpool
[2]Department of Mathematics, University of Bath
[3]Raytheon Company

November 6, 2015

Abstract

A series of novel filters for probabilistic inference called particle flow filters, which propose an alternate convenient way of performing Bayesian updates, has been much in evidence lately. Those filters lay out a procedure to approximately solve nonlinear filtering problems by which the prior probability density is updated continuously between two subsequent time steps. We propose a novel filter inspired by the particle flow methods to address the shortcomings of sequential Monte Carlo methods in solving important nonlinear high-dimensional filtering problems that arise in multi-target multi-sensor tracking. The novel filter establishes a Monte Carlo procedure for generating a sequence of samples that guide local solutions of the Fokker-Planck equation to compose a Gaussian mixture that approximates a filtering density. We show that the new filtering technique, called Stochastic Particle Flow, is adequate for nonlinear high-dimensional problems constituting a credible estimator of the filtering density. In addition, we extend the original particle flow filters for tackling multi-target multi-sensor tracking problems to enable a comparison with the new filter.

1 Introduction

Stochastic filtering in high-dimensional problems pose a great challenge for estimation methods because of two fundamental issues: (i) the curse of dimensionality, (ii) the infinite number of parameters required to represent exactly the general probability densities that arise from filtering on a continuous state space. Firstly, the curse of dimensionality emerges as a set of phenomena under the context of statistical analysis in high-dimensional spaces. Those phenomena are due to the fact that the volume enclosing all possible realisations of a given statistical experiment increases geometrically with the number of space dimensions, rendering any finite set of the experiment's outcomes to become sparse. Secondly, the infinite number of parameters required to represent exactly the continuous probability densities stems from the very nature of real functions whose complete description must be given as a power series with infinitely many terms. In practice this latter issue turns into a computational problem when one is required to represent the probability densities by a finite set of parameters that are desired to scale gently with the number of dimensions.

Whilst the vast majority of practical filters focus on how to accurately represent the probability densities, very few seem to work systematically on how to efficiently express densities in high-dimensional spaces. In spite of that, there appears to be a consensus that statistical efficiency in expressing high-dimensional filtering densities can be improved by simulating tempering distributions [1–4], which generally stabilises the filters and maintains the variance of Monte Carlo

*flavio.de-melo@liverpool.ac.uk
†s.maskell@liverpool.ac.uk
‡matteo.fasiolo@bath.edu
§frederick_e_daum@raytheon.com

weights at an acceptable level. It is conjectured by Bickel *et al.* [5] that a bootstrap particle filter for a high-dimensional problem would demand a prohibitively large number of intermediate steps which would cause it to be practically infeasible. This conjecture suggests that filtering by simulating continuously intermediating distributions [3] might be an idealised solution, and it is particularly well corroborated by the reported success of Monte Carlo Markov Chain algorithms that populate high-dimensional state-spaces efficiently through several sampling steps abstracting continuous-time transitions [6–9].

Solving the stochastic filtering problem formulated as a continuous-time inference procedure dates from the very seminal work by Stratonovich [10], Kushner [11] and Zakai [12] on the filtering theory. The most popular instance of such filters is the so-called Kalman-Bucy filter [13], that combines a continuous-time prediction step with a discrete-time measurement update step, under the assumption that the processes involved are linear Gaussian. More general filters directly approximate solutions to the Kushner-Stratonovich equation either by a finite-dimensional density parametrisation [14, 15] or by Monte Carlo methods [16–18]. Other important finite-order filters that appeal to an unusual formalism of multiple stochastic integrals [19, 20] are worth mentioning as well.

Although it is arguable that continuous-time filtering provides an idealised solution in terms of regularity and asymptotic variance, it has become clear recently [21, 22] that, at a practical level, there is a principle that is fundamental for the success of filtering in high-dimensional problems: the effects of local, continuous spatial properties of the observation process should be incorporated in the solution. As identified by Bickel *et al.* [5], the information contained in the observation process calls forth the notion of *effective dimension* of the space, which is what really affects the statistical efficiency of sequential Monte Carlo filters, leading to the conclusion that a tempering procedure only addresses part of the problem. Recently, a principled approach by Rebeschini & van Handel [22] proposes to structure the filtering problem in blocks of the state-space, so that the final solution is a global empirical measure combining all the local solutions to the separate blocks. As shown by Rebeschini & van Handel [22], by using the *decay of correlations* property[1], it is possible to develop particle filters based on local solutions whose approximation error does not depend on the state dimensions.

On the other hand, the idea of filtering continuously in time seems to have its appeal revigorated as several new methods have been proposed for progressive Bayesian updates, whose continuity is considered in the limit, aiming to gradually introduce the effect of each observation. Those filters have emerged either in a variational, ensemble-based, or sequential Monte Carlo framework. In the variational framework, the new methods presented in [23–25] pose the filtering problem as a multi-step optimisation problem for which the cost function is an approximated distance between a parameterised density and the actual filtering density. In the ensemble-based framework, the methods [26–28] are focused on data assimilation problems and apply ideas of optimal transport along with continuous-time filtering to generate multiple independent solutions that are combined to obtain a single solution of an inference problem. The methods in the sequential Monte Carlo framework explore extensions or alternatives to particle filters (e.g., [29–33]), or simply capitalise on techniques for properly choosing a sequence of intermediate *bridging* importance densities (e.g., [2–4, 34]), carrying on the intent to overcome the widely known problem of particle filters called *degeneracy* or collapse of weights [35–38].

Among those new sequential Monte Carlo methods one particular method stands out due to its applicability to a variety of Engineering problems and to its reported remarkable performance: particle flow. Particle flow algorithms were designed based on analogies to problems that arise in Fluid Dynamics and Electromagnetism, establishing an alternative to importance sampling for approximating a posterior filtering entity of interest. The literature on the particle flow algorithms [31, 39–50] is numerous, and the development of the technique has been rapid such that several variants of the filter now exist. These filters *flow* probability masses (particles) from a prior probability space to one that is updated according to a set of measurements without the need to perform a Bayesian update explicitly. All particle flow algorithms explore the concept of a homotopy between the prior and posterior probability spaces, implicitly describing a joint measure

[1] a spatial counterpart of the stability property of nonlinear filters, by which a probability mass is strongly correlated to masses within its neighbourhood but has negligible correlation with respect to the remaining areas of the state-space.

that couples both a prior and a posterior probability measures. This idea is in the heart of the Kantorovich's optimal tranportation problem [51], which evokes deterministic transport maps for very simple cost functions and dynamic constraints, endorsing the choice made by original particle flow methods to propose deterministic flow rules for the particles.

Nevertheless, proposing a deterministic transport map to solve a general filtering problem over a set of particles that are strongly correlated through a probability measure is not obvious, and requires non-trivial approximations for which not all the effects on the estimation errors are clearly known. A continuously evolving, exact, deterministic transport map would require the complete description at all time instants of an embedding dynamic field that induces the rule to correctly move the particles. A complete description of the optimal field is equivalent to solving the highly nonlinear Monge-Ampère equation [51] for any possible location of the particles on the space, which admits exact solutions only for few particular cases [52]. In this scenario, the best one can do, which is what the particle flow methods do, is to take simplifying assumptions on the embedding dynamic field that avoid both the optimisation over a parametric class of transport maps and the explicit solution of the associated elliptic partial differential equation. However, in our experience, these symplifying assumptions result in approximated filtering densities providing accurate estimates for the first-order moments but estimates for second and higher-order moments whose quality is highly dependent on the problem and the algorithm settings (e.g., [53]). In practice, particle flow methods address this latter issue by either relying on a companion filter [54, 55], or using the sample covariance matrix with shrinkage and Tikhonov regularisation [56] to be able to estimate the second-order moment.

Fortunately, a variational formulation of the Fokker-Planck equation as a gradient flow exposed by Jordan *et al.* [57] enables the precise interpretation that, if an optimal transport map is to be understood as a diffusion, then it minimises not only the Wasserstein distance metric, but also the free energy functional of the process with respect to the same metric. Relying on this formulation, it is straightforward to obtain an optimal transport map as a Langevin stochastic process based simply on the assumptions of stationarity of the filtering distribution (Gibb's distribution) and on potential conditions, for which an embedding stationary field is exactly derived.

In this article we take into consideration the findings presented by Jordan *et al.* [57] and incorporate the description of statistically efficient processes in high-dimensional spaces as proposed by Girolami & Calderhead [9], to formulate a stochastic particle flow[2] as an optimal transport map, representing the law of motion of the particles as a Langevin diffusion that is completely defined. This stochastic particle flow entails that a previous posterior measure under a known stationary potential field is diffused onto the current posterior measure, satisfying the Fokker-Planck equation and resulting in an accurate approximation to the filtered density. In practice, this novel interpretation of particle flow, herein called Stochastic Particle Flow (SPF), generates a sequence of samples that guide local solutions of the Fokker-Planck equation to construct a mixture that approximates the filtering density. As discussed later on, the SPF method we propose may be articulated either as a marginal particle filter (SPF-MPF) or as a Gaussian sum filter (SPF-GS), demonstrating versatility to algorithm settings and ability to address different forms of filtering problems.

It is worth mentioning that our resulting SPF technique is in the same ethos as the recent methods presented by Bunch & Godsill [34, 58], but with several substantial differences in concept and construction: (i) their filter is based on the homotopy between the prior and posterior spaces, i.e., a parameterised set of tempering distributions, whereas SPF filters do not construct the flow over a homotopy; (ii) their filter assumes the particle flow as an Ornstein-Uhlenbeck process whose scaling parameter (γ) determines the rate of diffusion of samples' paths, whereas the SPF filters are directly derived from a stationary solution of the Fokker-Planck equation; (iii) their filter's weights must be updated iteratively by a partial differential equation that describes how the logarithm of the unnormalised density evolves with a pseudo-time variable, whereas the SPF-based particle filter proposes a marginal importance density as a mixture whose weights are only updated at the end of the sampling process; (iv) their filter is articulated as a standard particle filter whereas our SPF particle filter is articulated as a marginal particle filter; (v) our method enables a direct filtering procedure that may avoid importance sampling for very high-dimensional problems.

[2]Existing particle flow algorithms (perhaps surprisingly including that known as non-zero diffusion particle flow [49]) flow particles deterministically.

The outline of the article is as follows. We start by reviewing the stochastic filtering problem in a sequential Monte Carlo framework in Section 2 and establishing the solution procedure in terms of a general map that may describe any valid method to perform the filtering update. In Section 3, we present a brief overview of the original particle flow methods and discuss their principles, in order to further clarify these methods and motivate the natural step towards the stochastic particle flow. Then the stochastic particle flow is derived in Section 4, by describing the dynamics of the probability masses, describing the associated stationary solution to the Fokker-Planck equation, constructing the filtering stochastic flow, and providing and justifying algorithm details on how to compute the diffusion matrix, how to integrate the stochastic flow, and how to select the simulation time horizon and integration step. We present the stochastic particle flow articulated as a Gaussian sum filter (SPF-GS) in Section 5, by abstracting the posterior Monte Carlo measure as a mixture of local solutions to the flow, and by discussing its essential characteristics. Similarly, in Section 6 we show the stochastic particle flow articulated as a marginal particle filter (SPF-MPF) by setting the importance density as a mixture of local solutions to the flow, and by describing the characteristics of the SPF-MPF. Finally, in Section 7 we illustrate the properties of the SPF technique using a series of toy problems, and evaluate it against state-of-the-art methods for two instructive multi-sensor and multi-target tracking problems: a multi-sensor bearing-only problem and a convoy tracking problem. In those evaluations, we included for comparison the extensions to two of the most effective (original) particle flows, namely, the Gaussian particle flow (GPF) [43] and the scaled-drift particle flow (SDPF) [49].

2 Sequential Monte Carlo filtering

In this section we lay out the filtering framework within which the particle flows are formalised. Let $\{\mathrm{x}_t \in \mathcal{X} : t \in \mathbb{R}^+\}$ be a sequence of states generated through time by a known continuous-time state process, generally modelled as a Markov process, and $\{\mathrm{y}_{t_k} \in \mathcal{Y} : t_k \in \mathbb{R}^+, k \in \mathbb{N}\}$ be a sequence of discrete-time observations of the process generated by an observation model. In the classical filtering problem, one is required to compute the best estimate of a function of interest φ of the state, given all observations realised up to the time instant t_k, i.e.,

$$\hat{\varphi}\left(\mathrm{x}_{t_k}\right) = \mathbb{E}\left[\varphi\left(\mathrm{x}_{t_k}\right) | \mathrm{y}_{t_1}, \mathrm{y}_{t_2}, \ldots, \mathrm{y}_{t_k}\right]. \tag{2.1}$$

To simplify notation, we will denote all variables at discretised time instants simply by the time indexes $k \in \mathbb{N}$, and write $\mathrm{y}_{1:k} \triangleq \{\mathrm{y}_1, \mathrm{y}_2, \ldots, \mathrm{y}_k\}$. Now consider a set of particles $\{\mathrm{x}_{k-1}^{(i)}, w_{k-1}^{(i)} : i = 1, \ldots, N\}$ constituting samples that can be used to approximate a filtering probability density $p\left(\mathrm{x}_{k-1} | \mathrm{y}_{1:k-1}\right)$ by means of a Monte Carlo measure satisfying

$$\sum_{i=1}^{N} w_{k-1}^{(i)} \delta(\mathrm{x}_{k-1} - \mathrm{x}_{k-1}^{(i)}) \overset{N\to\infty}{\longrightarrow} p(\mathrm{x}_{k-1} | \mathrm{y}_{1:k-1}). \tag{2.2}$$

Given a new observation obtained at k, one wishes to find a procedure to transform the set of particles $\{\mathrm{x}_{k-1}^{(i)}, w_{k-1}^{(i)}\}$ into a new set of particles $\{\mathrm{x}_k^{(i)}, w_k^{(i)} : i = 1, \ldots, N\}$ that incorporates the effect of the latest observation in order to estimate the filtered entity as

$$\hat{\varphi}(\mathrm{x}_k) = \sum_{i=1}^{N} w_k^{(i)} \varphi(\mathrm{x}_k^{(i)}). \tag{2.3}$$

In theory, the filtering problem in the sequential Monte Carlo form can be solved by any map $\mathcal{T} : \mathcal{X} \times \mathcal{Y} \to \mathcal{X}'$, $\mathcal{T} \in \mathcal{C}^{1,0}$, where $|\mathcal{X}'| = |\mathcal{X}|$[3], that accomplishes

$$\mathrm{x}_k^{(i)} \quad \coloneqq \quad \mathcal{T}(\mathrm{x}_{k-1}^{(i)}, \mathrm{y}_k);\ i = 1, \ldots, N; \tag{2.4}$$

$$w_k^{(i)} \quad \coloneqq \quad \left|\mathcal{J}_{\mathrm{x}_{k-1}}[\mathcal{T}]\right|^{-1} w_{k-1}^{(i)}; \tag{2.5}$$

[3] $|.|$ in this expression meaning the cardinality of a set, as opposed to the same symbol representing the determinant of a matrix in equation (2.5).

where $\mathcal{J}_{\mathrm{x}_{k-1}}[.]$ is the Jacobian matrix with respect to x_{k-1}, and such that

$$\sum_{i=1}^{N} w_k^{(i)} \delta(\mathrm{x}_k - \mathrm{x}_k^{(i)}) \overset{N\to\infty}{\longrightarrow} p(\mathrm{x}_k|\mathrm{y}_{1:k}). \tag{2.6}$$

Although most practical filters implement the mapping (2.4) in terms of discrete Bayesian updates, there should be no objection to the general idea of considering the map $\mathcal{T}$ as a transform continuous in time within $t_{k-1} < t \leq t_k$. This idea establishes the basis for the particle flow filters.

3 Particle flow

This section aims to present a brief overview on the particle flow methods, to discuss their principles, and to set the background for the introduction of the stochastic particle flow. The key idea of the particle flow is to transform a set of probability masses on a state space in a smooth way, in order to express a filtering entity, usually an estimate. The mechanism implied is, therefore, a filtering algorithm that avoids the need to perform a Bayesian measurement update explicitly.

Given a set of particles $\left\{\mathrm{x}^{(i)}(\lambda) \in \mathbb{R}^{n_x} : i = 1, \ldots, N\right\}$ dependent on a continuous pseudo-time variable $\lambda \in [0, 1]$, where n_x is the number of dimensions of the state space, and such that $\mathrm{x}^{(i)}(0) = \mathrm{x}_{k-1}^{(i)}$ and $\mathrm{x}^{(i)}(1) = \mathrm{x}_k^{(i)}$, the transformation of the particles is accomplished by solving through $0 < \lambda \leq 1$ an ordinary differential equation (ODE) referred to as the flow equation

$$\frac{d\mathrm{x}}{d\lambda} = \mu(\mathrm{x}, \lambda), \quad \mathrm{x}^{(i)}(0) \sim p_0(\mathrm{x}). \tag{3.1}$$

The varieties of particle flow methods rely on how one defines the flow drift $\mu(\mathrm{x}, \lambda)$, which in turn depends on the assumptions made to solve the associated continuity equation

$$\frac{\partial p}{\partial \lambda} = -\nabla_{\mathrm{x}} \cdot (\mu \cdot p), \quad p(\mathrm{x}, 0) = p_0(\mathrm{x}). \tag{3.2}$$

The operator $\nabla_{\mathrm{x}} \cdot (.)$ is the divergence operator and the drift can be understood as a vector field $\mu(\mathrm{x}, \lambda) \in \mathbb{R}^{n_x}$ that is not uniquely determined for a given probability density $p(\mathrm{x}, \lambda)$. In the optimal transportation literature the vector field is usually determined by the constraint that it minimises the kinetic energy. In that case, the flow equation (3.1) can be written in terms of a dynamic potential field as $\mu(\mathrm{x}, \lambda) = \mathcal{M}^{-1}\nabla_{\mathrm{x}}\psi(\mathrm{x}, \lambda)$ [51], where $\mathcal{M}$ is a positive-definite mass matrix, ∇_{x} is the gradient operator, and $\psi(\mathrm{x}, \lambda)$ is a dynamic potential function that satisfies a p-Laplacian equation of the form [51, 59]

$$\nabla_{\mathrm{x}} \cdot (a(\mathrm{x}, \lambda) \nabla_{\mathrm{x}}\psi(\mathrm{x}, \lambda)) = \pi(\mathrm{x}) - p(\mathrm{x}, \lambda), \tag{3.3}$$

where $\pi(\mathrm{x})$ is the target posterior probability density, the function $a(\mathrm{x}, \lambda) \in \mathbb{L}^{\infty}$[4], $a(\mathrm{x}, \lambda) \geq 0$, is a Lagrange multiplier that scales the distance of optimal transportation, whereas the term $\nabla_{\mathrm{x}}\psi(\mathrm{x}, \lambda)$ gives the direction of optimal tranportation. Nevertheless, the original particle flows do not follow the classical transport-based methodology but rather take simplifying assumptions on the dynamic potential field, avoiding the complexity of solving the elliptic partial differential equation (3.3). Specifically, the particle flows are derived from a programmed sequence of a dynamic potential field that roughly solves the equation (3.2). As examples we refer the reader to the incompressible particle flow [31], the Gaussian or exact particle flow [43], and the non-zero *"diffusion"* particle flow [49] which is not actually a diffusion, but simply takes into account a diffusion term to scale and/or offset the drift term.

Alternatively to a dynamic solution of (3.3) and to original particle flows, it is possible to demonstrate that if the drift is taken to solve the continuity equation (3.2) under a stationary

[4]The $\mathbb{L}^{\infty}$-space generalises the $\mathbb{L}^p$-spaces to $p = \infty$. An $\mathbb{L}^p$-space describes the set of all functions f for which the norm $\|f\|_p = \left(\int_{\mathcal{X}} |f|^p\right)^{1/p}$ converges. The concept is analogous for the $\mathbb{L}^{\infty}$-space although its norm is defined by the essential supremum.

potential field (conservative field) related to a stationary, locally[5] log-concave density of the form $p(\mathrm{x}, T) = \pi(\mathrm{x}) \propto \exp(-\psi(\mathrm{x}))$, then the flow (3.1) produces the maximum-a-posteriori estimate $\hat{\mathrm{x}}_{MAP}$ after an appropriate time horizon $\lambda \geq T$ (see *Theorem 3* in the Appendix A). A similar concept is used in optimisation algorithms based on gradient descent. The obvious problem with this approach is that it provides a first-order estimate, being unable to capture higher-order aspects of a target posterior density. Thus, on the assumption of a stationary potential field, in terms of minimising the free energy functional, the optimal way a particle flow could describe the filtering density precisely up to an arbitrary moment order is by being modeled as a diffusion and, therefore, assuming a stochastic form for which the probability density would follow the Fokker-Planck equation (see [57] for details). This observation becomes fundamental when we note that, generally speaking, obtaining an accurate approximation to a single stationary potential field is easier than obtaining a sequence of accurate approximations to a dynamic potential field, as proposed by filters based on the classical transport methodology (e.g., [26]).

4 Stochastic particle flow

This section derives the stochastic particle flow based on a stationary solution to the Fokker Planck equation. We capitalise on the fact that, under certain conditions on the drift and diffusion terms of a stochastic process, there is a stationary solution that satisfies a variational principle, minimising a certain convex free energy functional over an appropriate admissible class of probability densities. The Fokker–Planck equation is shown to follow the direction of steepest descent of the associated free energy functional [57] at each instant of time, which corresponds to solving the optimal mass transfer problem where the entropy is maximised, giving rise to a diffusion.

In the Subsection 4.1 we present the general dynamics proposed for a stochastic particle flow; in the Subsection 4.2 we obtain the corresponding stationary solution to the Fokker-Planck equation; in the Subsection 4.3 we present the stochastic particle flow based on the stationary solution; and in the Subsection 4.4 we discuss the interpretation of the diffusion matrix and possible choices for it.

4.1 Dynamics of the particles

Assuming that the particles $\left\{\mathrm{x}^{(i)}(\lambda) : i = 1, \ldots, N\right\}$ follow a diffusion process $\{X_\lambda\}_{\lambda \geq 0}$ when subject to a Bayesian measurement update, the dynamics of the particles can be generally described by the Îto stochastic differential equation

$$dX_\lambda = \mu(X_\lambda, \lambda)\, d\lambda + \sigma(X_\lambda, \lambda)\, dW_\lambda, \quad X_0 = X(0); \tag{4.1}$$

such that the associated probability distribution $p(\mathrm{x}, \lambda)$ is continuously evolving with respect to the time variable $\lambda \in \mathbb{R}^+$, where $\{W_\lambda\}$ is a standard Brownian motion, $\mu(X_\lambda, \lambda)$ is the drift vector and $\sigma(X_\lambda, \lambda)$ is the diffusion coefficient. It is well known [60, 61], that the probability density $p(\mathrm{x}, \lambda)$ of an n_x-dimensional random state vector x under the dynamics of (4.1) has a deterministic evolution according to the Fokker-Planck equation

$$\begin{aligned} \frac{\partial}{\partial \lambda} p(\mathrm{x}, \lambda) = &- \sum_{i=1}^{n_x} \frac{\partial}{\partial x_i} \left[\mu_i(\mathrm{x}, \lambda)\, p(\mathrm{x}, \lambda)\right] \\ &+ \frac{1}{2} \sum_{i=1}^{n_x} \sum_{j=1}^{n_x} \frac{\partial}{\partial x_i} \frac{\partial}{\partial x_j} \left[D_{ij}(\mathrm{x}, \lambda)\, p(\mathrm{x}, \lambda)\right], \\ &p(\mathrm{x}, 0) = p_0(\mathrm{x}),\ \lambda \geq 0; \end{aligned} \tag{4.2}$$

where $\mathrm{x} = [x_1, \ldots, x_{n_x}]^T$, $\mu = [\mu_1, \ldots, \mu_{n_x}]^T$, and

$$D_{ij}(\mathrm{x}, \lambda) = \sum_{k=1}^{n_x} \sigma_{ik}(\mathrm{x}, \lambda)\, \sigma_{jk}(\mathrm{x}, \lambda), \tag{4.3}$$

[5] log-concave in the vicinity of the density maxima.

for an n_x-dimensional Wiener process $\{W_\lambda\}$. In its usual form as described in Physics, the equation reads as

$$\frac{\partial}{\partial\lambda}p = -\nabla_{\mathrm{x}}\cdot[\mu p] + \frac{1}{2}\Delta_{\mathrm{x}}\left[\sigma\sigma^T p\right]. \tag{4.4}$$

where $\Delta_{\mathrm{x}}[.] = \nabla_{\mathrm{x}}\cdot\nabla_{\mathrm{x}}[.]$ is laplacian operator with respect to x. We assume that the diffusion coefficient σ is locally independent of x, giving rise to a local diffusion matrix $D(\lambda) = \sigma(\lambda)\,\sigma(\lambda)^T$ that is not affected by the laplacian operator in the vicinity of each particle. This means that, at a given time instant, the diffusion term in (4.2) evolves at a rate proportional to the curvature of a (Riemann) manifold that is approximately constant in the neighbourhood of each particle. This assumption does not affect the generality of the concepts applied in our derivation for two reasons: (i) the assumption results in a stochastic particle flow missing a simple term, whose univariate form is $\sigma(x,\lambda)\cdot\partial_x[\sigma(x,\lambda)]$, that can be easily incorporated; (ii) in practice, any probability density can be well approximated by a mixture of densities whose covariances are locally constant with respect to the state (i.e., $\partial_x[\sigma(x,\lambda)] = 0$ locally).

4.2 Stationary solution of the Fokker-Planck equation

A stationary solution to the equation (4.4) should obviously satisfy

$$\frac{\partial}{\partial\lambda}p(\mathrm{x},\lambda) \overset{\lambda\to\infty}{\longrightarrow} 0. \tag{4.5}$$

By writting

$$\nabla_{\mathrm{x}}\cdot S \triangleq \nabla_{\mathrm{x}}\cdot[\mu\, p] - \frac{1}{2}D\,\Delta_{\mathrm{x}}[p], \tag{4.6}$$

it becomes clear the definition of the probability current

$$\begin{aligned} S(\mathrm{x},\lambda) &= \mu(\mathrm{x},\lambda)\,p(\mathrm{x},\lambda) - \frac{1}{2}D(\lambda)\cdot\nabla_{\mathrm{x}}p(\mathrm{x},\lambda) \\ &= p(\mathrm{x},\lambda)\left[\mu(\mathrm{x},\lambda) - \frac{1}{2}D(\lambda)\cdot\nabla_{\mathrm{x}}\log p(\mathrm{x},\lambda)\right]. \end{aligned} \tag{4.7}$$

Since the stationary condition requires

$$\frac{\partial}{\partial\lambda}p(\mathrm{x},\lambda) = -\nabla_{\mathrm{x}}\cdot S(\mathrm{x},\lambda) \overset{\lambda\to\infty}{\longrightarrow} 0, \tag{4.8}$$

the probability current is required to vanish as $\lambda\to\infty$. The probability current can only vanish if the drift $\mu(\mathrm{x},\lambda)$ can be expressed as the gradient of a potential function [62], cancelling out the terms within brackets in (4.7). We write the drift as the gradient of a stationary potential function according to

$$\mu(\mathrm{x},\lambda) = -\frac{1}{2}D(\lambda)\cdot\nabla_{\mathrm{x}}\Phi(\mathrm{x}). \tag{4.9}$$

The necessary and sufficient conditions for the existence of $\Phi(\mathrm{x})$ are the potential conditions [62]

$$\frac{\partial\mu_i}{\partial x_j} = \frac{\partial\mu_j}{\partial x_i}, \quad \forall i\neq j. \tag{4.10}$$

Provided that the probability current vanishes as $\nabla_{\mathrm{x}}\log p(\mathrm{x},\lambda)\to-\nabla_{\mathrm{x}}\Phi(\mathrm{x})$, we obtain the stationary solution as

$$p(\mathrm{x},\lambda) \overset{\lambda\to\infty}{\longrightarrow} p_{st}(\mathrm{x}) = \frac{1}{Z}e^{-\Phi(\mathrm{x})}, \tag{4.11}$$

where

$$Z = \int_{\mathbb{R}^{n_x}} e^{-\Phi(\mathrm{x})} d\mathrm{x} \tag{4.12}$$

must be positive and finite. We promptly recognise (4.11) as analogous the Gibbs' distribution. It is verifiable that (see, for example, [63]) the Gibbs' distribution minimizes the free energy functional over all probability densities on $\mathbb{R}^{n_x}$. It can also be shown that the stationary solution is the first eigenfunction of the Fokker-Planck equation, corresponding to the eigenvalue zero [62].

4.3 The stochastic flow

The general stochastic particle flow is derived by setting the stationary solution to be the target posterior density $\pi(\mathrm{x}) = p(\mathrm{x}|\mathrm{y}_{1:k})$, to give

$$\begin{aligned} p_{st}(\mathrm{x}) &\coloneqq p(\mathrm{x}|\mathrm{y}_{1:k}), \\ \frac{e^{-\Phi(\mathrm{x})}}{Z} &= \frac{p(\mathrm{y}_k|\mathrm{x})\, p(\mathrm{x}|\mathrm{y}_{1:k-1})}{p(\mathrm{y}_k|\mathrm{y}_{1:k-1})}, \\ \Phi(\mathrm{x}) &= -\log p(\mathrm{y}_k|\mathrm{x}) - \log p(\mathrm{x}|\mathrm{y}_{1:k-1}). \end{aligned} \tag{4.13}$$

Given a valid potential function $\Phi(\mathrm{x})$ to provide the stationary solution, all potential functions of the form $\Phi(\mathrm{x}) \pm K$ for any constant $K \in \mathbb{R}$ are also valid, thus we can pick a valid potential function in (4.13) such that $p(\mathrm{y}_k|\mathrm{y}_{1:k-1}) = Z$.

By using equation (4.9), we obtain

$$\begin{aligned} \mu(\mathrm{x}, \lambda) &= -\frac{1}{2} D(\lambda) \cdot \nabla_{\mathrm{x}} \Phi(\mathrm{x}) = \frac{1}{2} D(\lambda) \cdot \nabla_{\mathrm{x}} \log \pi(\mathrm{x}) \\ &= \frac{1}{2} D(\lambda) \cdot \left[\nabla_{\mathrm{x}} \log p(\mathrm{y}_k|\mathrm{x}) + \nabla_{\mathrm{x}} \log p(\mathrm{x}|\mathrm{y}_{1:k-1})\right]. \end{aligned} \tag{4.14}$$

Substituting (4.14) into (4.7) it is easy to see that the probability current vanishes as $\lambda \to \infty$. Additionally, it is important to note that most of the continuous multivariate probability densities used in parametric statistics satisfy the potential conditions (4.10). Roughly speaking, if the drift does not comprise functions of products involving the state vector components, e.g., $\mu(\mathrm{x}) = [f_1(x_1 x_2 \ldots x_{n_x}), \ldots, f_{n_x}(x_1 x_2 \ldots x_{n_x})]^T$, and it does not comprise different functions across components, i.e., $\mu(\mathrm{x}) = [f_1(\mathrm{x}), \ldots, f_{n_x}(\mathrm{x})]^T$ where there is at least one $f_i \neq f_j$ for all $i \neq j$, the potential conditions hold.

Based on equation (4.1) and on the drift obtained from the stationary solution (4.14), the dynamics of a set of particles $\left\{\mathrm{x}^{(i)}(\lambda) : i = 1, \ldots, N\right\}$ can be described by the stochastic differential equation

$$\begin{aligned} d\mathrm{x} &= \mu(\mathrm{x}, \lambda)\, d\lambda + \sigma(\mathrm{x}, \lambda)\, d\mathrm{w}_\lambda, \quad \mathrm{x}_0^{(i)} = \mathrm{x}_{k-1}^{(i)}; \\ d\mathrm{x} &= \frac{1}{2} D \nabla_{\mathrm{x}} \log \pi(\mathrm{x})\, d\lambda + D^{1/2} d\mathrm{w}_\lambda; \end{aligned} \tag{4.15}$$

where $\pi(\mathrm{x})$ is the target (posterior) probability density, $\{\mathrm{w}_\lambda\}$ is the standard Wiener process (Brownian motion) and D is the diffusion matrix. The stochastic process described by (4.15) is known in the literature to follow the stochastic Langevin dynamics. If the SDE (4.15) is integrated over an appropriate finite time horizon $T \in \mathbb{R}^+$, then

$$\|P - P_\pi\|_{\mathrm{TV}} = \frac{1}{2} \int_{\mathbb{R}^{n_x}} |p(\mathrm{x}, \lambda) - \pi(\mathrm{x})|\, d\mathrm{x} \leq \varepsilon \tag{4.16}$$

for any $\lambda > T$, under a desired precision ε (see [64]), so that the stochastic particle flow implements the mapping (2.4). The left-hand side of expression (4.16) is the total-variation distance[6] between

[6] The total variation norm for probability measures have an equivalence to the $\mathbb{L}^1$-norm as presented in (4.16). A simple argument for this equivalence is given in [65], chapter 4, proposition 4.2.

the probability measures $P(dx)$ and $P_\pi(dx)$, defined on $(\mathbb{R}^{n_x}, \mathcal{B}(\mathbb{R}^{n_x}))$ and with the correspondences $dP = p(\mathrm{x}, \lambda)\, dx$ and $dP_\pi = \pi(\mathrm{x})\, dx$.

The stochastic particle flow can be interpreted as a continuous-time filtering method in the classical sense. Under the abstraction of a continuously interpolated observation process, the method has a direct correspondence to the Kallianpur-Striebel formula and satisfies the Zakai equation as we demonstrate by the *Theorem 8* and *Corollary 10* in the Appendix A.

4.4 The diffusion matrix

As exposed by Girolami & Calderhead [9], the space of parameterised probability density functions is endowed with a natural Riemann geometry, where the diffusion matrix arises as the inverse of a position-specific metric tensor, $G(\mathrm{x}(\lambda))$. This metric tensor maps the distances inscribed in a Riemann manifold to distances in the Euclidean space and, therefore, constitutes a mean to constrain the dynamics of any stochastic process to the geometric structure of the parametric probability space. Rao [66] showed the tensor $G(\mathrm{x}(\lambda))$ to be the expected Fisher information matrix

$$G(\mathrm{x}(\lambda)) = -\mathbb{E}_{\mathrm{y}|\mathrm{x}}\left[\mathcal{H}_{\mathrm{x}}\left[\log p(\mathrm{y}|\mathrm{x})\right]\right], \tag{4.17}$$

where $\mathcal{H}_{\mathrm{x}}[.]$ is the Hessian matrix with respect to x. In a Bayesian context, Girolami & Calderhead [9] suggested a metric tensor that includes the prior information as

$$G(\mathrm{x}(\lambda)) = -\mathbb{E}_{\mathrm{y}|\mathrm{x}}\left[\mathcal{H}_{\mathrm{x}}\left[\log p(\mathrm{y}|\mathrm{x})\right]\right] - \mathcal{H}_{\mathrm{x}}\left[\log p_x(\mathrm{x})\right], \tag{4.18}$$

although many possible choices of metric for a specific manifold could be advocated. Because we are interested in local (curvature) properties of the stochastic particle flow, a sensible choice for metric tensor $G(\mathrm{x}(\lambda))$ is the observed Fisher information matrix incorporating the prior information, locally evaluated, for which the density matrix becomes

$$D = G(\mathrm{x}(\lambda))^{-1} = \left[-\mathcal{H}_{\mathrm{x}}\left[\log \pi(\mathrm{x})\right]\right]^{-1}_{\mathrm{x}=\mathrm{x}_\lambda}. \tag{4.19}$$

An obvious problem with this choice is that the expression (4.19) may be not strictly positive definite at specific points of the state-space for some types of probability distributions (e.g., mixtures). In order to solve that problem, one could appeal to methods for regularising the diffusion matrix, such as the technique to find the nearest positive definite matrix with the minimum Fröbenius norm [67], or simply propose an empirical estimate to (4.18).

4.5 Integration method

Among the discretisation methods that could be used to integrate the SDE (4.15), we advocate the use of the Ozaki's discretisation [68] of the Langevin diffusion which is more accurate than methods based on the Euler discretisation. The Ozaki's discretisation is only possible for target densities that are continuously differentiable and have a smooth Hessian matrix. These requirements may be fulfilled by proposing a solution that constitutes a superposition of conveniently parameterised local approximations to a density.

The algorithm that enables simulation from the SDE (4.15) using the Ozaki's discretisation is generally called *Langevin Monte Carlo with Ozaki discretization* (LMCO) in the MCMC community (see [64]). Provided an appropriate time horizon T, by discretising the interval $0 \leq \lambda \leq T$ into L sub-intervals $\{\lambda_0 = 0, \lambda_1, \ldots \lambda_l, \ldots, \lambda_L = T\}$, the discretised particle flow equation using Ozaki's method is given by

$$\begin{aligned}\mathrm{x}(\lambda_{l+1}) = \mathrm{x}(\lambda_l) &+ \left(\mathrm{I}_{n_x} - e^{-\frac{1}{2}\Delta\lambda D(\lambda_l)^{-1}}\right) D(\lambda_l)^2 \nabla_{\mathrm{x}} \log \pi(\mathrm{x}(\lambda_l)) \\ &+ \left[\left(\mathrm{I}_{n_x} - e^{-\Delta\lambda D(\lambda_l)^{-1}}\right) D(\lambda_l)^2\right]^{1/2} \mathrm{w}_{l+1},\end{aligned} \tag{4.20}$$

where $\{\mathrm{w}_l : l = 1, \ldots, L\}$ is a sequence of independent random vectors distributed according to $\mathrm{w}_l \sim \mathcal{N}(\mathrm{w}; 0_{n_x}, \mathrm{I}_{n_x})$. The need to compute the exponential matrices in (4.20) implies an increment

in complexity typically bounded by $\mathrm{O}\left(NLn_x^3\right)$ computations, which may not be justifiable for some applications. A cheaper alternative is achieved by linearising (4.15) in the neighbourhood of the current state and assuming $D(\lambda)$ piecewise constant in time, transforming the linearised equation by the Laplace transform, solving it in the Laplace domain and transforming it back. The result is presented as follows

$$\begin{aligned}\mathrm{x}(\lambda_{l+1}) = \mathrm{x}(\lambda_l) &+ \left(1 - e^{-\frac{1}{2}\Delta\lambda}\right) D(\lambda_l)\nabla_{\mathrm{x}} \log \pi\left(\mathrm{x}(\lambda_l)\right) \\ &+ \left(1 - e^{-\Delta\lambda}\right)^{1/2} D(\lambda_l)^{1/2}\mathrm{w}_{l+1}. \end{aligned} \tag{4.21}$$

where the exponential matrices are avoided but the exponential effect on the integration variable (time step) is kept. See Appendix B for the derivation of this latter integration rule.

4.6 Selection of time horizon and integration step

A crucial requisite for successfully implementing the stochastic flow is to solve the problem of selecting an adequate time horizon T and integration step $\Delta\lambda$ so that

$$\left\|\hat{P}_L - P_\pi\right\|_{\mathrm{TV}} \leq \varepsilon \tag{4.22}$$

for a desired precision level ε, where $\hat{P}_L\left(d\mathrm{x}\right)$ is the approximating probability measure achieved by sampling from the discretised stochastic equation (4.21) over L steps.

There are several routes one could take to solve this problem depending on the assumptions made for the involved probability measures and on the regularity properties of the stationary distribution. Alternatively, one could pose associated problems concerning equally relevant questions, such as selecting the time horizon and integration step in order to minimise the weights' variance of an approximating Monte Carlo measure. Due to its generality and suitability to nicely measurable filtering entities, we advocate and recall the criteria established by Dalalyan [64] according to the following results.

Theorem 1. *[64] Let $\Phi : \mathbb{R}^{n_x} \to \mathbb{R}$ be a function satisfying*

$$\begin{aligned}\Phi\left(\mathrm{x}\right) - \Phi\left(\bar{\mathrm{x}}\right) - \nabla_{\mathrm{x}}\Phi\left(\bar{\mathrm{x}}\right)^T\left(\mathrm{x} - \bar{\mathrm{x}}\right) &\geq \frac{1}{2}m\left\|\mathrm{x} - \bar{\mathrm{x}}\right\|_2^2, \\ \left\|\nabla_{\mathrm{x}}\Phi\left(\mathrm{x}\right) - \nabla_{\mathrm{x}}\Phi\left(\bar{\mathrm{x}}\right)\right\|_2 &\leq M\left\|\mathrm{x} - \bar{\mathrm{x}}\right\|_2, \\ &\forall \mathrm{x}, \bar{\mathrm{x}} \in \mathbb{R}^{n_x}; \end{aligned} \tag{4.23}$$

for two existing positive constants m and M, and $\bar{\mathrm{x}} \in \mathbb{R}^{n_x}$ be its global minimum point. Assume that for some $\gamma \geq 1$, we have $\Delta\lambda \leq (\gamma M)^{-1}$ and $L \geq \gamma$. Then, for any time horizon $T = L\Delta\lambda$, the total-variation distance between the target measure P_π and the approximation $\hat{P}_L$ furnished by a Langevin Monte Carlo algorithm with the initial distribution $\nu_0\left(\mathrm{x}\right) = \mathcal{N}(\mathrm{x}; \bar{\mathrm{x}}, M^{-1}\mathrm{I}_{n_x})$ satisfies

$$\begin{aligned}\left\|\hat{P}_L - P_\pi\right\|_{TV} \leq \frac{1}{2}\exp\left\{\frac{n_x}{4}\log\left(\frac{M}{m}\right) - \frac{Tm}{2}\right\} \\ + \left\{\frac{n_x M^2 T\Delta\lambda\gamma}{4\left(2\gamma - 1\right)}\right\}^{1/2}. \end{aligned} \tag{4.24}$$

Corollary 2. *[64] Let $n_x \geq 2$, Φ satisfies (4.23) and $\varepsilon \in (0, 1/2)$ be a desired precision level. Let the time horizon T and the step size $\Delta\lambda$ be defined by*

$$T = \frac{4\log\left(\frac{1}{\varepsilon}\right) + n_x\log\left(\frac{M}{m}\right)}{2m}, \tag{4.25}$$

$$\Delta\lambda = \frac{\varepsilon^2\left(2\gamma - 1\right)}{M^2 T n_x \gamma}, \tag{4.26}$$

where $\gamma = (1 + Mn_xT\varepsilon^{-2})/2$. Then the resulting probability distribution of a Langevin Monte Carlo algorithm after $L = \lceil T/\Delta\lambda \rceil$ steps, satisfies (4.22).

It is obvious that *Corollary 2* is a direct criteria for selecting the time horizon and step size, arising for the right-hand side of the inequality (4.24) set to be a desired precision level. Obviously, the initial distribution defined by the *Theorem 1* is just a reference distribution that enables a closed formula for the bound, which may be well understood as a parameterised empirical distribution that encompass (spatially) all initial samples.

It is worth noting though that the solution assumes the positive constants m and M are known a priori. We propose to obtain these constants by first computing the maximum-a-posteriori estimate $\bar{\mathrm{x}} = \operatorname{argmin}[\Phi(\mathrm{x})] = \operatorname{argmax}[\pi(\mathrm{x})]$ of the filtering problem, and applying the inequalities (4.23) for the initial sample that would produce the maximum m and the minimum M.

5 Stochastic particle flow as a Gaussian sum filter

In this section we derive a filter that approximates the posterior probability density as a Gaussian mixture by means of the stochastic particle flow, referred to as the stochastic-particle-flow Gaussian sum filter (SPF-GS).

5.1 The mixture-based approximating measure

The key idea for the derivation of the SPF-GS is explained as follows. Given a set of samples $\{\mathrm{x}^{(i)} \in \mathcal{X} : i = 1, \ldots, N\}$ drawn from an appropriate distribution, if one is required to solve the filtering problem by a standard Monte Carlo method, then the filter entails the following approximation

$$\begin{aligned}\hat{\varphi}(\mathrm{x}) &= \int_{\mathcal{X}} \varphi(\mathrm{x})\,\pi(\mathrm{x})\,dx \\ &\approx \int_{\mathcal{X}} \varphi(\mathrm{x}) \sum_{i=1}^{N} w(\mathrm{x}^{(i)})\delta(\mathrm{x}-\mathrm{x}^{(i)})d\mathrm{x} \\ &= \sum_{i=1}^{N} w^{(i)}\varphi(\mathrm{x}^{(i)}),\end{aligned} \tag{5.1}$$

where $w(\mathrm{x}^{(i)}) = w^{(i)}$ are the importance weights. Now suppose that we have access to an approximating measure $\hat{P}_\pi(d\mathrm{x})$ on $(\mathcal{X}, \mathcal{B}(\mathcal{X}))$ with an associated density such that $d\hat{P}_\pi = \hat{\pi}d\mathrm{x}$. If the density $\hat{\pi}$ involves a superposition of N Gaussians according to

$$\begin{aligned}\hat{\pi}(\mathrm{x}) &= \sum_{i=1}^{N} w_m(\mathrm{x}^{(i)})\mathcal{N}(\mathrm{x};\mu_m(\mathrm{x}^{(i)}),\Sigma_m(\mathrm{x}^{(i)})) \\ &= \sum_{i=1}^{N} w_m^{(i)}\mathcal{N}(\mathrm{x};\mu_m^{(i)},\Sigma_m^{(i)}),\end{aligned} \tag{5.2}$$

where $\{w_m^{(i)}, \mu_m^{(i)}, \Sigma_m^{(i)}\}$ are computed based on the samples $\{\mathrm{x}^{(i)}\}$, then the solution is given by

$$\begin{aligned}\hat{\varphi}(\mathrm{x}) &= \int_{\mathcal{X}} \varphi(\mathrm{x})\,\pi(\mathrm{x})\,d\mathrm{x} \\ &\approx \int_{\mathcal{X}} \varphi(\mathrm{x}) \sum_{i=1}^{N} w_m^{(i)}\mathcal{N}(\mathrm{x};\mu_m^{(i)},\Sigma_m^{(i)})d\mathrm{x} \\ &= \sum_{i=1}^{N} w_m^{(i)} \int_{\mathcal{X}} \varphi(\mathrm{x})\,\mathcal{N}(\mathrm{x};\mu_m^{(i)},\Sigma_m^{(i)})d\mathrm{x} \\ &= \sum_{i=1}^{N} w_m^{(i)}\mathbb{E}_{\mathcal{N}}\left[\varphi(\mathrm{x})\,|\mu_m^{(i)},\Sigma_m^{(i)}\right].\end{aligned} \tag{5.3}$$

In this setting, it is possible to prove that $\hat{\pi}(\mathrm{x}) \to \pi(\mathrm{x})$ as $N \to \infty$ almost surely if $\mu_m^{(i)} \to \mathrm{x}^{(i)}$ and $\Sigma_m^{(i)} \to 0$, by appealing to convergence proofs for mixture-based estimators (see [69], pages 197–199). Also, it is worth noting that this procedure is quite general in the sense that (5.2) could be replaced by a mixture of any convenient parametric distribution.

5.2 The stochastic-particle-flow Gaussian sum filter

Building upon the results presented in the previous subsection, stochastic particle flow uses samples to populate the state space so that they guide an accurate approximation to the posterior probability density of the form (5.2).

From a known set of samples and parameters $\{\mathrm{x}^{(i)}(\lambda), w_m^{(i)}(\lambda), \mu_m^{(i)}(\lambda), \Sigma_m^{(i)}(\lambda)\}$, the filtering procedure consists in integrating the SDE (4.15) for each particle and propagating the associated parameters through the interval $0 < \lambda \leq T$, which corresponds to the interval $t_{k-1} < t \leq t_k$. The integration process is performed until one achieves the posterior set of samples and parameters $\{\mathrm{x}^{(i)}(T), w_m^{(i)}(T), \mu_m^{(i)}(T), \Sigma_m^{(i)}(T)\}$, where $\mathrm{x}^{(i)}(0) = \mathrm{x}_{k-1}^{(i)}$ and $\mathrm{x}^{(i)}(T) = \mathrm{x}_k^{(i)}$, so that

$$\frac{1}{2}\int_{\mathcal{X}} \left| \sum_{i=1}^{N} w_m^{(i)}(T)\mathcal{N}(\mathrm{x}; \mu_m^{(i)}(T), \Sigma_m^{(i)}(T)) - \pi(\mathrm{x}) \right| d\mathrm{x} \leq \varepsilon,$$

under a desired precision level ε as $N \to \infty$. In practice, the integration of the stochastic flow (4.15) over $0 < \lambda \leq T$ involves multiple intermediate sampling steps that propagate the samples $\mathrm{x}^{(i)}(\lambda)$ in order to populate the state space accordingly. Assuming approximate local linearity of the flow drift in the neighbourhood of a probability mass located at x_l, which should produce a negligible error for a small state displacement given a small increment of pseudo-time $\Delta\lambda$, the stochastic particle flow (4.15) can be approximated within the region $\|\mathrm{x} - \mathrm{x}_l\| < \zeta$, for a sufficiently small $\zeta \in \mathbb{R}^+$, as

$$\begin{aligned} d\mathrm{x} &= \frac{1}{2}D(\lambda)\nabla_{\mathrm{x}} \log \pi(\mathrm{x})\, d\lambda + D(\lambda)^{1/2} d\mathrm{w}_\lambda, \quad \lambda \in (\lambda_l, \lambda_l + \Delta\lambda],\ \mathrm{x}(\lambda_l) = \mathrm{x}_l; \\ d\mathrm{x} &\approx [C(\mathrm{x}_l, \lambda) \cdot \mathrm{x} + c(\mathrm{x}_l, \lambda)]\, d\lambda + D(\lambda)^{1/2} d\mathrm{w}_\lambda. \end{aligned} \tag{5.4}$$

As a consequence of integrating the flow, the corresponding component moments are evolved according to the locally approximated ordinary differential equations

$$\frac{d\mu_m^{(i)}(\lambda)}{d\lambda} = C(\mathrm{x}_l^{(i)})\mu_m^{(i)}(\lambda) + c(\mathrm{x}_l^{(i)}), \tag{5.5}$$

$$\frac{d\Sigma_m^{(i)}(\lambda)}{d\lambda} = C(\mathrm{x}_l^{(i)})\Sigma_m^{(i)}(\lambda) + \Sigma_m^{(i)}(\lambda)C^T(\mathrm{x}_l^{(i)}) + D^{(i)}; \tag{5.6}$$

where

$$\begin{aligned} C(\mathrm{x}_l, \lambda) = &-\frac{1}{2}D(\lambda)P_{k|k-1}^{-1} \\ &-\frac{1}{2}D(\lambda)\mathcal{J}_{\mathrm{x}}[h(\mathrm{x}_l)]^T R_k^{-1}\mathcal{J}_{\mathrm{x}}[h(\mathrm{x}_l)], \end{aligned} \tag{5.7}$$

$$\begin{aligned} c(\mathrm{x}_l, \lambda) = &\ \frac{1}{2}D(\lambda)P_{k|k-1}^{-1} f(\mu_{m,k-1}) \\ &+\frac{1}{2}D(\lambda)\mathcal{J}_{\mathrm{x}}[h(\mathrm{x}_l)]^T R_k^{-1}\mathcal{J}_{\mathrm{x}}[h(\mathrm{x}_l)] \cdot \mathrm{x}_l \\ &+\frac{1}{2}D(\lambda)\mathcal{J}_{\mathrm{x}}[h(\mathrm{x}_l)]^T R_k^{-1}(\mathrm{y}_k - h(\mathrm{x}_l)), \end{aligned} \tag{5.8}$$

$f(.)$ is the state process function, $h(.)$ is the observation function, and

$$P_{k|k-1} = \mathbb{E}\left[(\mathrm{x}_{k|k-1} - f(\mu_{m,k-1}))(\mathrm{x}_{k|k-1} - f(\mu_{m,k-1}))^T\right], \tag{5.9}$$
$$R_k \quad = \mathbb{E}\left[(\mathrm{y}_k - h(\mathrm{x}_k))(\mathrm{y}_k - h(\mathrm{x}_k))^T\right], \tag{5.10}$$

are the covariance matrix of the prior probability density and the covariance matrix of the observation noise, respectively.

The method for propagating the moments of the mixture components is analogous to the Kalman-Bucy filter, however it does not perform an explicit discrete-time measurement update. The equations (5.5) and (5.6) are integrated for each particle. The mixture weights can be shown to be (see [69], pages 214 and 215)

$$\begin{aligned} w_m\left(\mathrm{x}(T)\right) &\propto w_m\left(\mathrm{x}(0)\right) \int_{\mathcal{X}} p\left(\mathrm{y}_k|\mathrm{x}'(T)\right) p\left(\mathrm{x}'(T)|\mathrm{y}_{1:k-1}\right) d\mathrm{x}', \\ w_m^{(i)}\left(T\right) &\propto w_m^{(i)}\left(0\right) \int_{\mathcal{X}} p\left(\mathrm{y}_k|\mathrm{x}'_k\right) p_i\left(\mathrm{x}'_k|\mathrm{y}_{1:k-1}\right) d\mathrm{x}'_k, \\ w_{m,k}^{(i)} &\propto w_{m,k-1}^{(i)} \int_{\mathcal{X}} p\left(\mathrm{y}_k|\mathrm{x}'_k\right) p_i\left(\mathrm{x}'_k|\mathrm{y}_{1:k-1}\right) d\mathrm{x}'_k. \end{aligned} \tag{5.11}$$

where, for a known Markov transition density $p\left(\mathrm{x}'_k|\mathrm{x}_{k-1}\right)$, the local prior density is computed as

$$\begin{aligned} p_i\left(\mathrm{x}'_k|\mathrm{y}_{1:k-1}\right) &= \int_{\mathcal{X}} p(\mathrm{x}'_k|\mathrm{x}_{k-1}) \mathcal{N}(\mathrm{x}_{k-1}; \mu_m^{(i)}(0), \Sigma_m^{(i)}(0)) d\mathrm{x}_{k-1} \\ &= \int_{\mathcal{X}} p(\mathrm{x}'_k|\mathrm{x}_{k-1}) \mathcal{N}(\mathrm{x}_{k-1}; \mu_{m,k-1}^{(i)}, \Sigma_{m,k-1}^{(i)}) d\mathrm{x}_{k-1}. \end{aligned} \tag{5.12}$$

It is important to make it clear the distinction $\mathrm{x}'_k \neq \mathrm{x}_k$ in the expressions (5.11) and (5.12), bearing in mind that x'_k corresponds to the state that the flow would reach when considering only the prior density as the target $\pi_{\text{prior}}(\mathrm{x}') = p_x(\mathrm{x}') \triangleq p(\mathrm{x}'|\mathrm{y}_{1:k-1})$.

Although the resulting Gaussian sum filter based on the stochastic particle flow appears to have features similar to the ones of the Gaussian sum particle filter [70], in reality these filters rely on distinct fundamental principles that render them to be very different. The fundamental principle of the Gaussian sum particle filter is using importance sampling to estimate the component moments of a mixture that approximates a target density; whereas the SPF-GS filter, in order to approximate the posterior density, propagates a mixture through multiple intermediate steps by exploring the local properties of a stochastic flow that transforms probability masses from the previous posterior to the current posterior probability space. In practice, the SPF-GS filter can be understood as a Monte-Carlo realisation of the continuous-time version of the original Gaussian sum filter [71, 72], by appropriately exploring the Riemannian geometric structure of the probability space. The SPF-GS is also very different from the one proposed by Terejanu *et al.* [73], which is a Gaussian sum filter analogous to an extended Kalman-Bucy filter, but providing an optimal estimate of the predicted mixture weights based on an optimisation procedure.

The stochastic-particle-flow Gaussian sum filter is summarised by *Algorithm 1.*

5.3 The collapsing of mixands and resampling for the SPF Gaussian sum

A well known limitation of the Gaussian sum filter and the Gaussian sum particle filter is a phenomenon referred to as the *collapsing of the mixands* [70]. In these filters the covariances of the mixands can grow significantly because they are filtered by targeting the posterior density globally. As a consequence, the Gaussian mixture approximations become increasingly coarse and all the mixands collapse into multiple copies of the same mixand. This process results in the posterior distribution being approximated as a single Gaussian, which may be a poor representation, and additionally, it leads to a waste of computation to update identical mixands. Conceptually, the

Algorithm 1 Stochastic-particle-flow Gaussian sum filter

Initialisation

- Generate the initial set of samples and mixture parameters $\{\mathrm{x}_0^{(i)}, w_{m,0}^{(i)}, \mu_{m,0}^{(i)}, \Sigma_{m,0}^{(i)}\}_{i=1}^{N}$ as

$$\mathrm{x}_0^{(i)} \sim p(\mathrm{x}_0),$$

$$w_{m,0}^{(i)} = N^{-1},\ \mu_{m,0}^{(i)} = \mathbb{E}_{\mathrm{x}_0}\left[\mathrm{x}_0\right],\ \Sigma_{m,0}^{(i)} = \mathbb{E}_{\mathrm{x}_0}\left[(\mathrm{x}_0 - \bar{\mathrm{x}}_0)(\mathrm{x}_0 - \bar{\mathrm{x}}_0)^T\right].$$

Steps $k = 1, \ldots, T_f$

- Compute the time horizon T (4.25) and the step size $\Delta\lambda$ (4.26)
- Discretise the interval $0 \leq \lambda \leq T$ into L sub-intervals

$$\{\lambda_0 = 0,\ \lambda_1, \ldots \lambda_l, \ldots,\ \lambda_L = T\}$$

- For all particles and mixture components $i = 1, \ldots, N$,
  - Set $\mathrm{x}_{l=0}^{(i)} = \mathrm{x}_{k-1}^{(i)}$, $\mu_{l=0}^{(i)} = \mu_{m,k-1}^{(i)}$, $\Sigma_{l=0}^{(i)} = 0_{n_x \times n_x}$
  - Propagate samples by simulating from the diffusion
    - For $l = 1, \ldots, L$,

$$\mathrm{x}_l^{(i)} = \mathrm{x}_{l-1}^{(i)} + \frac{1}{2}\int_{\lambda_{l-1}}^{\lambda_l} D(\mathrm{x}_{l-1}^{(i)}) \nabla_{\mathrm{x}} \log \pi(\mathrm{x}_{l-1}^{(i)}) d\lambda + \int_{\lambda_{l-1}}^{\lambda_l} D(\mathrm{x}_{l-1}^{(i)})^{1/2} d\mathrm{w}_\lambda, \tag{5.13}$$

$$\mu_l^{(i)} = \mu_{l-1}^{(i)} + \int_{\lambda_{l-1}}^{\lambda_l} \left[C(\mathrm{x}_{l-1}^{(i)})\mu_{l-1}^{(i)} + c(\mathrm{x}_{l-1}^{(i)})\right] d\lambda, \tag{5.14}$$

$$\Sigma_l^{(i)} = \Sigma_{l-1}^{(i)} + \int_{\lambda_{l-1}}^{\lambda_l} \left[C(\mathrm{x}_{l-1}^{(i)})\Sigma_{l-1}^{(i)} + \Sigma_{l-1}^{(i)} C^T(\mathrm{x}_{l-1}^{(i)})\right] d\lambda + \int_{\lambda_{l-1}}^{\lambda_l} D(\mathrm{x}_{l-1}^{(i)}) d\lambda. \tag{5.15}$$

  - Compute normalised mixture weights as

$$w_{m,k}^{(i)} \propto w_{m,k-1}^{(i)} \int p\left(\mathrm{y}_k | \mathrm{x}_k'\right) p_i\left(\mathrm{x}_k' | \mathrm{y}_{1:k-1}\right) d\mathrm{x}_k'.$$

  - Set $\mathrm{x}_k^{(i)} = \mathrm{x}_{l=L}^{(i)}$, $\mu_{m,k}^{(i)} = \mu_{l=L}^{(i)}$, $\Sigma_{m,k}^{(i)} = \Sigma_{l=L}^{(i)}$.

Optional step

- Resample particles and mixture components by the *Algorithm 2* if the effective number of mixands is smaller than a threshold:

$$ENM = \left(\sum_{i=1}^{N} w_{m,k}^{(i)\,2}\right)^{-1} < N_{\text{threshold}}.$$

Algorithm 2 Resampling for the SPF-GS

Initialisation

- Construct the empirical cumulative distribution function

$$c_m(i) = \sum_{n=1}^{i} w_m^{(i)}, \quad i = 1, \ldots, N.$$

Steps

- For all particles and mixture components $i = 1, \ldots, N$,
  - Draw a sample from the uniform distribution in $(0, 1]$: $\mathrm{u}^{(i)} \sim \mathrm{U}(0, 1]$;
  - Obtain the corresponding index from the inverse of the cumulative distribution function as

$$j(i) = c_m^{-1}(\mathrm{u}^{(i)}) \,|\, c_m^{-1}(u) = j \text{ if } u \in (c_m(j-1), c_m(j)].$$

- Set $\mathrm{x}^{*(i)} = \mathrm{x}^{(j(i))}$, $\mu_m^{*(i)} = \mu_m^{(j(i))}$, $\Sigma_m^{*(i)} = \Sigma_m^{(j(i))}$.
- Replace original particles and mixture components by the resampled ones:

$$\left\{\mathrm{x}^{(i)}, w_m^{(i)}, \mu_m^{(i)}, \Sigma_m^{(i)}\right\} \coloneqq \left\{\mathrm{x}^{*(i)}, w_m^{*(i)}, \mu_m^{*(i)}, \Sigma_m^{*(i)}\right\}.$$

SPF-GS is much less vulnerable to the collapsing phenomenon for two main reasons: (i) the mixands are guided by propagated companion samples that are spread over the state space upon a spatially structured concentration (histogram) describing the posterior density; (ii) the filtering of each mixand is highly dependent on the local curvature of the posterior density in the neighbourhood of its companion sample, which is clearly observable from the expressions (4.19) and (5.7). The general effect stemming from those facts is that the SPF-GS produces a very heterogeneous population of mixands, which are highly dependent on the local properties of the target posterior density.

Despite the SPF-GS being robust to the collapsing of the mixands, it is prone to situations where the sampling process lead to a set of outliers, causing some filtered mixture components to have small weights and to be irrelevant to the global approximation of the posterior density. Although this circumstance per se does not degrade the quality of the density approximation noticeably, it affects crucially the effectiveness of the sampling process for the subsequent filtering cycle. In that situation, the outliers from one cycle will drive their following samples to become even worst after few sampling steps of the next cycle. Moreover, in filtering problems prone to the appearance of sampling outliers, as a natural consequence of the diffusion dynamics, the population of outliers tends to increase as the sequential filtering progresses.

In order to cope with this problem, we advocate a resampling algorithm equivalent to the multinomial resampling, intended to remove the outliers (samples and mixands) and replicate the samples and mixands with probability proportional to the weights of the mixture components. The resampling algorithm for the SPF-GS is presented in the frame *Algorithm 2*.

6 Stochastic particle flow as a marginal particle filter

In this section we derive a marginal particle filter that relies on a proposal density built as a Gaussian mixture by means of the stochastic particle flow. The resulting filter is referred to as the

stochastic-particle-flow marginal particle filter (SPF-MPF).

6.1 Marginal particle filtering

In the standard setting particle filters don't target the marginal filtering distribution $p(\mathrm{x}_k|\mathrm{y}_{1:k})$, a characteristic stemming from the origins of these filters, which were designed to be relatively simple to implement. The main problem with the standard particle filters then arises because they construct importance densities that target the joint filtering density $p(\mathrm{x}_{0:k}|\mathrm{y}_{1:k})$. A typical particle filter incrementally draws *path* samples $\{\mathrm{x}_{0:k}^{(i)} \in \mathcal{X}^{k+1} : i = 1, \ldots, N\}$ from a joint importance density $q(\mathrm{x}_{0:k}|\mathrm{y}_{1:k})$ and ignores the past of the sampled paths $\{\mathrm{x}_{0:k-1}^{(i)} \in \mathcal{X}^k\}$ in order to compute the filtering expectations of interest. Thus, despite these algorithms provide a simple way to perform the measurement update, they perform importance sampling in the joint space over all time steps $\mathcal{X}^{k+1} = \mathcal{X}(0) \times \mathcal{X}(1) \times \cdots \times \mathcal{X}(k)$. The result is the precipitation of the degeneracy phenomenon: the set of paths become increasingly sparse on the joint space, leading to a quick increase in the variance of the importance weights so that most paths have vanishingly small probability. In high-dimensional applications this problem becomes even more pronounced, rendering the standard particle filters to be practically infeasible.

With the mindset of improving this crucial shortcoming of particle filters, Klaas *et al.* [74] proposed the marginal particle filter. The marginal particle filter targets the posterior distribution $p(\mathrm{x}_k|\mathrm{y}_{1:k})$, performing importance sampling directly on the marginal state space $\mathcal{X}(k)$ that is commensurate at all time steps. The samples are drawn from an importance density of the form

$$q(\mathrm{x}_k|\mathrm{y}_{1:k}) \propto \int_{\mathcal{X}} q(\mathrm{x}_k|\mathrm{x}_{k-1}, \mathrm{y}_k)\, q(\mathrm{x}_{k-1}|\mathrm{y}_{1:k-1})\, d\mathrm{x}_{k-1}, \tag{6.1}$$

to target the posterior density

$$p(\mathrm{x}_k|\mathrm{y}_{1:k}) \propto p(\mathrm{y}_k|\mathrm{x}_k) \int_{\mathcal{X}} p(\mathrm{x}_k|\mathrm{x}_{k-1})\, p(\mathrm{x}_{k-1}|\mathrm{y}_{1:k-1})\, d\mathrm{x}_{k-1}, \tag{6.2}$$

with the importance weights

$$w(\mathrm{x}_k) \propto \frac{p(\mathrm{x}_k|\mathrm{y}_{1:k})}{q(\mathrm{x}_k|\mathrm{y}_{1:k})}. \tag{6.3}$$

In practical terms, the particles and importance weights of one iteration are used to compose both an approximation for the target density (6.2) and the importance density (6.1) in order to obtain the particles and weights for the next iteration. Even though the marginal particle filter is more robust against degeneracy than the standard particle filters, and so more suitable to high-dimensional problems in principle, its success is highly dependent on the validity of the sequential representation of the target density. Problems may arise in situations where the usual approximation

$$\hat{p}(\mathrm{x}_k|\mathrm{y}_{1:k}) \propto p(\mathrm{y}_k|\mathrm{x}_k) \sum_{i=1}^{N} w_{k-1}^{(i)} p(\mathrm{x}_k|\mathrm{x}_{k-1}^{(i)}), \tag{6.4}$$

is prone to relevant statistical and numerical errors, e.g., when the transition density $p(\mathrm{x}_k|\mathrm{x}_{k-1})$ describes a Markov process with small variance and the observation y_k lies relatively far on the space from the current set of particles $\{\mathrm{x}_{k-1}^{(i)}, \mathrm{w}_{k-1}^{(i)}\}$ (see the linear, univariate example in Section 7). Moreover, owing to the curse of dimensionality, the usual approximation (6.4) is corrupted by a Monte Carlo error that increases exponentially with the number of state dimensions, which cripples the marginal particle filter to solve very high-dimensional problems. Because of this limitation, the marginal particle filters are likely to be suitable for only moderately high-dimensional problems. We illustrate these limitations of the marginal particle filter by examples in the Section 7.

As well explored in [74], there exist several possibilities to choose the marginal importance density (6.1), but the auxiliary marginal proposal density is particularly interesting because it emulates an optimal importance density, in the sense of minimising the variance of the weights. The marginal optimal (auxiliary) proposal density is constructed as

$$q\left(\mathrm{x}_k|\mathrm{y}_{1:k}\right) = \sum_{i=1}^{N} w_{q,k-1}^{(i)} p(\mathrm{x}_k|\mathrm{x}_{k-1}^{(i)}, \mathrm{y}_k), \tag{6.5}$$
$$w_{q,k-1}^{(i)} \propto w_{k-1}^{(i)} p(\mathrm{y}_k|\mathrm{x}_{k-1}^{(i)}).$$

It is straightforward to verify that the marginal optimal proposal implies weights that never change:

$$\begin{aligned} w_k &\propto \frac{\hat{p}\left(\mathrm{x}_k|\mathrm{y}_{1:k}\right)}{q\left(\mathrm{x}_k|\mathrm{y}_{1:k}\right)} \propto \frac{p(\mathrm{y}_k|\mathrm{x}_k)\sum_{i=1}^{N} w_{k-1}^{(i)} p(\mathrm{x}_k|\mathrm{x}_{k-1}^{(i)})}{\sum_{i=1}^{N} w_{q,k-1}^{(i)} p(\mathrm{x}_k|\mathrm{x}_{k-1}^{(i)}, \mathrm{y}_k)} \\ &\propto \frac{p(\mathrm{y}_k|\mathrm{x}_k)\sum_{i=1}^{N} w_{k-1}^{(i)} p(\mathrm{x}_k|\mathrm{x}_{k-1}^{(i)})}{\sum_{i=1}^{N} w_{k-1}^{(i)} p(\mathrm{y}_k|\mathrm{x}_{k-1}^{(i)}) \cdot \frac{p(\mathrm{y}_k|\mathrm{x}_k)p(\mathrm{x}_k|\mathrm{x}_{k-1}^{(i)})}{p(\mathrm{y}_k|\mathrm{x}_{k-1}^{(i)})}} \\ &= \text{constant}. \end{aligned}$$

This feature is crucial because it endows a particle filter with low variance of weights, which essentially turns into statistical efficiency. This finding motivates the marginal optimal proposal density as the foundation for a marginal particle filter based on the stochastic flow for moderately high-dimensional problems.

6.2 Difficulties from a standard marginal importance density

This subsection is intended to discuss the problems that naturally arise when considering a standard Monte Carlo setting as (5.1) to build a marginal importance density based on the stochastic flow. If one regards the proposal distribution as the result of a sequence of L Markov transitions through a discretisation of the interval $0 < \lambda \leq T$ onto the sub-intervals $\{\lambda_0 = 0, \lambda_1, \ldots \lambda_l, \ldots, \lambda_L = T\}$, where $\mathrm{x}_k \triangleq \mathrm{x}_L$ and $\mathrm{x}_{k-1} \triangleq \mathrm{x}_0$, then the succession of transitions would provide an importance density as

$$\begin{aligned} q\left(\mathrm{x}_k|\mathrm{y}_{1:k}\right) = \int_{\mathcal{X}}\int_{\mathcal{X}}\cdots\int_{\mathcal{X}} & q(\mathrm{x}_L|\mathrm{x}_{L-1}, \mathrm{y}_k) q(\mathrm{x}_{L-1}|\mathrm{x}_{L-2}, \mathrm{y}_k)\cdots \\ & q(\mathrm{x}_1|\mathrm{x}_0, \mathrm{y}_k) q(\mathrm{x}_0|\mathrm{y}_{1:k-1}) d\mathrm{x}_{L-1} d\mathrm{x}_{L-2}\ldots d\mathrm{x}_0. \end{aligned} \tag{6.6}$$

In order to evaluate this importance density over a set of N particles, incorporating the previous set of samples and importance weights, one would be required to compute

$$q(\mathrm{x}_k^{(i)}|\mathrm{y}_{1:k}) = \sum_{j=1}^{N} w_{k-1}^{(j)} q(\mathrm{x}_k^{(i)}|\mathrm{x}_{k-1}^{(j)}, \mathrm{y}_k); \tag{6.7}$$
$$i = 1, \ldots, N.$$

This implementation depends on the set of conditional densities $q(\mathrm{x}_k|\mathrm{x}_{k-1}, \mathrm{y}_k)$ that could be achieved in terms of a recursion of the form

$$w_1^{(i|j)} \triangleq q(\mathrm{x}_1^{(i)}|\mathrm{x}_0^{(j)}, \mathrm{y}_k); \quad i, j = 1, \ldots, N; \tag{6.8}$$
$$w_2^{(i|j)} \triangleq q(\mathrm{x}_2^{(i)}|\mathrm{x}_0^{(j)}, \mathrm{y}_k) = \sum_{n=1}^{N} w_1^{(n|j)} q(\mathrm{x}_2^{(i)}|\mathrm{x}_1^{(n)}, \mathrm{x}_0^{(j)}, \mathrm{y}_k);$$
$$\vdots$$
$$w_l^{(i|j)} \triangleq q(\mathrm{x}_l^{(i)}|\mathrm{x}_0^{(j)}, \mathrm{y}_k) = \sum_{n=1}^{N} w_{l-1}^{(n|j)} q(\mathrm{x}_l^{(i)}|\mathrm{x}_{l-1}^{(n)}, \mathrm{x}_0^{(j)}, \mathrm{y}_k);$$

where $q(\mathrm{x}_l|\mathrm{x}_{l-1}, \mathrm{x}_0, \mathrm{y}_k)$ are the one-step Markov transition densities conditioned on the initial state (prior samples), which are directly available from the discretised version of (4.15). Besides the high complexity involved in computing the conditional probability densities (6.8), which is bounded by $\mathrm{O}\left((L-1)N^3 + N^2\right)$ evaluations, the main complication of this realisation is due to the mixing properties of (6.7) that encompass significant errors built up through the sequence of finite-sample approximations along with the prohibitively high variance of the resulting importance weights.

Whilst these problems could be tentatively worked around by a judicious choice of a variance reduction method, it is worth looking how the implementation difficulties would turn out to be by evoking the hypothetical continuity over the sampling steps. It is well known that in the limit $\Delta\lambda \to 0$, the proposal density (6.6) defines a path integral. Based on the definition of the path probability density of a Markov process [75]

$$W_\infty\left[\mathrm{x}\left(\lambda\right)\right]\left[d\mathrm{x}\right] \propto e^{-\int_0^T \left[\frac{1}{2}(\dot{\mathrm{x}}-\mu(\mathrm{x}))^T D^{-1}(\dot{\mathrm{x}}-\mu(\mathrm{x}))+\frac{1}{2}\nabla_{\mathrm{x}}\cdot\mu(\mathrm{x})\right]d\lambda}, \tag{6.9}$$

for particles describing continuous paths, the proposal should be written as a functional integral of the form [76]

$$q_c\left(\mathrm{x}_k|\mathrm{y}_{1:k}\right) \propto \int e^{-\int_0^T \left[\frac{1}{2}(\dot{\mathrm{x}}-\mu(\mathrm{x}))^T D^{-1}(\dot{\mathrm{x}}-\mu(\mathrm{x}))+\frac{1}{2}\nabla_{\mathrm{x}}\cdot\mu(\mathrm{x})\right]d\lambda}\left[d\mathrm{x}\right], \tag{6.10}$$

where $[d\mathrm{x}] = d\mathrm{x}_{L-1}\ldots d\mathrm{x}_0$ as $\Delta\lambda \to 0$. Solving path integrals in general is a daunting task, nevertheless, a density of interest could be approximately integrated if formulated as a mixture of Gaussians, under the assumption of local Gaussianity. Within this framework, an ensemble of independently selected Gaussian densities can be analytically integrated to achieve local solutions to (6.10). This crucial idea is exactly what the stochastic flow proposes when the filtering solution is formulated as the mixture (5.2).

6.3 The stochastic-particle-flow marginal particle filter

In marginal particle filtering, the best importance density one could construct in general is the proposal density (6.1) that infers an approximation to the actual posterior pdf. Composing the marginal optimal proposal requires computing $p(\mathrm{y}_k|\mathrm{x}_{k-1}^{(i)})$ exactly, which is not possible in general. In addition, the same scenarios that cause considerable errors in the computation of the empirical target $\hat{p}\left(\mathrm{x}_k|\mathrm{y}_{1:k}\right)$ (6.4) will also affect the evaluation of the proposal (6.5), as illustrated by the first example in Section 7. In these cases, one can benefit from the inherent characteristics of the stochastic flow to construct a proposal density with better regularity properties by doing

$$\begin{aligned}
q\left(\mathrm{x}_k|\mathrm{y}_{1:k}\right) &= \sum_{i=1}^{N} w_{k-1}^{(i)} p(\mathrm{y}_k|\mathrm{x}_k) p(\mathrm{x}_k|\mathrm{x}_{k-1}^{(i)}) \\
&= \sum_{i=1}^{N} w_{k-1}^{(i)} \frac{p(\mathrm{x}_k|\mathrm{x}_{k-1}^{(i)})}{p_i(\mathrm{x}_k|\mathrm{y}_{1:k-1})} p(\mathrm{y}_k|\mathrm{x}_k) p_i(\mathrm{x}_k|\mathrm{y}_{1:k-1}) \\
&\propto \sum_{i=1}^{N} w_{k-1}^{(i)} \frac{p(\mathrm{x}_k|\mathrm{x}_{k-1}^{(i)})}{p_i(\mathrm{x}_k|\mathrm{y}_{1:k-1})} w_{m,k}^{(i)} \mathcal{N}(\mathrm{x}_k; \mu_{m,k}^{(i)}, \Sigma_{m,k}^{(i)}), \\
q\left(\mathrm{x}_k|\mathrm{y}_{1:k}\right) &= \sum_{i=1}^{N} w_q^{(i)}(\mathrm{x}_k) \mathcal{N}(\mathrm{x}_k; \mu_{m,k}^{(i)}, \Sigma_{m,k}^{(i)});
\end{aligned} \tag{6.11}$$

where

$$\tilde{w}_q^{(i)}(\mathrm{x}_k) = w_{k-1}^{(i)} w_{m,k}^{(i)} \frac{p(\mathrm{x}_k|\mathrm{x}_{k-1}^{(i)})}{p_i(\mathrm{x}_k|\mathrm{y}_{1:k-1})}, \tag{6.12}$$

$$w_q^{(i)}(\mathrm{x}_k) = \frac{\tilde{w}_q^{(i)}(\mathrm{x}_k)}{\sum_{i=1}^{N} \tilde{w}_q^{(i)}(\mathrm{x}_k)}; \tag{6.13}$$

and $p_i(\mathrm{x}_k|\mathrm{y}_{1:k-1})$ is given by (5.12). This formulation evokes the stochastic flow to guide an accurate approximation to the marginal optimal proposal density. Similarly to the SPF-GS, from a previous set of samples and parameters $\{\mathrm{x}_{k-1}^{(i)}, w_{k-1}^{(i)}, w_{m,k-1}^{(i)}, \mu_{m,k-1}^{(i)}, \Sigma_{m,k-1}^{(i)}\}$, where $w_{k-1}^{(i)}$ are importance weights, the marginal particle filter integrates the SDE (4.15) for each particle and propagates the associated parameters through the interval $0 < \lambda \leq T$, to acquire the samples and parameters that compose the proposal density and enable filtering: $\{\mathrm{x}_k^{(i)}, w_k^{(i)}, w_{m,k}^{(i)}, \mu_{m,k}^{(i)}, \Sigma_{m,k}^{(i)}\}$. The mixture component moments are evolved in accordance with equations (5.5) and (5.6), the mixture weights are computed by equation (5.11), and the importance weights are updated by

$$w_k(\mathrm{x}_k) \propto \frac{\sum_{j=1}^{N} w_{k-1}^{(j)} p(\mathrm{y}_k|\mathrm{x}_k) p(\mathrm{x}_k|\mathrm{x}_{k-1}^{(j)})}{\sum_{j=1}^{N} w_q^{(j)}(\mathrm{x}_k) \mathcal{N}(\mathrm{x}_k; \mu_{m,k}^{(j)}, \Sigma_{m,k}^{(j)})}. \tag{6.14}$$

The resulting filter is called the stochastic-particle-flow marginal particle filter (SPF-MPF). It is worth noting that a simpler alternative to (6.11) could be chosen by considering

$$q\left(\mathrm{x}_k|\mathrm{y}_{1:k}\right) = \sum_{i=1}^{N} w_{m,k}^{(i)} \mathcal{N}(\mathrm{x}_k; \mu_{m,k}^{(i)}, \Sigma_{m,k}^{(i)}), \tag{6.15}$$

however, in that case, the importance density would not be affected by the same errors as the empirical target $\hat{p}\left(\mathrm{x}_k|\mathrm{y}_{1:k}\right)$ (6.4) because each component in (6.15) targets a local instance of the posterior density itself. As a result, even though the importance density could approximate the true posterior density accurately, it would not directly approach the target density. In situations where the approximated target density $\hat{p}\left(\mathrm{x}_k|\mathrm{y}_{1:k}\right)$ cannot represent the true posterior density as well as a mixture of the form (6.15), the SPF-MPF with such a proposal would fail because of the mismatch arising from the distinctions in the approximation methods. As a consequence, the importance weights would have infeasibly high variance. The described issue is equivalent to treat the errors in the standard empirical measure (5.1) as comparable to the errors in the mixture measure (5.3), which is not true except for few cases. This scenario is well illustrated by two examples in Section 7.

The stochastic-particle-flow marginal particle filter is summarised in the frame *Algorithm 3*.

7 Examples

In this section we present some illustrative toy examples and experimental results for two instructive applications for the multi-sensor multi-target tracking community: a multi-sensor bearing-only problem and a convoy tracking problem.

In the experimental results for the multi-sensor and multi-target examples, we compared the SPF-GS against standard multi-target trackers and extensions to two of the most effective particle flows, namely, the Gaussian particle flow (GPF) and the scaled-drift particle flow (SDPF). The former was first called *exact particle flow* in [43] and the latter was first called *non-zero diffusion particle flow* in [49], however, it is actually a particle flow with the drift scaled by a diffusion coefficient, but the filter itself is not a diffusion.

It is important to mention that, in order to work properly, both the Gaussian particle flow and the scaled-drift particle flow rely on a companion filter to estimate the covariance matrix correctly. These implementation details have been explicitly presented by Choi *et al.* [54] and Ding & Coates [55], that advocate the use of either the EKF or UKF as a companion filter to estimate the associated covariance matrices. In contrast, the stochastic particle flow does not require any auxiliary filter to estimate higher-order moments, relying solely on its own empirical Monte Carlo measure.

For the toy examples the companion filter was not necessary for the original particle flows since a single filtering cycle has been analysed. For the multi-sensor and multi-target examples we adopted baseline filters, which are the most structurally similar to the EKF, as companion filters for the original particle flows.

Algorithm 3 Stochastic-particle-flow marginal particle filter

Initialisation

- Generate the initial set of samples, importance weights and mixture parameters $\{\mathrm{x}_0^{(i)}, w_0^{(i)}, w_{m,0}^{(i)}, \mu_{m,0}^{(i)}, \Sigma_{m,0}^{(i)}\}_{i=1}^N$ as

$$\mathrm{x}_0^{(i)} \sim p(\mathrm{x}_0),\ w_0^{(i)} = N^{-1},$$

$$w_{m,0}^{(i)} = N^{-1},\ \mu_{m,0}^{(i)} = \mathbb{E}_{\mathrm{x}_0}\left[\mathrm{x}_0\right],\ \Sigma_{m,0}^{(i)} = \mathbb{E}_{\mathrm{x}_0}\left[(\mathrm{x}_0 - \bar{\mathrm{x}}_0)(\mathrm{x}_0 - \bar{\mathrm{x}}_0)^T\right].$$

Steps $k = 1, \ldots, T_f$

- Compute the time horizon T (4.25) and the step size $\Delta\lambda$ (4.26)
- Discretise the interval $0 \leq \lambda \leq T$ into L sub-intervals

$$\{\lambda_0 = 0,\ \lambda_1, \ldots \lambda_l, \ldots,\ \lambda_L = T\}$$

- For all particles and mixture components $i = 1, \ldots, N$,
  - Set $\mathrm{x}_{l=0}^{(i)} = \mathrm{x}_{k-1}^{(i)}$, $\mu_{l=0}^{(i)} = \mu_{m,k-1}^{(i)}$, $\Sigma_{l=0}^{(i)} = 0_{n_x \times n_x}$
  - Propagate samples by simulating from the diffusion
    - For $l = 1, \ldots, L$, propagate each particle, mixture component mean and covariance using equations (5.13), (5.14), and (5.15).
  - Compute normalised mixture weights as

$$w_{m,k}^{(i)} \propto w_{m,k-1}^{(i)} \int p\left(\mathrm{y}_k|\mathrm{x}_k'\right) p_i\left(\mathrm{x}_k'|\mathrm{y}_{1:k-1}\right) d\mathrm{x}_k'.$$

  - Set $\mathrm{x}_k^{(i)} = \mathrm{x}_{l=L}^{(i)}$, $\mu_{m,k}^{(i)} = \mu_{l=L}^{(i)}$, $\Sigma_{m,k}^{(i)} = \Sigma_{l=L}^{(i)}$.
  - Compute importance weights as

$$w_k^{(i)} \propto \frac{\sum_{j=1}^N w_{k-1}^{(j)} p(\mathrm{y}_k|\mathrm{x}_k^{(i)}) p(\mathrm{x}_k^{(i)}|\mathrm{x}_{k-1}^{(j)})}{\sum_{j=1}^N w_q^{(j)}(\mathrm{x}_k^{(i)}) \mathcal{N}(\mathrm{x}_k^{(i)}; \mu_{m,k}^{(j)}, \Sigma_{m,k}^{(j)})}.$$

Optional step

- Resample particles and mixture components if the effective sample size is smaller than a threshold.

7.1 Toy examples

The toy examples are Gaussian processes chosen to demonstrate the properties of the stochastic particle flow methods, summarised as

- Univariate
  - linear,
  - quadratic,
  - cubic;
- Bivariate
  - multimodal, linear,
  - nonlinear (banana-shaped pdf).

In all cases, we analyse the filters for a single filtering cycle. We generally describe the state process, the observation process and the initial proposal distribution for these examples as

$$\mathrm{x}_k = f(\mathrm{x}_{k-1}) + \mathrm{u}_k,\ \mathrm{u}_k \sim \mathcal{N}(\mathrm{u}_k; 0, Q_k), \tag{7.1}$$

$$\mathrm{y}_k = h(\mathrm{x}_k\ \ ) + \mathrm{v}_k,\ \mathrm{v}_k \sim \mathcal{N}(\mathrm{v}_k; 0, R_k), \tag{7.2}$$

$$p_0(\mathrm{x}_{k-1}) = \mathcal{N}(\mathrm{x}_{k-1}; \bar{\mathrm{x}}_{k-1}, P_{k-1}). \tag{7.3}$$

For these toy examples, we considered for comparison four different types of particle filters based on the marginal importance density

$$q\left(\mathrm{x}_k|\mathrm{y}_{1:k}\right) = \sum_{i=1}^{N} w_{k-1}^{(i)} q(\mathrm{x}_k|\mathrm{x}_{k-1}^{(i)}, \mathrm{y}_k),$$

where

- for the marginal bootstrap particle filter (MBPF), the local components are the Markov transition pdf: $q(\mathrm{x}_k|\mathrm{x}_{k-1}^{(i)}, \mathrm{y}_k) = p(\mathrm{x}_k|\mathrm{x}_{k-1}^{(i)})$;
- for the marginal EKF-based particle filter (MEPF), the local components are computed by the EKF: $q(\mathrm{x}_k|\mathrm{x}_{k-1}^{(i)}, \mathrm{y}_k) = p_{\mathrm{EKF}}(\mathrm{x}_k|\mathrm{x}_{k-1}^{(i)}, \mathrm{y}_k)$;
- for the marginal UKF-based particle filter (MUPF), the local components are computed by the UKF: $q(\mathrm{x}_k|\mathrm{x}_{k-1}^{(i)}, \mathrm{y}_k) = p_{\mathrm{UKF}}(\mathrm{x}_k|\mathrm{x}_{k-1}^{(i)}, \mathrm{y}_k)$; and
- for the marginal (optimal) auxiliary particle filter (MAPF) [74], the importance density is given by (6.5).

In addition, we include in the comparison the evaluation of the empirical marginal target $\hat{p}\left(\mathrm{x}_k|\mathrm{y}_{1:k}\right)$ defined by (6.4). For all filters, when applicable, we calculate the average of the effective sample size

$$\mathrm{ESS} = \left(\sum_{i=1}^{N} w_k^{(i)\,2}\right)^{-1} \tag{7.4}$$

over 100 Monte Carlo runs, for 1000 particles. For all marginal proposal densities, we analyse their similiarity to the true posterior probability density by averaging their corresponding empirical Jensen-Shannon divergence with respect to the true posterior, which is obtained to high numerical precision. The Jensen-Shannon divergence is defined as

$$\mathrm{JSD}\left(P \parallel Q\right) = \frac{1}{2}\mathrm{D}_{\mathrm{KL}}(P \parallel \left(P+Q\right)/2) + \frac{1}{2}\mathrm{D}_{\mathrm{KL}}(Q \parallel \left(P+Q\right)/2), \tag{7.5}$$

where the Kullback–Leibler divergence is computed using the base-2 logarithm so that the Jensen-Shannon divergence is bounded as $0 \leq \mathrm{JSD}\left(P \parallel Q\right) \leq 1$. The Jensen-Shannon divergence is symmetric and equals zero when the compared densities are equal.

For the bivariate examples, we also consider the original particle flow methods, the Gaussian particle flow and scaled-drift particle flow, for which the Jensen-Shannon divergence with respect to the true posterior is evaluated based on empirical densities constructed by (bidimensional) histograms of the particles.

7.1.1 Linear, univariate model

The simplest example is a linear, univariate model, with the parameters shown in the table below.

Parameters for the linear, univariate model	
Initial distribution	$\bar{\mathrm{x}}_{k-1} = 0$, $P_{k-1} = 20$
Markov transition pdf	$f(\mathrm{x}_{k-1}) = \mathrm{x}_{k-1}$, $Q_k = 5$
Likelihood function	$h(\mathrm{x}_k) = \mathrm{x}_k$, $R_k = 10$
Observation	$\mathrm{y}_k = 30$

Although very simple, this example was proposed to demonstrate the scenario where the empirical marginal target (6.4) is prone to relevant statistical and numerical errors, by setting a situation where the transition density describes a Markov process with small variance and the observation lies relatively far from the initial distribution. In this scenario, the statistical inefficiency emerges because the observation provides little information on the space region where the state process is most likely to populate with probability masses at a significant density. Incidentally, this is also the main source of degeneracy in standard particle filters for low-dimensional problems. On the other hand, there may exist round-off errors when evaluating the empirical marginal target owing to the samples being located relatively far from the first moment, several standard deviations apart in the tail of each proposal component.

As depicted in Figure 7.1, the importance density established by the SPF-MPF (red x's) is successful at aiming the empirical marginal target (blue circles), generating a high effective sample size. However, as the empirical target constitutes a poor approximation to the true posterior pdf, the importance sampling clearly fails and the SPF-MPF leads to a solution excessively biased. In opposition, the direct filtering density generated by the SPF-GS approximates the true posterior pdf accurately, generating a satisfactory solution. These findings are quantified by the Jensen-Shannon divergences averaged over 100 Monte Carlo runs and presented in Table 1, which shows a neglible divergence between the density filtered by the SPF-GS and the true posterior while the divergences for the target density and for the importance density constructed by the SPF-MPF are significant.

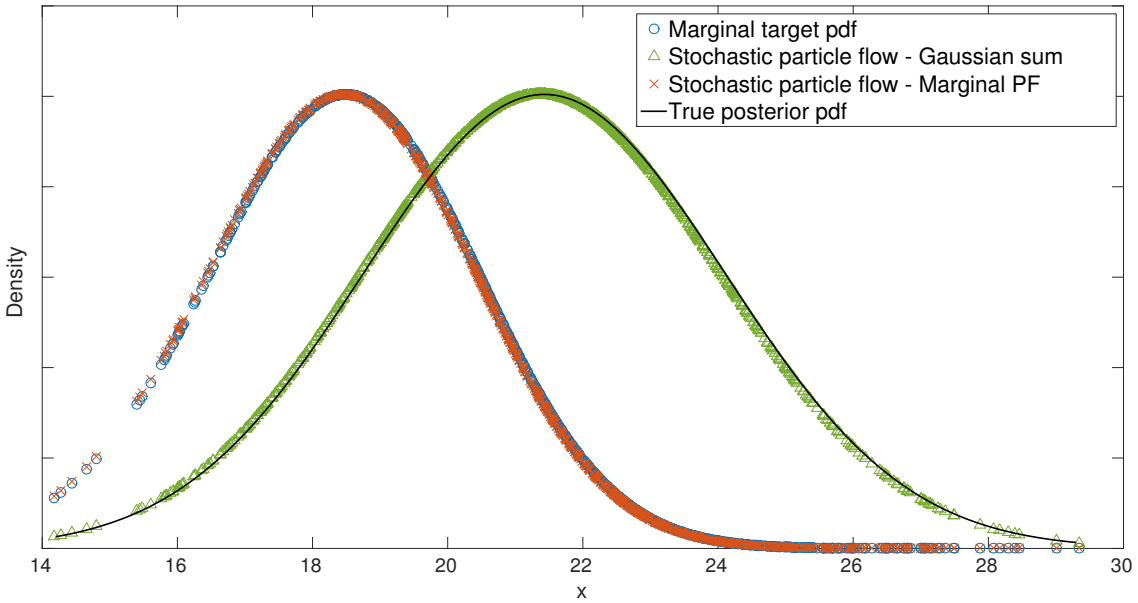

Figure 7.1: Densities generated by the SPF-GS and SPF-MPF for the linear, univariate example

7.1.2 Quadratic, univariate model

The quadratic, univariate model was tested with parameters shown in the following table. This model is particularly interesting because the nonlinearity of the observation process leads to bimodality of the filtered density.

Parameters for the quadratic, univariate model	
Initial distribution	$\bar{\mathrm{x}}_{k-1} = 0,\ P_{k-1} = 20$
Markov transition pdf	$f(\mathrm{x}_{k-1}) = \mathrm{x}_{k-1},\ Q_k = 20$
Likelihood function	$h(\mathrm{x}_k) = \mathrm{x}_k^2/20,\ R_k = 50$
Observation	$\mathrm{y}_k = 30$

This example was set to be favorable for marginal importance sampling so that it is possible to compare different marginal particle filters against the SPF-MPF for this nonlinear model. In addition, the original particle flows are compared to the SPF-MPF as well. The quantified performances of these filters for the quadratic univariate model are shown in Table 1.

Firstly, we compare the sequence of histograms achieved by propagating samples for the Gaussian particle flow, the scaled-drift particle flow and the stochastic particle flow. As it can be seen in Figure 7.2, the stochastic particle flow provides the best distribution of particles to approximate the posterior density, denoting a higher level of accuracy and regularity of the flow approximation as a diffusion for this example.

Regarding the marginal importance densities illustrated in Figure 7.3, we observe a high degree of similarity of the SPF-MPF proposal density to the marginal target density. In the same manner, the filtering density achieved by the SPF-GS accurately approximates the true posterior density, as shown in Table 1. In Figure 7.4 we can see in detail the proximity of the SPF-MPF proposal density to both the marginal target density and to the true posterior density, along with some of the proposal mixture components (unweighted). The density proposed by the marginal (optimal) auxiliary particle filter is also very similar to the marginal target, providing an accurate solution, whereas all other filters propose densities less effective for this example. These observations are quantitatively captured by the performance data summarised in Table 1.

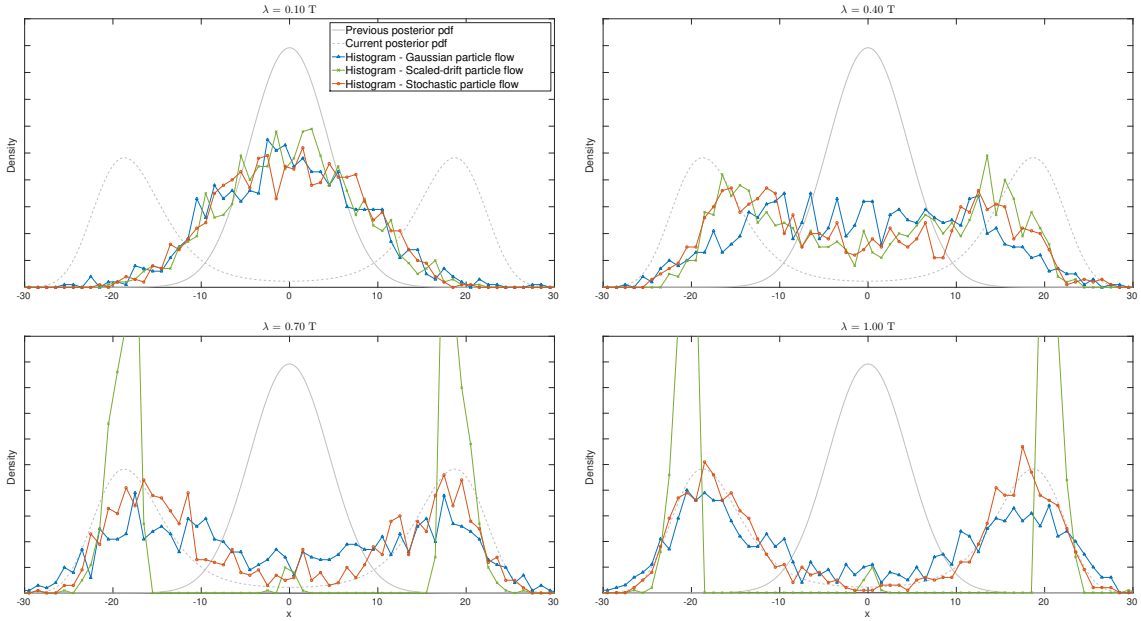

Figure 7.2: Sequence of histograms achieved by propagating particles for the quadratic, univariate example

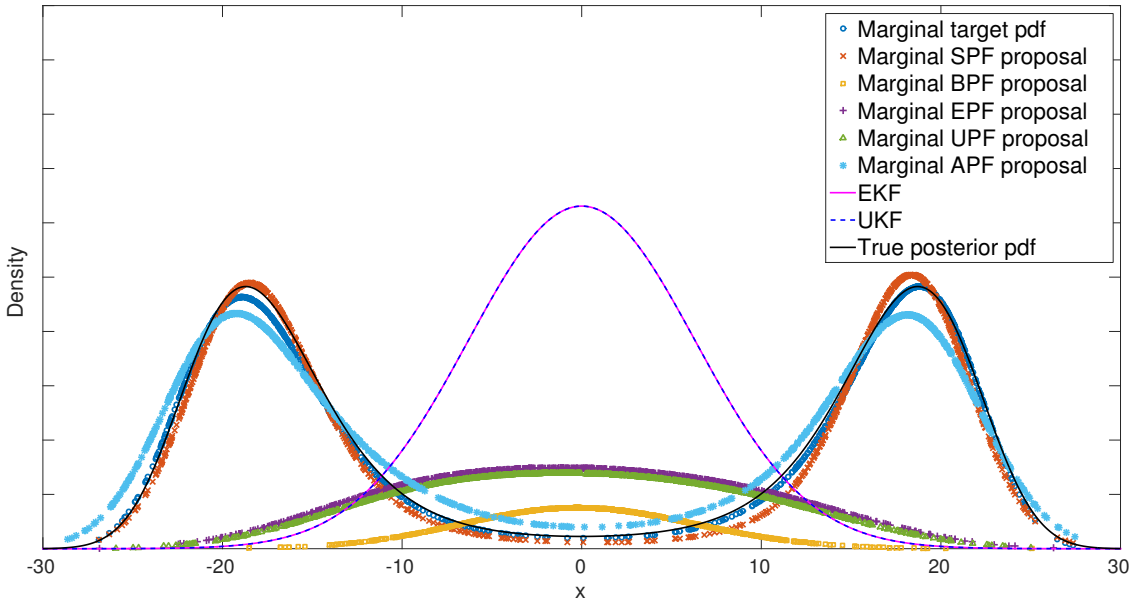

Figure 7.3: Comparison of proposal densities for the quadratic, univariate example

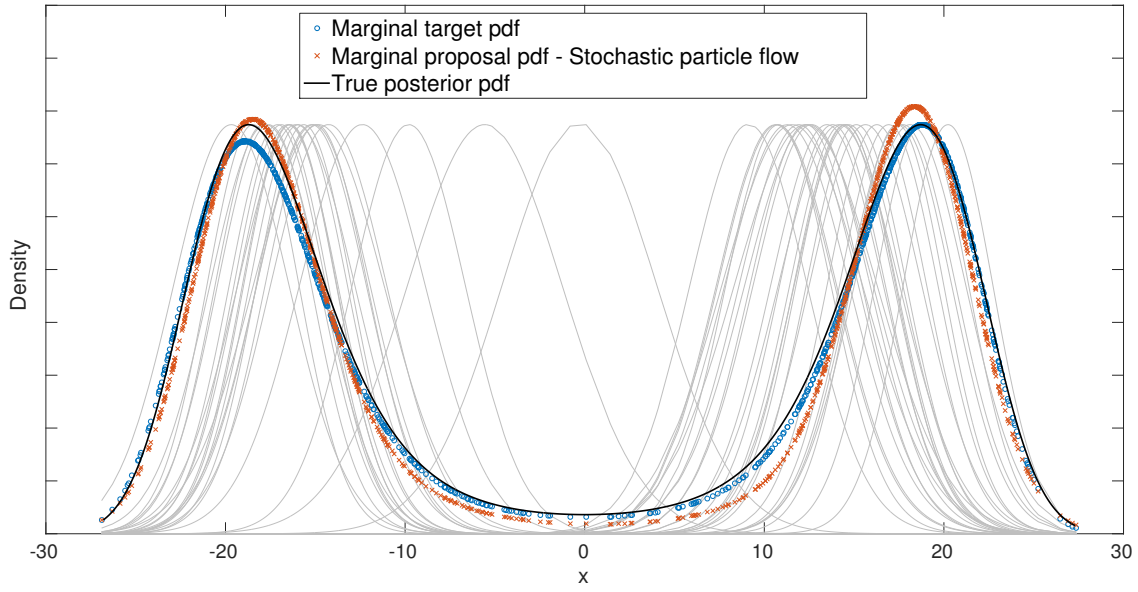

Figure 7.4: Marginal proposal density based on the stochastic particle flow

7.1.3 Cubic, univariate model

The cubic, univariate model was tested with parameters shown in the following table.

Parameters for the cubic, univariate model	
Initial distribution	$\bar{\mathrm{x}}_{k-1} = 0$, $P_{k-1} = 20$
Markov transition pdf	$f(\mathrm{x}_{k-1}) = \mathrm{x}_{k-1}$, $Q_k = 20$
Likelihood function	$h(\mathrm{x}_k) = \mathrm{x}_k^3/120$, $R_k = 50$
Observation	$\mathrm{y}_k = 20$

This example was also set to be favorable for marginal importance sampling, i.e., avoiding the scenario described in the first example where importance sampling fails.

By comparing the resulting histograms achieved by propagating samples for the Gaussian particle flow, the scaled-drift particle flow and the stochastic particle flow, it is remarkable in Figure 7.5 that the stochastic particle flow provides a fairly superior distribution of particles to approximate the posterior density. This superiority is extended to the importance density proposed by the SPF-MPF as can be seen in Figure 7.6. The importance density proposed by the marginal auxiliary particle filter also provides an accurate solution to the filtering problem, but it is slightly less effective than the SPF-MPF. The remaining marginal particle filters present less effective solutions. The comparison of all filters for this example is quantified in Table 1.

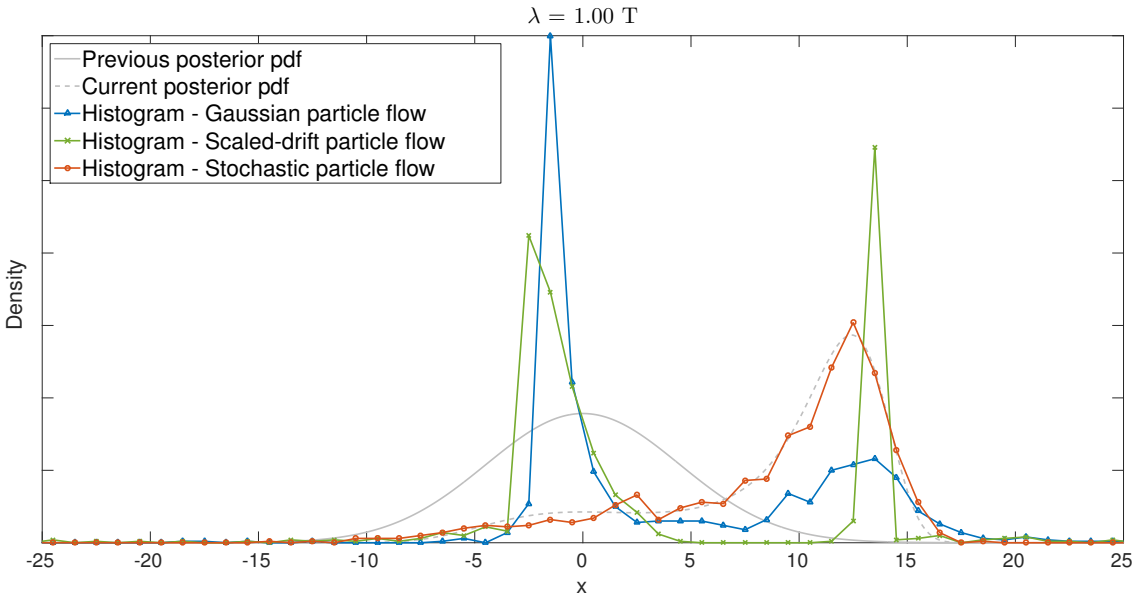

Figure 7.5: Resulting histograms of particles for the cubic, univariate example

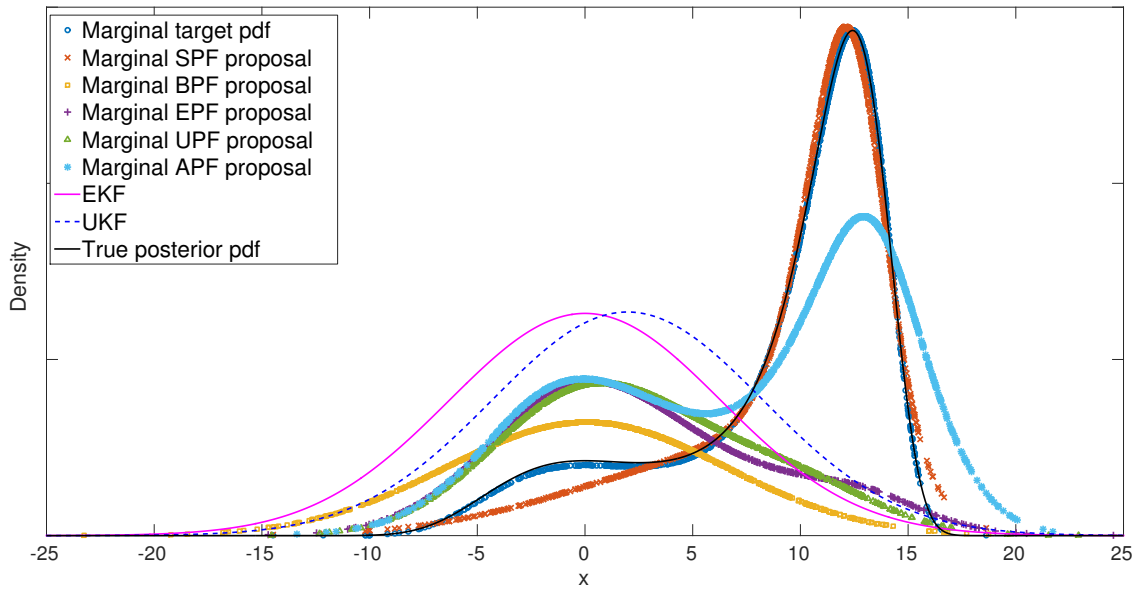

Figure 7.6: Comparison of proposal densities for the cubic, univariate example

7.1.4 Linear, bimodal, bivariate model

This example poses a bimodal model where the modes arise from two different observations with a joint likelihood explicitly known. We implemented a scheme of flowing the particles that selects the samples to be filtered for each of the modes according to a set of indexes that are sampled from a binomial distribution $B\left(u_1, u_2; 1, w_{l,(1)}, w_{l,(2)}\right) \propto w_{l,(1)}^{u_1} w_{l,(2)}^{u_2}$ where $u_1, u_2 \in [0, 1]$, $u_1 + u_2 = 1$,

Density	*Linear*		*Quadratic*		*Cubic*	
	JSD_{avg}	ESS_{avg}	JSD_{avg}	ESS_{avg}	JSD_{avg}	ESS_{avg}
Marginal target	0.2930	-	0.0037	-	0.0000	-
SPF-GS	0.0001	-	0.0052	-	0.0080	-
SPF-MPF	0.1477	99.89%	0.0050	96.97%	0.0020	94.13%
Marginal BPF	0.9875	0.24%	0.2667	1.79%	0.1735	12.69%
Marginal EPF	0.7861	2.02%	0.3093	17.26%	0.1803	28.72%
Marginal UPF	0.7853	1.98%	0.3112	14.80%	0.1664	25.42%
Marginal APF	0.0683	100.00%	0.0149	92.68%	0.0587	72.12%

Table 1: Comparison of densities for the univariate examples

such that the indexes are uniquely associated to u_1, u_2. The linear, bimodal, bivariate model was tested with parameters shown in Table 2. The parameters were chosen to result in quite distinct local properties between the two modes.

Parameters for the linear, bimodal, bivariate model	
Initial distribution	$\bar{\mathrm{x}}_{k-1} = \begin{pmatrix} 0 \\ 0 \end{pmatrix}$, $P_{k-1} = \begin{pmatrix} 9 & 0 \\ 0 & 9 \end{pmatrix}$
Markov transition pdf	$f(\mathrm{x}_{k-1}) = \mathrm{x}_{k-1}$, $Q_k = \begin{pmatrix} 16 & 0 \\ 0 & 16 \end{pmatrix}$
Likelihood function:	$h(\mathrm{x}_k) = \mathrm{x}_k$
Mode 1	$R_{k,(1)} = \begin{pmatrix} 0.8 & 0 \\ 0 & 0.2 \end{pmatrix}$, $w_{l,(1)} = 0.2$
Mode 2	$R_{k,(2)} = \begin{pmatrix} 4.0 & 0 \\ 0 & 1.0 \end{pmatrix}$, $w_{l,(2)} = 0.8$
Observations	$\mathrm{y}_{k,(1)} = \begin{pmatrix} +10 \\ +20 \end{pmatrix}$, $\mathrm{y}_{k,(2)} = \begin{pmatrix} +10 \\ -20 \end{pmatrix}$

Table 2: Parameters for the bimodal bivariate model

For this example, we solely analyse the stochastic particle flow methods, SPF-GS and SPF-MPF, against the original particle flow methods. We exemplify the sequence of particles' distributions acquired by the Gaussian particle flow, the scaled-drift particle flow and the stochastic particle flow in Figure 7.7, from which it becomes clear that the final distribution generated by the stochastic particle flow is highly similar to the true posterior density, precisely describing the local moments of the two modes. In opposition, the Gaussian particle flow generates a distribution that is excessively biased for the most peaky mode whereas the scaled-drift particle flow generates a distribution that does not describe correctly the local covariances for each mode.

These findings are quantified by the average Jensen-Shannon divergences presented in Table 5. The Table 5 shows a low divergence between the density filtered by the SPF-GS and the true posterior, a low divergence for the SPF-MPF proposal density as well as for the target density, whereas the divergences for the original particle flows are fairly high. The SPF-MPF provides a high effective sample size.

7.1.5 Nonlinear, unimodal, bivariate model

The nonlinear bivariate model was tested in two cases: 1) favorable for marginal particle filters, and 2) unfavorable, i.e., emulating a scenario similar to the one presented in the first example

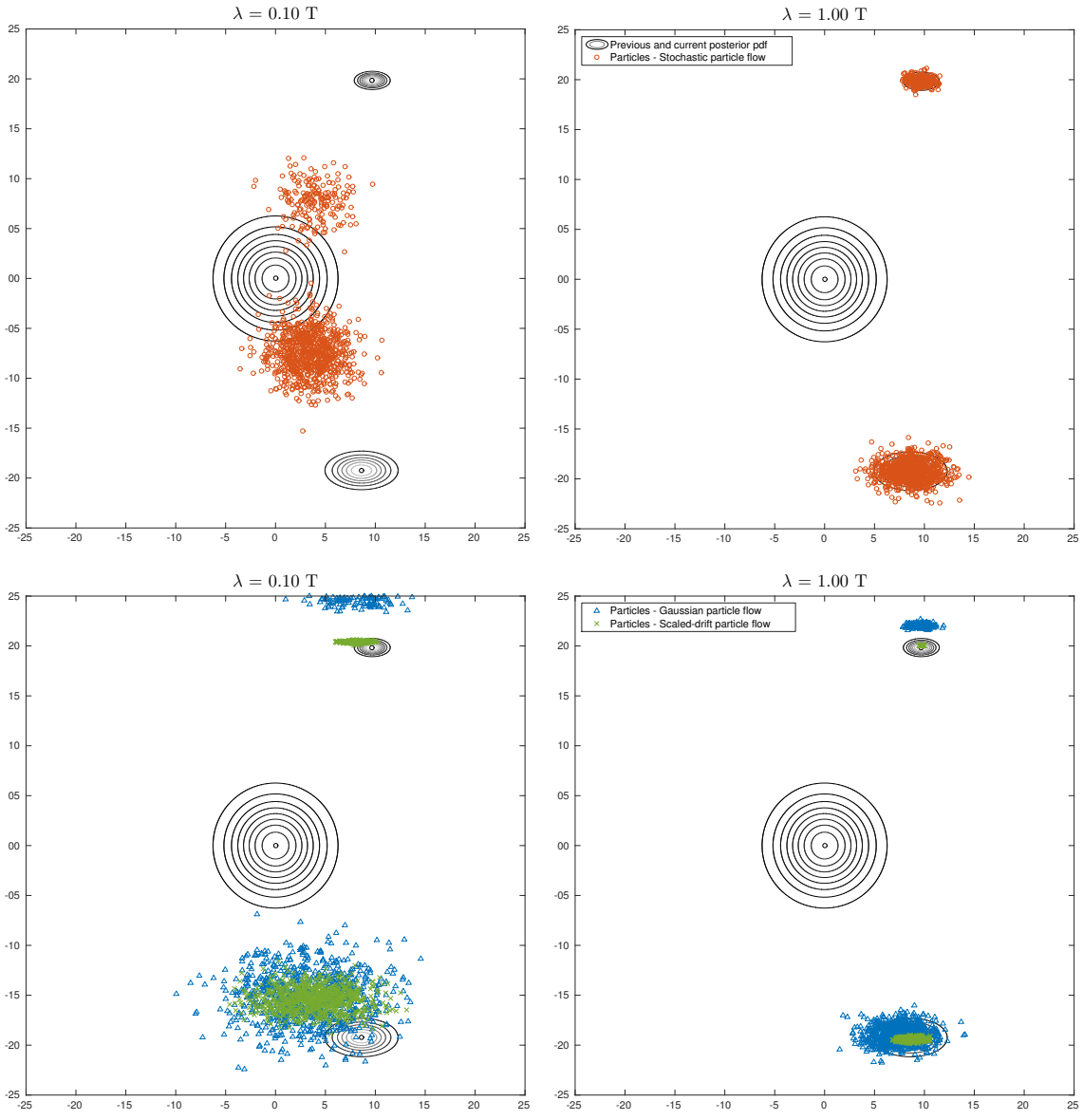
λ = 0.10 T
λ = 1.00 T
Previous and current posterior pdf
Particles - Stochastic particle flow
λ = 0.10 T
λ = 1.00 T
Particles - Gaussian particle flow
Particles - Scaled-drift particle flow

Figure 7.7: Sequence of distributions achieved by propagating particles for the bimodal, bivariate example

Parameters for the nonlinear bivariate model, case 1	
Initial distribution	$\bar{\mathrm{x}}_{k-1} = \begin{pmatrix} 0 \\ 0 \end{pmatrix}$, $P_{k-1} = \begin{pmatrix} 20 & 0 \\ 0 & 20 \end{pmatrix}$
Markov transition pdf	$f(\mathrm{x}_{k-1}) = \mathrm{x}_{k-1}$, $Q_k = \begin{pmatrix} 20 & 0 \\ 0 & 20 \end{pmatrix}$
Likelihood function	$h(\mathrm{x}_k) = \begin{pmatrix} \sqrt{\mathrm{x}_k(1)^2 + \mathrm{x}_k(2)^2} \\ \operatorname{atan}\left(\mathrm{x}_k(2)/\mathrm{x}_k(1)\right) \end{pmatrix}$, $R_k = \begin{pmatrix} 1.00 & 0 \\ 0 & 0.16 \end{pmatrix}$
Observation	$\mathrm{y}_k = \begin{pmatrix} 20 \\ 0^\circ \end{pmatrix}$

Table 3: Parameters for the nonlinear bivariate model, case 1

where importance sampling fails. The parameters used for the *case 1* and *case 2* are presented in Table 3 and Table 4, respectively.

In either cases the sequence of distributions generated by the original particle flows and by the stochastic particle flow are as illustrated in Figure 7.8. Once more it is evident that the stochastic particle flow provides a superior distribution of particles to approximate the posterior density, which demonstrates a higher level of accuracy and regularity of the stochastic flow approximation, as opposed to the deterministic particle flows. Similarly to the results presented for previous examples, the Gaussian particle flow seems to generate substantially biased distributions whereas the scaled-drift particle flow seems highly prone to regularity problems. These aspects are well corroborated by the average Jensen-Shannon divergences presented in Table 5.

We also included in the comparison the marginal particle filters. For *case 1* (favorable), we illustrate in Figure 7.9 how the marginal importance densities, projected (marginalised) onto the vertical and horizontal planes, would look like for the marginal auxiliary particle filter and for the SPF-MPF. It is clear that in this case both filters generate proposal densities quite proximate to the empirical marginal target, which in turn approximates well the true posterior. Additionally, it is possible to visualise that the SPF-MPF provides a slightly better proposal density in terms of similarity to the target density, which is corroborated by a greater average effective sample size as presented in Table 5. The remaining marginal particle filters don't generate effective importance densities either in terms of approximating the true posterior or approximating the target density.

For the *case 2* (unfavorable), importance sampling fails as exemplified by the projections of the importance density proposed by the marginal auxiliary particle filter depicted in Figure 7.10. By the same reason explained before, the importance sampling procedure fails to provide a satisfactory filtering density owing to the errors that affect the evaluations of both the marginal target density and the marginal importance density. The consequence is that any marginal particle filter generates a poor solution, despite the marginal auxiliary particle filter provides a high effective sample size for this example. The SPF-MPF generates a remarkably poor solution for the *case 2* because it distributes the particles to generally approximate the true posterior density but constrains the associated (proposal) mixture components to match a very inaccurate empirical target density.

In contrast, in both the *case 1* and *case 2* the SPF-GS proposes a direct filtering density that accurately approximates the true posterior density, being insensitive to the sparsity caused by an observation located relatively far from the initial distribution. These features are quantitatively captured by the performance data summarised in Table 5.

Parameters for the nonlinear bivariate model, case 2	
Initial distribution	$\bar{\mathrm{x}}_{k-1} = \begin{pmatrix} 0 \\ 0 \end{pmatrix}$, $P_{k-1} = \begin{pmatrix} 10 & 0 \\ 0 & 10 \end{pmatrix}$
Markov transition pdf	$f(\mathrm{x}_{k-1}) = \mathrm{x}_{k-1}$, $Q_k = \begin{pmatrix} 5 & 0 \\ 0 & 5 \end{pmatrix}$
Likelihood function	$h(\mathrm{x}_k) = \begin{pmatrix} \sqrt{\mathrm{x}_k(1)^2 + \mathrm{x}_k(2)^2} \\ \mathrm{atan}\left(\mathrm{x}_k(2)/\mathrm{x}_k(1)\right) \end{pmatrix}$, $R_k = \begin{pmatrix} 1.00 & 0 \\ 0 & 0.16 \end{pmatrix}$
Observation	$\mathrm{y}_k = \begin{pmatrix} 20 \\ 0^\circ \end{pmatrix}$

Table 4: Parameters for the nonlinear bivariate model, case 2

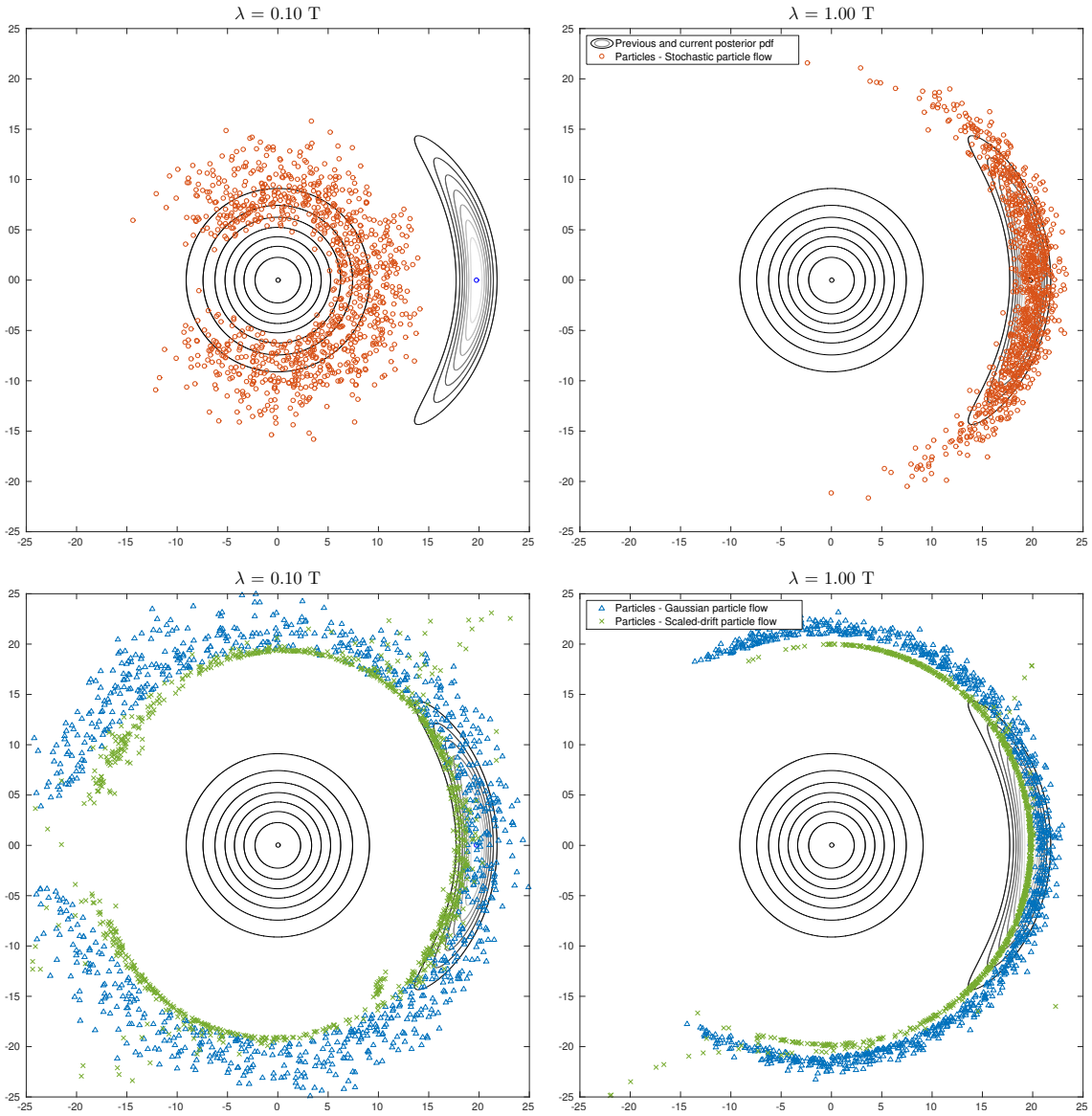
λ = 0.10 T
λ = 1.00 T
Previous and current posterior pdf
Particles - Stochastic particle flow
λ = 0.10 T
λ = 1.00 T
Particles - Gaussian particle flow
Particles - Scaled-drift particle flow

Figure 7.8: Sequence of distributions achieved by propagating particles for the nonlinear, bivariate example

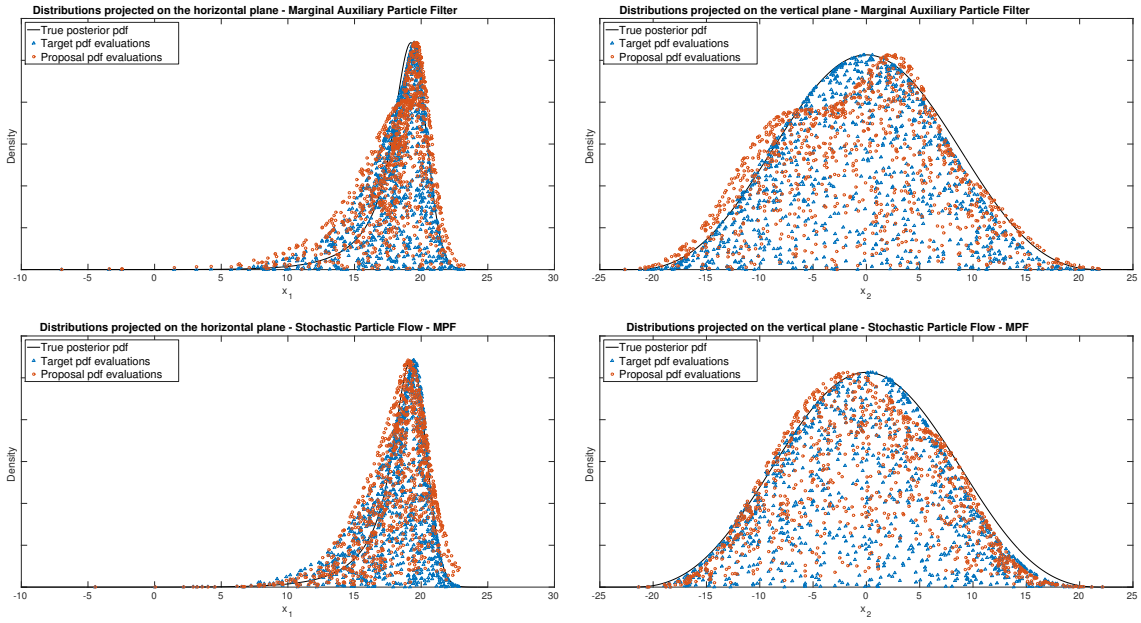
Distributions projected on the horizontal plane - Marginal Auxiliary Particle Filter
Distributions projected on the vertical plane - Marginal Auxiliary Particle Filter
Distributions projected on the horizontal plane - Stochastic Particle Flow - MPF
Distributions projected on the vertical plane - Stochastic Particle Flow - MPF
True posterior pdf
Target pdf evaluations
Proposal pdf evaluations
Density
x1
x2

Figure 7.9: Comparison between the SPF-MPF and the MAPF for the nonlinear, bivariate example

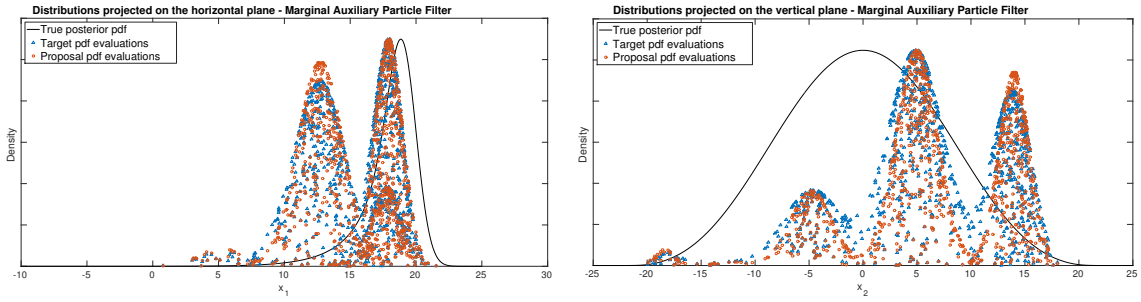
Distributions projected on the horizontal plane - Marginal Auxiliary Particle Filter
Distributions projected on the vertical plane - Marginal Auxiliary Particle Filter
True posterior pdf
Target pdf evaluations
Proposal pdf evaluations
Density
x1
x2

Figure 7.10: Failure of marginal importance sampling for the nonlinear example

7.2 Multi-sensor bearings-only tracking

The estimation of a target position and velocity based solely on angular measurements in clutter is a relevant problem that finds direct application in airborne radar and sonar in passive listening mode. In this example a single target is observed by a circumferential array of sensors that measure the bearing of the target with respect to their own position.

We compare the performance of following filters:

- a multi-sensor EKF that performs a series of centralised measurement updates, taking into account each sensor in sequence;
- the Information Matrix Fusion filter [77], that fuses distributed estimates (in parallel) into a global estimate using the Information Matrix form of the EKF;
- a bootstrap particle filter;
- a Gaussian particle flow;
- a scaled-drift particle flow; and

Density	*Multimodal, linear*		*Nonlinear - case 1*		*Nonlinear - case 2*	
	JSD_{avg}	ESS_{avg}	JSD_{avg}	ESS_{avg}	JSD_{avg}	ESS_{avg}
Marginal target	0.0082	-	0.0073	-	0.1822	-
SPF-GS	0.0034	-	0.0201	-	0.0328	-
SPF-MPF	0.0193	92.55%	0.0167	84.26%	0.2776	7.27%
Gaussian particle flow	0.2653	-	0.6573	-	0.5300	-
Scaled-drift particle flow	0.3861	-	0.4956	-	0.5804	-
Marginal BPF	-	-	0.9968	0.37%	0.9998	0.13%
Marginal EPF	-	-	0.3206	27.62%	0.5764	9.53%
Marginal UPF	-	-	0.7748	4.54%	0.8148	2.51%
Marginal APF	-	-	0.0130	81.19%	0.1663	84.75%

Table 5: Comparison of densities for the bivariate examples

- a stochastic particle flow, Gaussian sum (SPF-GS).

As mentioned before, in order to work properly, both the Gaussian particle flow and the scaled-drift particle flow rely on a companion filter to estimate the covariance matrix correctly, according to Choi *et al.* [54] and Ding & Coates [55]. For this example, we used the multi-sensor (serial) EKF as the companion filter for the original particle flows. In contrast, the stochastic particle flow does not require a companion filter.

The bootstrap particle filter, the Gaussian and scaled-drift particle flows, and the stochastic particle flow consider all measurements jointly according to a joint likelihood function described in the next subsection. The filters performance is analysed by computing the root-mean-square error (RMSE) of the estimates and the normalised estimation error squared (NEES) over 100 Monte Carlo runs. The original particle flows and the stochastic particle flow use 250 samples.

7.2.1 A multi-sensor bearings-only model

When tracking in clutter based on multiple measurements, the usual treatment rests on the probabilistic data association (PDA) [78]. In the PDA model, a set of m_k valid measurements is received at each time step k and assumed to be generated according to the possibilities: (i) all measurements are spurious false alarms (clutter), (ii) one of the measurements is originated from the target and the remaining are false alarms. Provided a formulation of the association event $\theta_{k,i}$ that the ith measurement is target-originated, the PDA filter computes the association probabilities $p(\theta_{k,i}|\mathrm{y}_{1:k})$ conditional on the set of all received measurements up to time instant k, and calculates the target state posterior density $p(\mathrm{x}_k|\mathrm{y}_{1:k})$ by marginalising the joint density $p(\mathrm{x}_k, \theta_{k,1:m_k}|\mathrm{y}_{1:k})$ over all possible associations.

We propose an example where a single target is tracked by a set of N_s sensors located along a circumference enclosing the surveillance region, at equally spaced angular positions. As per the PDA model, one target is known to exist a priori, detected with probability $P_{d,j}$ by the jth sensor; and the number of clutter detections per sensor is Poisson-distributed with mean $\lambda_c \cdot V$, where λ_c is the clutter spatial density and V is the volume of the surveillance region. For any given set of N_s sensors, the expected likelihood can be easily obtained by extending the procedure established by Marrs *et al.* [79] to multiple sensors, to give

$$p\left(\mathrm{y}_k|\mathrm{x}_k, \mathrm{y}_{1:k-1}\right) = \prod_{j=1}^{N_s} V^{-m_{k,j}} \frac{\left(\lambda_c V\right)^{m_{k,j}} e^{-\lambda_c V}}{m_{k,j}!} \times \left[\lambda_c \left(1 - P_{d,j}\right) + \sum_{i=1}^{m_{k,j}} P_{d,j} \mathcal{N}\left(\mathrm{y}_{k,i(j)}; h_j(\mathrm{x}_k), R_{k,j}\right)\right], \tag{7.6}$$

where $m_{k,j}$ is the total number of validated measurements for the jth sensor, $\mathrm{y}_{k,i(j)}$ is the ith measurement received by the jth sensor, $h_j(.)$ and $R_{k,j}$ are the observation function and the observation noise variance for the jth sensor, respectively.

On a bidimensional state space, the bearing observations are defined so that

$$h_j(\mathrm{x}_k) = \operatorname{atan}\left(\frac{\mathrm{x}_k\,(2) - p_{2,j}}{\mathrm{x}_k\,(1) - p_{1,j}}\right), \tag{7.7}$$

where $\mathrm{p}_j = (p_{1,j}, p_{2,j})^T$ are the position coordinates for the jth sensor. We assume a target moving according to the nearly-constant velocity model

$$\mathrm{x}_k = F\mathrm{x}_{k-1} + \mathrm{u}_k,\ \mathrm{u}_k \sim \mathcal{N}(\mathrm{u}_k; 0_{n_x}, Q_k), \tag{7.8}$$

where $\mathrm{x}_k = (p_{x_1}, p_{x_2}, v_{x_1}, v_{x_2})_k^T$ is the state vector composed of position and velocity in Cartesian coordinates (x_1, x_2), and

$$F = \begin{pmatrix} 1 & 0 & dt & 0 \\ 0 & 1 & 0 & dt \\ 0 & 0 & 1 & 0 \\ 0 & 0 & 0 & 1 \end{pmatrix}, \tag{7.9}$$

$$Q_k = \begin{pmatrix} {dt^3}/{3} & 0 & {dt^2}/{2} & 0 \\ 0 & {dt^3}/{3} & 0 & {dt^2}/{2} \\ {dt^2}/{2} & 0 & dt & 0 \\ 0 & {dt^2}/{2} & 0 & dt \end{pmatrix} \sigma_q^2. \tag{7.10}$$

The multi-sensor joint likelihood (7.6) is incorporated in the bootstrap filter, the Gaussian and scaled-drift particle flows, and the stochastic particle flow by considering their filtering densities to target a posterior density involving the joint likelihood. Regarding the implementation of the particle flows, the Gaussian and scaled-drift particle flows reinterpret the filtered density empirically as a Gaussian pdf at the end of each cycle in order to avoid the exponential growth of the number of mixture components over time. This practical aspect does not affect the stochastic particle flow, whose filtered density is a mixture composed invariably of N local solutions to the actual posterior pdf, where N is the number of samples.

Generally speaking, the multi-sensor bearings-only tracking is a difficult problem to solve when the observation noise has high variance, the probability of detection is relatively low and the probability of having clutter in the surveillance region is not negligible. The difficulty stems from the fact that the joint multi-sensor likelihood (7.6) is a product of mixtures composed of several nonlinear and non-informative likelihood terms: when the nonlinearity is pronounced by a high-variance observation noise, the resulting posterior density may not be well expressed by simple parametric densities. In addition, this difficulty is modulated by the amount of information available: the fewer the number of sensors the more difficult to solve the problem. Other aspect that pose additional concern is the observability of the system that is highly dependent on the relative position of a sensor with respect to the trajectory, i.e., trajectories radially aligned with the sensor position provide less information to infer the velocity of the target.

7.2.2 Results

For a moderately difficult scenario, where the state process noise is assumed with variance scaled by $\sigma_q^2 = 25\,m^2$, the observation noise variance is $R_k = 100\,deg^2$, $P_d = 0.80$ and $\lambda_c \times V = 1.00$ false alarm/sensor/scan, for identical sensors, the resulting track of an exemplar run is shown in Figure 7.11. The track initiation is based on an overdetermined triangulation of the measurements for the first two steps. No gating has been performed for this problem, i.e., no preprocessing to discard measurements that fall outside a high-confidence region for each sensor. The Figure 7.11 depicts a sucessful tracking of the target despite the moderately difficult scenario.

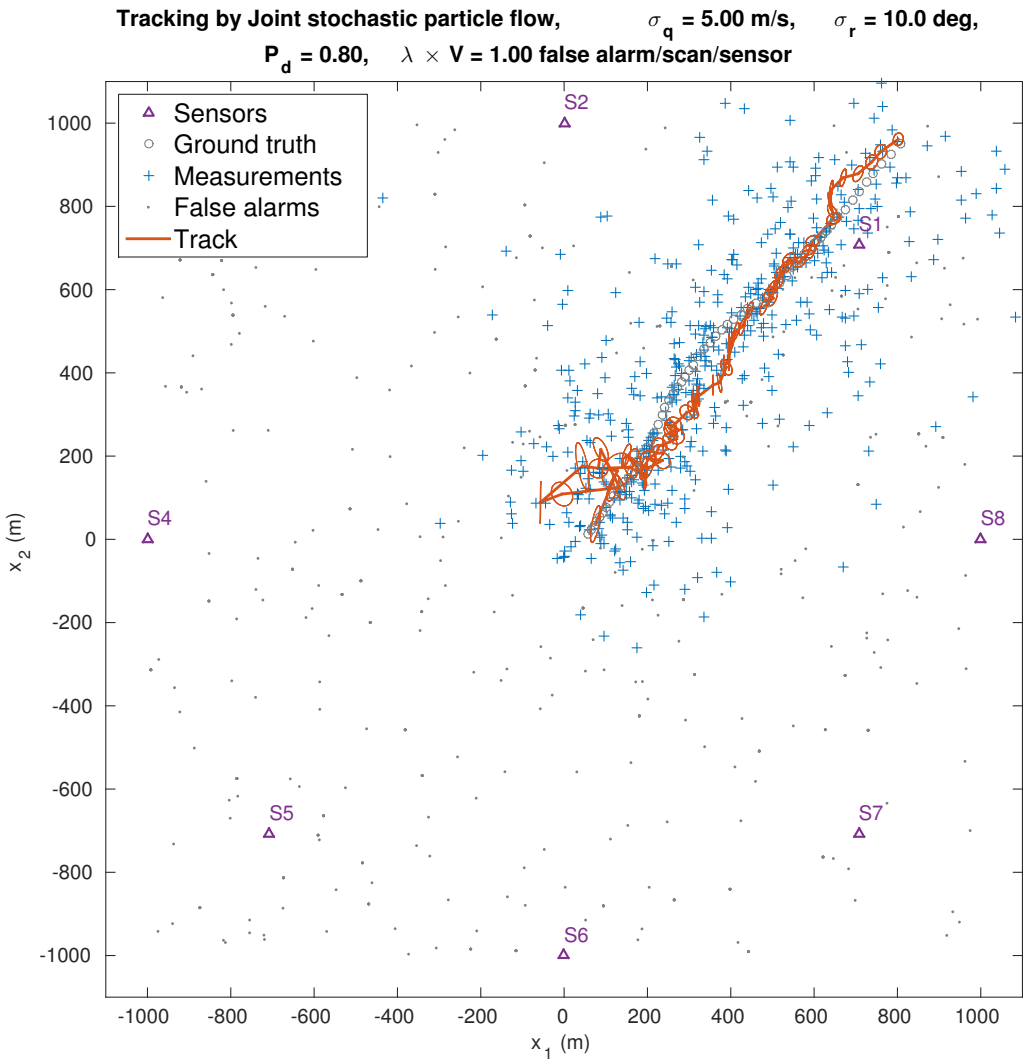

Figure 7.11: Illustration of bearing-only multi-sensor tracking

An even more challenging scenario was set for comparing the filters in order to exacerbate the differences of their performances to a noticeable level. In this very difficult scenario, we set $\sigma_q^2 = 25\,m^2$, $R_k = \sigma_r^2 = 400\,deg^2$, $P_d = 0.50$ and $\lambda_c \times V = 1.00$ false alarm/sensor/scan. Even though it is arguable that the estimation errors generated for such a scenario might not be feasible as an Engineering solution, it is certainly of practical interest to examine how the estimate errors scale to extreme scenarios that happen quite often in real applications.

The resulting root mean square error (RMSE) and normalised estimation error squared (NEES) of all filters for different numbers of sensors are shown in Figure 7.12. The following important aspects can be observed from Figure 7.12:

- the somewhat counterintuitive fact that the multi-sensor serial EKF provides better estimates than the Information Matrix Fusion EKF (parallel), both in terms of precision (RMSE) and credibility (NEES);
- the remarkably poor performance provided by the multi-sensor (bootstrap) particle filter, which becomes even worst as the number of sensors increase;
- the commensurate performances shown by the particle flows and by the stochastic particle flow, outperforming the multi-sensor (bootstrap) particle filter and the Information Matrix Fusion EKF;

- the remarkably good performance shown by the multi-sensor serial EKF, similar to the particle flows and to the stochastic particle flow;
- the overall improvement of estimation accuracy as the numbers of sensors is increased, as expected, except for the multi-sensor particle filter;
- the higher estimation accuracy and credibility provided by the stochastic particle flow in more difficult scenarios, with few sensors;
- the overall higher credibility of the stochastic particle flow, which is denoted by its NEES closer to 1 ($\log_{10} NEES \to 0$) from above.

It is worth commenting on the results comparing the particle flows and the stochastic particle flow. Specifically for this problem, the particle flows provide the most accurate state estimate and rely on a fairly good approximation to the estimate covariance matrix given by the companion filter, the multi-sensor serial EKF. It is remakable the successful synergy between the original particle flows and their companion filter, despite the fact that it is difficult to justify the calculated NEES for these filters since their first and second moment estimates stem from distinct filtering methods. On the other hand, the stochastic particle flow (SPF-GS) provides an equally accurate state estimate and securely constitutes the most credible estimator among all filters.

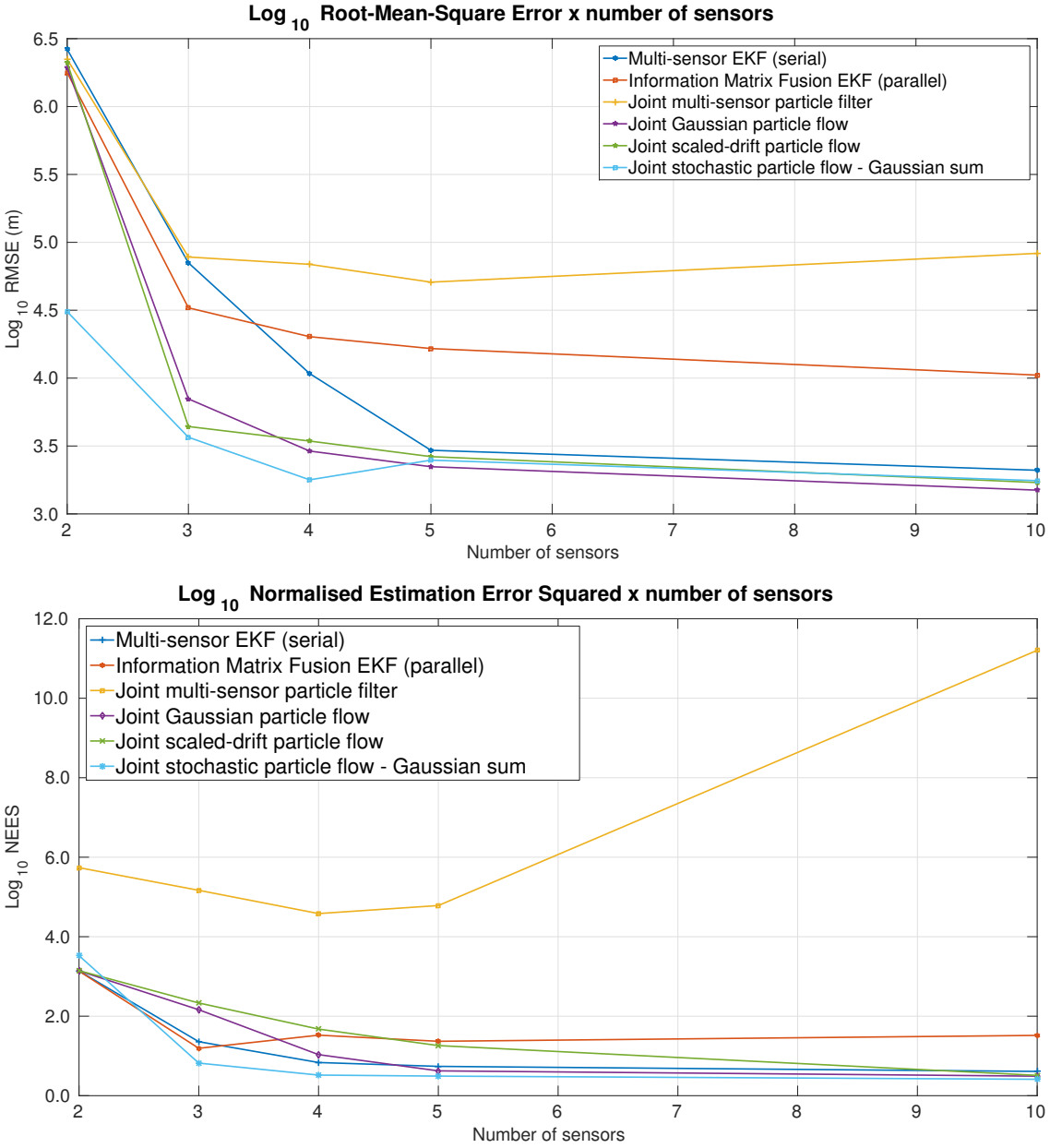
Log 10 Root-Mean-Square Error x number of sensors
Log 10 RMSE (m)
Number of sensors
Multi-sensor EKF (serial)
Information Matrix Fusion EKF (parallel)
Joint multi-sensor particle filter
Joint Gaussian particle flow
Joint scaled-drift particle flow
Joint stochastic particle flow - Gaussian sum
Log 10 Normalised Estimation Error Squared x number of sensors
Log 10 NEES
Number of sensors
Multi-sensor EKF (serial)
Information Matrix Fusion EKF (parallel)
Joint multi-sensor particle filter
Joint Gaussian particle flow
Joint scaled-drift particle flow
Joint stochastic particle flow - Gaussian sum

Figure 7.12: Performance for the multi-sensor bearing-only tracking example

7.3 Convoy tracking

Tracking multiple objects in clutter is as challenging as important for real applications. In the multi-target tracking standard methods, the most common treatment assumes the targets' states to be independent so that the joint probability density is the product of their marginal densities. Whilst this assumption is fairly reasonable for applications where the objects are far apart most of the time, the same cannot be stated for cases where the objects are in proximity for a considerable part of time. This latter cases elicit tracking all targets jointly in the hope to implicitly capture the dependencies between targets and, therefore, become problems whose dimension scales with the number of targets.

To illustrate this situation, we propose an example of a convoy of vehicles trafficking on a road that are forced into mutual proximity. The vehicles have explicit interactions as each driver aims

driving at the maximum allowed speed unless there is another vehicle immediately in front at a slower speed, which demands the care for a safety distance. The intent of the tracker is then to provide the best estimate of each vehicle on the convoy, given a set of non-identified measurements corrupted by noise and possible false alarms (clutter) reported by a position sensor.

We compare the performance of following filters:

- the Joint Probabilistic Data Association (JPDA) filter [78];
- the Global Nearest Neighbor Data Association (GNN) filter;
- the JPDA with a Gaussian mixture per target, applying mixture reduction [80];
- the Coupled Probabilistic Data Association (CPDA) filter [81];
- a joint multi-target bootstrap particle filter based on the description by Blom & Bloem [82];
- a Gaussian particle flow;
- a scaled-drift particle flow; and
- a stochastic particle flow, Gaussian sum (SPF-GS).

The Gaussian particle flow and the scaled-drift particle flow rely on a companion filter to estimate the covariance matrix correctly, according to Choi *et al.* [54] and Ding & Coates [55]. For this example, we used the CPDA [81] as the companion filter for the original particle flows. In contrast, the stochastic particle flow does not require a companion filter.

The CPDA, the joint multi-target bootstrap particle filter, the Gaussian and scaled-drift particle flows, and the stochastic particle flow consider all targets' states jointly, as a single high-dimensional state. In opposition, the classical multi-target filters track the targets separately, based on the nearly-constant velocity model. The filters' performance is analysed by computing the root-mean-square error (RMSE) of the estimates and the normalised estimation error squared (NEES) over 100 Monte Carlo runs. The original particle flows and the stochastic particle flow use 250 samples.

7.3.1 The Intelligent Driver Model

The Intelligent Driver Model (IDM) [83] is a model[7] used in Traffic Engineering to simulate phenomena such as congestion and analyse the traffic behaviour as a response to changes in the transport system. Because the interaction between vehicles is explicitly taken into account by the IDM, tracking based on it involves consideration of the joint state of multiple targets. Even though the IDM establishes an empirical description of traffic for multiple vehicles, it has not been previously used in the context of multi-target tracking. We propose an stochastic version of the IDM and discretise it in order to make it compatible with multi-target trackers formulated on the joint state space.

The IDM describes the dynamics of the positions and velocities of vehicles in traffic, incorporating the interaction between each vehicle and the vehicle directly in front. Provided a vehicle indexed as α with length l_α, the dynamics of its position x_α and velocity v_α are given by the following (continuous-time) stochastic differential equations:

$$dx_\alpha = v_\alpha dt, \tag{7.11}$$

$$dv_\alpha = \underbrace{a\left[1-\left(\frac{v_\alpha}{v_0}\right)^{\delta}\right]}_{\dot{v}_\alpha^{\text{free road}}} dt - \underbrace{a\left[\frac{\bar{s}}{s_\alpha}\right]^2}_{\dot{v}_\alpha^{\text{interaction}}} dt + dw_t, \tag{7.12}$$

where $\{w_t\}_{t\geq 0}$ is a Wiener process, $s_\alpha = x_{\alpha-1} - x_\alpha - l_\alpha$ is the net distance between vehicles, $\Delta v_\alpha = v_{\alpha-1} - v_\alpha$ is the approaching rate, and $\bar{s} = \bar{s}\,(v_\alpha, \Delta v_\alpha)$ is the expected distance defined as

[7] In its simplest form, the IDM is focused on the interaction of vehicles moving along a single-carriageway road. More complex variants exist to model overtaking, for example, and consider factors such as the politeness of the driver.

$$\bar{s}\left(v_\alpha, \Delta v_\alpha\right) = s_0 + v_\alpha T_h + \frac{v_\alpha \Delta v_\alpha}{2\sqrt{a \cdot b}}. \tag{7.13}$$

The model dynamics is such that when a vehicle is travelling on a free road it will predominantly accelerate according to $\dot{v}_\alpha^{\text{free road}}$ up to the maximum allowed speed v_0, whereas when it approaches another vehicle immediately in front, the decrement in acceleration according to $\dot{v}_\alpha^{\text{interaction}}$ becomes relevant to maintain a safe-time headway T_h and avoid approaching closer than the minimum safe distance s_0. The IDM parameters are summarised in the following table.

Parameter	**Description**
a	nominal maximum acceleration
b	comfortable braking decceleration
δ	acceleration exponent (driver dynamics)
v_0	free-road desired velocity
s_0	minimum allowed distance between vehicles
T_h	safe-time headway
$\alpha - 1$	index of the vehicle direcly in front

In order to use the stochastic IDM as the state process for a multi-target tracker, its continuous-time equations are discretised by a first-order approximation. This assumes that the derivative of the state is linear in time between two subsequent measurements, but the interactions between non-adjacent vehicles are negligible when compared to the interactions between adjacent vehicles. The discretised version of the stochastic IDM is presented in the Appendix C.

7.3.2 The multi-target joint likelihood function

The joint multi-target filters extend the joint probabilistic data association (JPDA) [78] framework for situations where the targets' states are not mutually independent conditioned on the past observations. This formulation has been first proposed as the JPDA coupled filter (JPDAC) [78] and further generalised by Blom & Bloem [81, 82], that consider the measurement-to-target associations implicitly.

In the JPDA model, a set of N_m valid measurements is received at each time step k and assumed to be generated according to the possibilities: (i) each of the measurements may be originated from each target, considering all possible associations, (ii) a measurement not originated from any target is due to a false alarm (clutter). These possibilities are exhaustive so that a measurement can have only one source, and at most one of the validated measurements can originate from a target.

Provided the association event $\phi_{k,i} \in \{0, 1, \ldots, N_m\}$ that maps each target i to the measurement indexed as $\phi_{k,i}$, and $\phi_{k,i} = 0$ meaning that no measurement is associated to the target, the coupled JPDA filter computes the joint association probabilities $p(\phi_{k,1:N_t}|\mathrm{y}_{1:k})$ conditional on the set of all received measurements up to time instant k, and calculates the joint state posterior density $p(\mathrm{x}_{k,1:N_t}|\mathrm{y}_{1:k})$ by marginalising $p(\mathrm{x}_{k,1:N_t}, \phi_{k,1:N_t}|\mathrm{y}_{1:k})$ over all possible joint associations.

In the JPDA framework, N_t targets are known to exist a priori, detected with probability P_d by a single sensor; the number of clutter detections is Poisson-distributed with mean $\lambda_c \cdot V$, where λ_c is the clutter spatial density and V is the volume of the surveillance region; the location of each clutter detection is independently distributed according to a spatial density $\eta_c(\mathrm{y})$; and the likelihood function of the jth measurement being originated from the ith detected target is $p(\mathrm{y}_{k,j}|\mathrm{x}_{k,i})$. Denoting the joint multi-target state as $\mathrm{x}_{k,1:N_t}$ and the joint observation as $\mathrm{y}_{k,1:N_m}$, the joint likelihood can be either obtained by the filter of Blom & Bloem [82] or in a formulation equivalent to the coupled JPDA as

$$p\left(\mathrm{y}_{k,1:N_m}|\mathrm{x}_{k,1:N_t}\right) = \frac{\left[\prod_{j=1}^{N_m}\eta_c\left(\mathrm{y}_{k,j}\right)\right]}{N_t!}$$
$$\times \sum_{N_d=0}^{N_t} \frac{(\lambda_c V)^{N_m-N_d}\, e^{-\lambda_c V}}{(N_m-N_d)!} P_d^{N_d}\left(1-P_d\right)^{N_t-N_d}$$
$$\times \sum_{\phi_{k,1:N_t}|N_d} \prod_{i=1}^{N_t} \frac{p\left(\mathrm{y}_{k,\phi_{k,i}}|\mathrm{x}_{k,i}\right)}{\eta_c\left(\mathrm{y}_{k,\phi_{k,i}}\right)}. \tag{7.14}$$

The joint state vector $\mathrm{x}_{k,1:N_t} = (p_1, \ldots, p_{N_t}, v_1, \ldots, v_{N_t})_k^T$ is composed of position and velocity of all vehicles in the convoy, and the joint observation $\mathrm{y}_{k,1:N_m} = (\mathrm{y}_1, \ldots, \mathrm{y}_{N_m})_k^T$ contains position measurements of all targets and possible false alarms obtained at a given time instant k.

The joint bootstrap particle filter, the Gaussian and scaled-drift particle flows, and the stochastic particle flow consider their filtering densities to target a joint posterior density incorporating the multi-target joint likelihood function (7.14). Regarding the implementation of the original particle flows, the Gaussian and scaled-drift particle flows reinterpret the filtered density empirically as a Gaussian pdf at the end of each cycle in order to avoid the exponential growth of the number of mixture components over time. In contrast, this practical aspect does not affect the stochastic particle flow, whose filtered density is a mixture composed of a fix number of local solutions to the actual posterior pdf.

7.3.3 Results

We simulated the trajectories of vehicles on a ring road by integrating the continuous-time stochastic IDM over 60 seconds with the parameters presented as follows. The convoy was set to start from rest with the vehicles initially positioned apart, lead by a truck so that the queue of cars is slowed down and forced into mutual proximity. The minimum allowed distance between vehicles was set to be exaggeratedly small ($s_0 = 0.5\,m$) to induce the model to control the distance between cars mainly based on the safe-time headway T_h. In this case, the safe-time headway indirectly determines the desired distance between vehicles, which is denoted as *target distance* in the table below. At the final steady state, the net speed of the convoy is dominated by the target speed of the truck, which motivates the safe-time headway being computed based on $v_{0,\mathrm{truck}}$.

Parameter	**car**	**truck**
a	$0.5\,m/s^2$	$0.4\,m/s^2$
b	$1.5\,m/s^2$	$1.2\,m/s^2$
δ	4	4
v_0	$15\,m/s$	$10\,m/s$
s_0	$0.5\,m$	$0.5\,m$
T_h	$\frac{\{\text{target distance (m)}\}}{v_{0,\mathrm{truck}}}$	-
l_α	$5\,m$	$20\,m$

The state process noise is assumed with the joint state process covariance matrix scaled by $\sigma_q^2 = 0.0625\ (m/s)^2$, each position observation has variance $\sigma_r^2 = 4\,m^2$, $P_d = 0.80$ and $\lambda_c \times V = 0.01$ false alarm/scan, and the "volume" of the surveillance region V is in fact the length covered by a confidence region ($\approx 99.73\%$) that contains all the vehicles. Proposing a method to effectively initiate tracks was out of the example's scope, thus the track initiation was considered to be ideal, i.e., the initial position and velocity of the targets is known with an initial uncertainty scaled by the observation noise.

The Figure 7.14 shows two frames of an exemplar run, demonstrating the situation where a queue of cars is slowed down by a truck, forcing them into proximity. The non-filled rectangles depicted in Figure 7.14 denote the position estimates provided by the filter applied for that run. The involved interactions between the vehicles in the convoy can be well perceived in the exemplar run shown in Figure 7.15.

The resulting root mean square error (RMSE) and normalised estimation error squared (NEES) of all filters for different numbers of vehicles, and target distance between vehicles $d = 10\,m$, are shown in Figure 7.13. The RMSE of the estimates and the NEES were computed over 100 Monte Carlo runs, with the particle-based filters using 250 samples. The following important aspects can be noted from Figure 7.13:

- in general, the trackers that estimate in the joint $2N_t$-dimensional state space clearly outperform the classical multi-target trackers (JPDA, GNN and JPDA with mixture reduction), both in terms of precision (RMSE) and credibility (NEES);
- as the number of targets increases, the Global Nearest Neighbor association filter is the one amongst the classical multi-target trackers that provides the most accurate estimates, owing to the increasingly detrimental effect of the association uncertainty on the estimation, that is more prominent in the JPDA;
- the estimation errors committed by the joint multi-target (bootstrap) particle filter grow exponentially with the number of dimensions of the problem ($2N_t$), as expected, due to the curse of dimensionality;
- the commensurate root-mean-square errors presented for the CPDA, original particle flows, and the stochastic particle flow, suggesting that most of their accuracy gain stems from tracking in the joint $2N_t$-dimensional state space and estimating the inherent dependencies between targets;
- the oscillations in the NEES calculated for the original particle flows, which most likely evidence the fact that these methods cannot provide reliable estimates for the state covariance matrices and depend on a dissimilar companion filter to work it around, affecting the credibility of the estimation;
- the overall higher estimation accuracy (RMSE) and credibility (NEES) provided by the stochastic particle flow, with low sensitivity to the increase in the number of dimensions of the problem.

The NEES slightly smaller than 1 for the JPDA with one Gaussian mixture per target (yellow line), at the evaluation for 2 vehicles, reflects an overestimated state covariance matrix. This is due to the relative high importance of all association hypotheses for only two targets involved.

Based on the results for this example, two important remarks are worth making. Firstly, the results show a notable performance improvement with the adoption of filtering on the joint $2N_t$-dimensional state-space: about 15-fold improvement in estimation precision (RMSE) and nearly 10-fold in credibility (NEES). The fact that the Coupled PDA performs as well as the stochatic particle flow suggests that modeling the inherent dependencies between targets and filtering in the joint space provides most of the performance gain. Secondly, the example not only illustrates well the curse of dimensionality for the joint multi-target (bootstrap) particle filter, but also corroborates the success of the principled choices made to formulate the stochastic particle flow in order to avoid degeneracy in high-dimensional problems. This latter observation becomes clear when we realise that the performance indexes for the stochastic particle flow scale gently with the number of dimensions.

Additionally, it is also worth noting that the original particle flows provide very accurate estimates, relying on the fairly precise estimate covariance matrices given by the CPDA as a companion filter. However, the calculated NEES for these filters is not reliable since their first and second moment estimates stem from distinct filtering methods. Whilst this fact does not disqualify the original particle filters per se, it is arguable that the true credibility of their estimates cannot be quantified and, ultimately, evokes the question about to what extent the success of these algorithms is due to the companion filter.

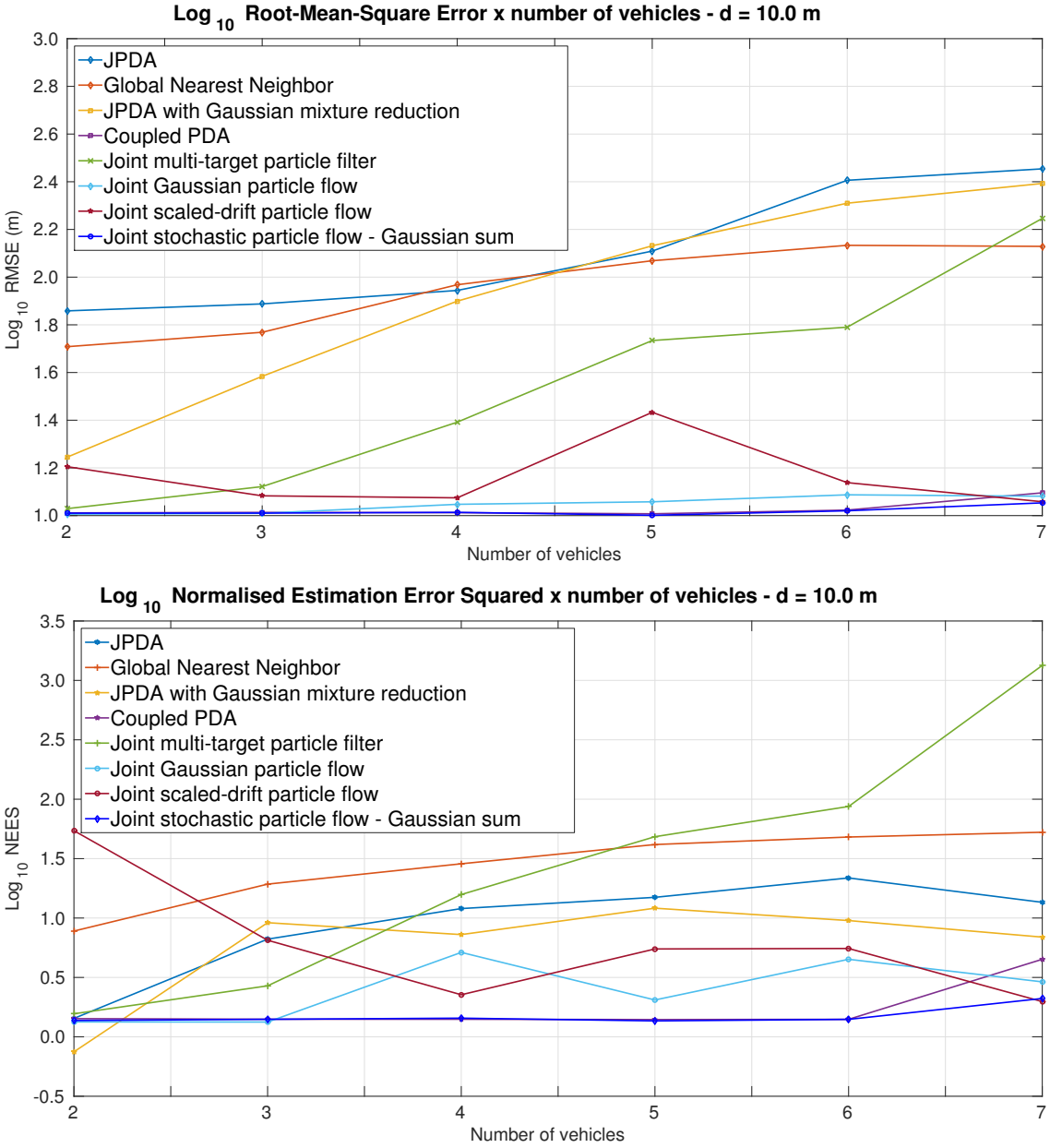
Log 10 Root-Mean-Square Error x number of vehicles - d = 10.0 m
JPDA
Global Nearest Neighbor
JPDA with Gaussian mixture reduction
Coupled PDA
Joint multi-target particle filter
Joint Gaussian particle flow
Joint scaled-drift particle flow
Joint stochastic particle flow - Gaussian sum
Log 10 RMSE (m)
Number of vehicles
Log 10 Normalised Estimation Error Squared x number of vehicles - d = 10.0 m
JPDA
Global Nearest Neighbor
JPDA with Gaussian mixture reduction
Coupled PDA
Joint multi-target particle filter
Joint Gaussian particle flow
Joint scaled-drift particle flow
Joint stochastic particle flow - Gaussian sum
Log 10 NEES
Number of vehicles

Figure 7.13: Performance for the convoy tracking example

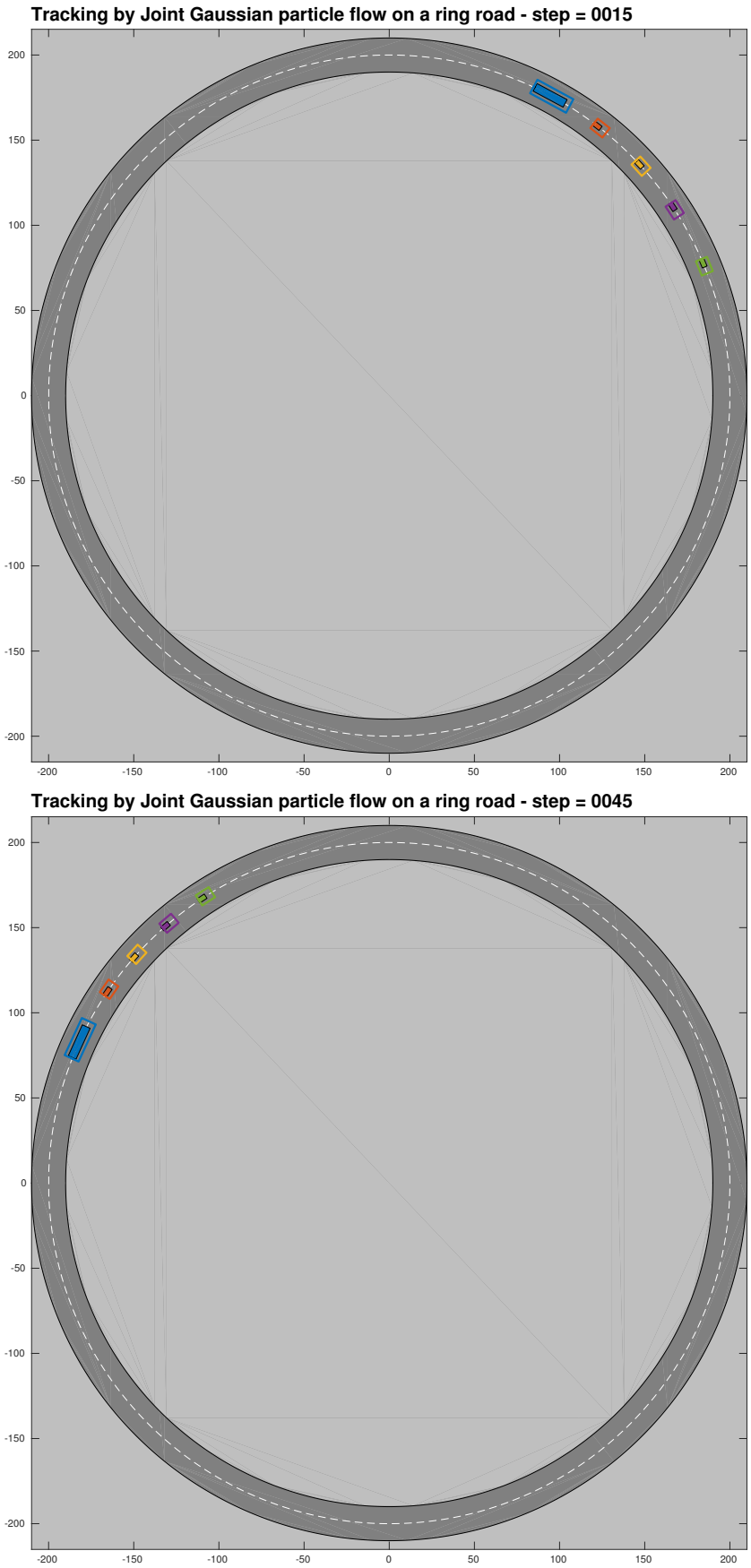

Figure 7.14: Illustration of convoy tracking on a ring road

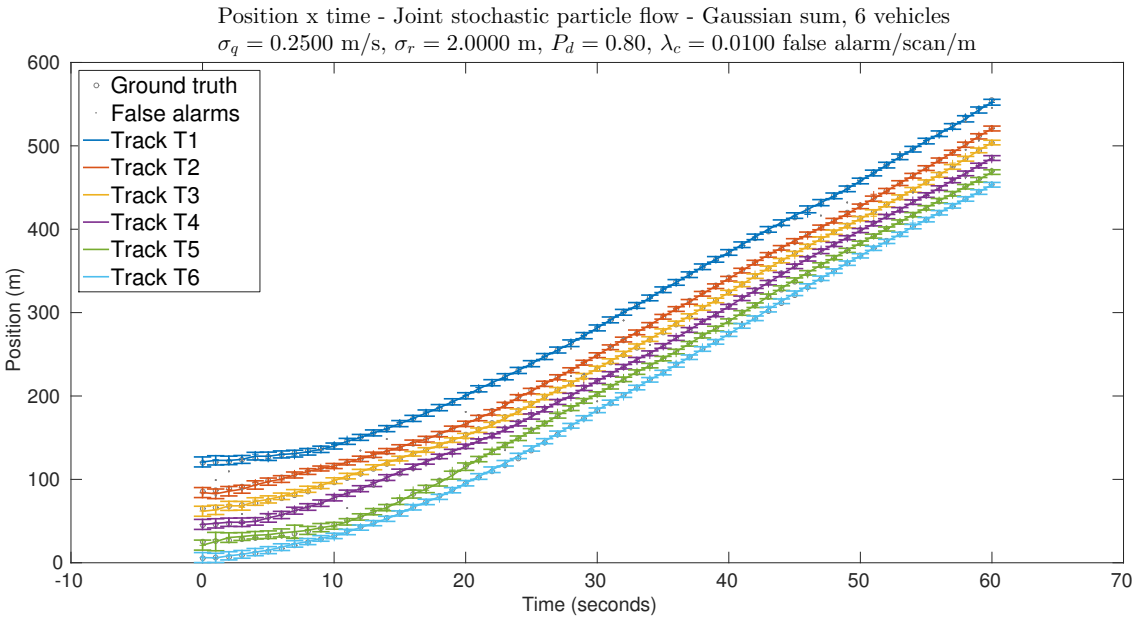

Figure 7.15: Position estimates for an exemplar run of the convoy tracking

8 Conclusions and future work

This paper is intended to bring new elements into the practical solution of nonlinear high-dimensional filtering problems, both by exploring ideas under intense revisitation by the research community, such as filtering in continuous-time, and capitalising on the fast-paced increment of the knowledge basis for sequential Monte Carlo methods. In addition, the article aims to contribute to a theoretical middle-ground between the highly abstract field that the sequential Monte Carlo filtering theory has become and the necessity for new tools in order to effectively solve more difficult real problems.

The particle flow methods can be interpreted in the framework of well established ideas, such as annealing sampling, simulating diffusions, transferring mass optimally, and exploring the homotopy between topological spaces. A particularly interesting and promising avenue for this class of methods may lie in the recent development of the transportation theory. For an a recent review on the optimal transport theory, see Villani's book [84], that builds on the classical Monge-Kantorovich problem to provide a comprehensive understanding and explore important connections with the probability theory and variational methods. Not less important is the link between solving the Fokker-Planck equation and minimising a cost functional involving the Wasserstein metric and the free-energy, as described by Jordan *et al.* [57]. Understanding these theories enables new ways of transporting probability masses to solve inference problems.

It is remarkable that the sequential Monte Carlo community have augmented focus in addressing problems in high-dimensional spaces recently. We believe that this is an obvious step if one considers the increasing demand for more statistically efficient methods to solve difficult inference problems when dealing with massive amounts of data, or daunting numbers of parameters. This is specially true for problems involving big data and pattern recognition in multivariate systems. Some important findings have been reported recently [21, 22] regarding how the local properties of sequential Monte Carlo filtering measures affect the ability to solve high-dimensional problems. As shown by Rebeschini & van Handel [22], by using the decay of correlations property, it is possible to develop particle filters based on local solutions whose approximation error does not depend on the state dimensions. These findings certainly bring new thoughts on how to construct new filters.

Within this context, we proposed a novel type of filters inspired by the particle flow methods [31, 39–50, 54, 55, 85–89], envisaging to address well known shortcomings of sequential Monte Carlo methods in solving nonlinear high-dimensional filtering problems, such as the ones that arise in multi-target and multi-sensor tracking. The novel method establishes a Monte Carlo procedure for generating a sequence of samples that guide local solutions of the Fokker-Planck equation to compound a mixture that approximates a filtering density. The ultimate result is a statistically-sound general-purpose class of algorithms that has been shown to be adequate for solving nonlinear high-dimensional inference problems, as demonstrated by the series of simple, though not trivial, illustrations proposed by this article. It is worth recalling that the stochastic particle flow, filtering on the joint multi-target (or multi-sensor) space, provides highly accurate estimates and securely constitutes the most credible estimator among all evaluated filters, outperforming classical multi-target filters.

Our investigation reveals that further consideration is required in order to explore fully the potential of the stochastic particle flow, specially concerning the computational cost of the algorithms and the crucial properties required for the diffusion matrix, such as positive definiteness and non-singularity. In its most general form, the algorithm's complexity is bounded by $O\left(NLn_x^3 + N + N^2\right)$ computations owing to the diffusion matrix calculated over L steps, as an inversion of a Hessian matrix, the evaluation of the mixture weights, and the evaluation of the filtering (or importance) density. It is important to remark that the stochastic particle flow is much more computationally complex than the original particle flows, which are generally bounded by $O\left(N\right)$ computations both in theory and practice.

Concerning alleviation of the computational complexity, it should be possible to explore the natural sparsity present in the diffusion matrix for some statistical models or, as a last resort, to incorporate methods that uncorrelate partially the states in order to partition the matrix inversion. Girolami & Calderhead [9] suggest that the use of guiding Hamiltonians [6] could provide a way of reducing such computational cost, but it is still unclear as a solution.

Regarding the properties of the diffusion matrix, possible issues arise when either dealing with statistical models for which the Hessian matrix (or the observed Fisher information matrix) is not available in closed analytic form, or when the models inhabit a space where the Hessian is not negative definite. In those cases, Girolami & Calderhead [9] advocate to employ the empirical Fisher information matrix as an estimate of the covariance of the score, with the advantage that the method would only deal with second-order derivatives, however, the filter would lose part of its locality that is inherently present in the local curvature provided by the Hessian. It is clear that there are several possible numerical and computational methods that could be investigated in order to solve these issues.

In conclusion, we hope that the methods proposed herein offer not only a way of solving nonlinear high-dimensional problems but also bridges the seminal knowledge on continuous-time filtering to reach its way into Engineering applications.

A Proofs

Theorem 3. *Define* $\mathrm{x} \in \mathbb{R}^{n_x}$ *to describe an* n_x*-dimensional vector state. Let the vector field* $\mu : \mathbb{R}^{n_x} \to \mathbb{R}^{n_x}$, $\mu\left(\mathrm{x}\right) \in \mathcal{C}^{1^{n_x}}$, *be a conservative field, i.e., there exists a scalar potential function* $\psi : \mathbb{R}^{n_x} \to \mathbb{R}$, $\psi\left(\mathrm{x}\right) \in \mathcal{C}^{2^{n_x}}$, *such that*

$$\mu\left(\mathrm{x}\right) = -\nabla_{\mathrm{x}}\psi\left(\mathrm{x}\right). \tag{A.1}$$

Let $p\left(\mathrm{x}, \lambda\right)$ *be the density of an ensemble of particles and, without loss of generality, can be assumed to be a continuous probability density function on* $\mathbb{R}^{n_x}$ *that depends on the pseudo-time variable* $\lambda \in \mathbb{R}$, $\lambda \geq 0$.

Set $\pi\left(\mathrm{x}\right) \propto e^{-\psi(\mathrm{x})}$ *to be an invariant, locally log-concave probability density to which the density* $p\left(\mathrm{x}, \lambda\right)$ *is expected to converge weakly at a stationary state in a finite time horizon* $\lambda \geq T$, $T \in \mathbb{R}^{+}$, *i.e.,*

$$\mathbb{E}_p\left[\varphi\left(\mathrm{x}\right)\right] \to \mathbb{E}_\pi\left[\varphi\left(\mathrm{x}\right)\right], \quad \lambda \to T; \tag{A.2}$$

for all bounded, continuous functions φ, and where $\mathbb{E}_p[.]$ is the expectation with respect to the probability density $p(\mathrm{x}, \lambda)$.

If the probability density $p(\mathrm{x}, \lambda)$ satisfies the continuity equation (Liouville's equation)

$$\frac{\partial p}{\partial \lambda} = -\nabla_{\mathrm{x}} \cdot (p\,\mu), \quad \lambda \geq 0; \tag{A.3}$$

with the initial condition

$$p(\mathrm{x}, \lambda) = p_0(\mathrm{x}), \quad \lambda = 0; \tag{A.4}$$

then any probability mass (particle) $\mathrm{x}_m(0) \sim p_0(\mathrm{x})$, when evolved according to the associated state equation

$$d\mathrm{x}_m(\lambda) = \mu(\mathrm{x}_m(\lambda))\, d\lambda, \quad \lambda \geq 0; \tag{A.5}$$

converges to

$$\mathrm{x}_m(T) = argmax[\pi(\mathrm{x})], \quad \lambda \geq T, \tag{A.6}$$

at a stable equilibrium.

Proof. The general solution of the continuity equation without sources (A.3) assumes the form (see for example [90])

$$\begin{aligned} p(\mathrm{x}, \lambda) &= p_0(\mathrm{x}_m(\mathrm{x}, \lambda)) \left| \frac{\partial \mathrm{x}_m}{\partial \mathrm{x}} \right| \\ &= p_0(\mathrm{x}_m(\mathrm{x}, \lambda)) \left| \mathcal{J}_{\mathrm{x}}[\mathrm{x}_m(\mathrm{x}, \lambda)] \right|, \end{aligned} \tag{A.7}$$

where $\mathrm{x}_m(\mathrm{x}, \lambda)$ is an arbitrary element of mass that is regarded as a function of the pseudo-time λ and of the state x that it can possibly reach. The matrix $\mathcal{J}_{\mathrm{x}}[\mathrm{x}_m(\mathrm{x}, \lambda)]$ is the Jacobian matrix of $\mathrm{x}_m(\mathrm{x}, \lambda)$ with respect to x. Conceptually, at the stationary state $\mathrm{x}_m(\mathrm{x}_T, T) = \mathrm{x}_T$ the continuity equation (A.3) reads

$$\frac{\partial p}{\partial \lambda} = 0, \quad \lambda \geq T. \tag{A.8}$$

Using the general solution (A.7) to verify the stationary condition (A.8), we conclude that $p_0(\mathrm{x}_m(\mathrm{x}_T, T)) \left| \mathcal{J}_{\mathrm{x}}[\mathrm{x}_m(\mathrm{x}_T, T)] \right|$ must be constant with respect to the pseudo-time, thus

$$\frac{d\mathrm{x}_m(\lambda)}{d\lambda} = \mu(\mathrm{x}_m(\lambda)) = 0, \quad \lambda \geq T. \tag{A.9}$$

Following the assumption of conservative field, $\mu(\mathrm{x}_T) = -\nabla_{\mathrm{x}}\psi(\mathrm{x}_T) = 0$ implies that the stationary state x_T is an equilibrium point, i.e., an extreme of the potential function ψ. In addition, since the potential function is assumed to be related to the stationary distribution as $\psi(\mathrm{x}) \propto -\log \pi(\mathrm{x})$, the stationary state x_T is an extreme of the stationary density.

A valid Lyapunov function of the flow is $V(\mathrm{x}) = \psi(\mathrm{x})$, which is positive semi-definite ($\psi(\mathrm{x}) \geq 0$) in the neighbourhood of the equilibrium point due to the local log-concavity of the invariant density $\pi(\mathrm{x})$. Analysing the (Lie) time derivative of the Lyapunov function in the neighbourhood of the equilibrium point, $\|\mathrm{x} - \mathrm{x}_T\| < \varepsilon$ for a sufficiently small $\varepsilon \in \mathbb{R}^+$, we have

$$\begin{aligned} &\frac{dV(\mathrm{x})}{d\lambda} = \nabla_{\mathrm{x}} V(\mathrm{x})^T \cdot \frac{d\mathrm{x}}{d\lambda} = \nabla_{\mathrm{x}} V(\mathrm{x})^T \cdot \mu(\mathrm{x}), \\ &\dot{V}(\mathrm{x}) = \nabla_{\mathrm{x}} \psi(\mathrm{x})^T \cdot (-\nabla_{\mathrm{x}} \psi(\mathrm{x})), \\ &\dot{V}(\mathrm{x}) = -\left\| \nabla_{\mathrm{x}} \psi(\mathrm{x}) \right\|^2 \leq 0, \ \|\mathrm{x} - \mathrm{x}_T\| < \varepsilon; \end{aligned} \tag{A.10}$$

from which we conclude that x_T is a point of (uniformily) stable equilibrium.

Therefore, under the established hypotheses, any arbitrary probability mass $\mathrm{x}_m(\lambda)$ evolved according to (A.5) converges to

$$\mathrm{x}_m(T) = \operatorname{argmin}[\psi(\mathrm{x})] = \operatorname{argmin}[-\log \pi(\mathrm{x})],$$
$$\mathrm{x}_m(T) = \operatorname{argmax}[\pi(\mathrm{x})], \quad \lambda \geq T;$$

at a stable equilibrium. □

Lemma 4. *Let $\{\mathrm{X}_\lambda : t \leq \lambda \leq T\}$ be a diffusion process in $\mathbb{R}^{n_x}$ (hence a Markov process), solution of*

$$d\mathrm{X}_\lambda = \mu_f(\mathrm{X}_\lambda, \lambda)\, d\lambda + D_f(\lambda)^{1/2}\, dW_\lambda^P, \tag{A.11}$$
$$\mathrm{X}_\lambda(t) = \mathrm{x}_t, t \leq \lambda \leq T;$$

where $\{W_\lambda : t \leq \lambda \leq T\}$ is a standard Wiener process in $\mathbb{R}^{n_x}$ under the probability measure P, $\mu_f : \mathbb{R}^{n_x} \times [t,T] \to \mathbb{R}^{n_x}$ is the drift and $D_f : [t,T] \to \mathbb{R}^{n_x \times n_x}$ is a diffusion coefficient invariant over the space at any time instant. There exists an equivalent process $\left\{\bar{\mathrm{X}}_\tau, \mathcal{V}_\tau : t \leq \tau \leq T\right\}$, which is probabilistically the same as the original process, called reverse process *on the interval $[t,T]$ (see [91]), that provides the solution of the stochastic system*

$$d\bar{\mathrm{X}}_\tau = \mu_r\left(\bar{\mathrm{X}}_\tau, \tau\right) d\tau + D_r(\tau)^{1/2}\, d\bar{W}_\tau^P,\ \bar{\mathrm{X}}_\tau(t) = \bar{x}_t; \tag{A.12}$$
$$d\mathcal{V}_\tau = v_r\left(\bar{\mathrm{X}}_\tau, \tau\right)\mathcal{V}_\tau d\tau, \qquad \mathcal{V}_\tau(t) = 1; \tag{A.13}$$

for a standard Wiener process $\left\{\bar{W}_\tau : t \leq \tau \leq T\right\}$ in $\mathbb{R}^{n_x}$ under the measure P, with the reverse drift and diffusion coefficients given, respectively, by

$$\mu_r\left(\bar{\mathrm{X}}_\tau, \tau\right) = -\mu_f\left(\bar{\mathrm{X}}_\tau, T + t - \lambda\right), \tag{A.14}$$
$$D_r(\tau) = \quad D_f(T + t - \lambda). \tag{A.15}$$

Proof. The Markov process $\{\mathrm{X}_\lambda\}$, as an existing solution to the SDE (A.11), has an associated probability density $p(\mathrm{x}_\lambda, \lambda)$ that must satisfy the Kolmogorov forward equation (Fokker-Planck equation):

$$\frac{\partial}{\partial\lambda} p = -\nabla_{\mathrm{x}} \cdot (\mu_f p) + \frac{1}{2} D_f \Delta_{\mathrm{x}} p,\ \lambda \geq t,$$
$$p(\mathrm{x}_\lambda, t) = p_t(\mathrm{x}_t), \mathrm{x}_\lambda \in \mathbb{R}^{n_x}.$$

The Fokker-Planck equation can be written in the non-divergence form as

$$\frac{\partial}{\partial\lambda} p = \tilde{\mu}^T \nabla_{\mathrm{x}} p + \frac{1}{2} D_f \Delta_{\mathrm{x}} p + \tilde{v} \cdot p, \tag{A.16}$$

where

$$\tilde{\mu}(\mathrm{x}_\lambda) = -\mu_f(\mathrm{x}_\lambda),$$
$$\tilde{v}(\mathrm{x}_\lambda) = -\nabla_{\mathrm{x}} \cdot \mu_f(\mathrm{x}_\lambda).$$

We introduce the reverse time variable $\tau = T + t - \lambda$, so that

$$p(\mathrm{x}_\lambda(T + t - \lambda), T + t - \lambda) \equiv \tilde{p}(\bar{\mathrm{x}}_\tau, \tau),$$

and hence $-\partial_\lambda \tilde{p} = \partial_\tau \tilde{p}$. Thus, rewritting (A.16) with respect to $\tilde{p}(\bar{\mathrm{x}}_\tau, \tau)$ for $\tau \leq T$, $\bar{\mathrm{x}}_\tau \in \mathbb{R}^{n_x}$, and performing the substitutions

$$\mu_r(\bar{\mathrm{x}}_\tau, \tau) = -\mu_f(\mathrm{x}_\lambda(T + t - \lambda), T + t - \lambda),$$
$$D_r(\tau) = \quad D_f(T + t - \lambda),$$

we obtain

$$\begin{aligned}
\frac{\partial}{\partial\lambda}p &= -\mu_f^T\nabla_{\mathrm{x}}p + \frac{1}{2}D_f\Delta_{\mathrm{x}}p + (-\nabla_{\mathrm{x}}\cdot\mu_f)\cdot p,\\
-\frac{\partial}{\partial\tau}\tilde{p} &= \mu_r^T\nabla_{\mathrm{x}}\tilde{p} + \frac{1}{2}D_r\Delta_{\mathrm{x}}\tilde{p} - (-\nabla_{\mathrm{x}}\cdot\mu_r)\cdot\tilde{p},\\
-\frac{\partial}{\partial\tau}\tilde{p} &= \mu_r^T\nabla_{\mathrm{x}}\tilde{p} + \frac{1}{2}D_r\Delta_{\mathrm{x}}\tilde{p} - v_r\cdot\tilde{p},\ \tau\leq T,\\
&\quad\ \tilde{p}\left(\bar{\mathrm{x}}_\tau, T\right) = \tilde{p}_T\left(\bar{\mathrm{x}}_T\right) = p_t\left(\mathrm{x}_t\right), \bar{\mathrm{x}}_\tau\in\mathbb{R}^{n_x};
\end{aligned} \tag{A.17}$$

where

$$v_r\left(\bar{\mathrm{x}}_\tau,\tau\right) = -\nabla_{\mathrm{x}}\mu_r\left(\bar{\mathrm{x}}_\tau,\tau\right). \tag{A.18}$$

Solving (A.17) corresponds to the Cauchy problem in reverse time $\tau\leq T$, which is equivalent to solve the stochastic system stated by (A.12) and (A.13). Therefore, because the solution to the SDE (A.11) is assumed to exist and corresponds to the solution of (A.17) for $\tau\leq T$, then there exists the equivalent reverse process $\left\{\bar{\mathrm{X}}_\tau,\mathcal{V}_\tau\right\}$ that solves the stochastic system (A.12) and (A.13). □

Remark 5. Despite its name, inherited from [91], it is worth stressing that $\left\{\bar{\mathrm{X}}_\tau,\mathcal{V}_\tau\right\}$ is the solution of a stochastic system forward in time on the interval $[t,T]$, which may be properly understood as a smoothing process.

Remark 6. It is clear that the general solution to (A.13) is

$$\mathcal{V}_\tau\left(T\right) = e^{-\int_t^T v_r\left(\bar{\mathrm{x}}_\tau,\tau\right)d\tau},$$

which leads to the solution of (A.17) by the Feynman-Kac formula

$$\tilde{p}\left(\mathrm{x},\tau\right) = \mathbb{E}^P\left[e^{-\int_\tau^T v_r\left(\bar{\mathrm{x}}_{\tau'},\tau'\right)d\tau'}\tilde{p}_T\left(\bar{\mathrm{x}}_T\right)|\bar{\mathrm{x}}_\tau=\mathrm{x}\right]. \tag{A.19}$$

A more general form of the *Lemma 4* can be found in [91].

Lemma 7. *The reverse process* $\left\{\bar{\mathrm{X}}_\tau,\mathcal{V}_\tau : t\leq\tau\leq T\right\}$ *described by (A.12) and (A.13), has an associated smooth probability density* $\tilde{p}\left(\bar{\mathrm{x}}_\tau,\tau\right)$ *that satisfies, for the initial value problem, the Kolmogorov forward equation*

$$\begin{aligned}
\frac{\partial}{\partial\tau}\tilde{p} &= -\nabla_{\mathrm{x}}\cdot\left(\mu_r\tilde{p}\right) + \frac{1}{2}D_r\Delta_{\mathrm{x}}\tilde{p} - v_r\cdot\tilde{p},\ t\leq\tau\leq T,\\
&\quad\ \tilde{p}\left(\bar{\mathrm{x}}_\tau(t),\tau=t\right) = \tilde{p}_t\left(\bar{\mathrm{x}}_t\right), \bar{\mathrm{x}}_\tau\in\mathbb{R}^{n_x}.
\end{aligned} \tag{A.20}$$

Proof. We assume a bounded, continuous function of the process $\left\{\bar{\mathrm{X}}_\tau,\mathcal{V}_\tau\right\}$, $\varphi:\mathbb{R}^{n_x}\times\mathbb{R}^{n_x}\to\mathbb{R}^{n_x}$, $\varphi(\bar{\mathrm{X}}_\tau,\mathcal{V}_\tau)\in\mathcal{C}^{2^{n_x}}$, apply the Îto's lemma to it and substitute (A.12) and (A.13) to obtain

$$\begin{aligned}
d\varphi &= \partial_{\bar{\mathrm{X}}_\tau}\varphi\, d\bar{\mathrm{X}}_\tau + \frac{1}{2}D_r\partial^2_{\bar{\mathrm{X}}_\tau\bar{\mathrm{X}}_\tau}\varphi\, d\tau + \partial_{\mathcal{V}_\tau}\varphi\, d\mathcal{V}_\tau\\
&= \partial_{\bar{\mathrm{X}}_\tau}\varphi\cdot\left(\mu_r d\tau + {D_r}^{1/2}d\bar{W}_\tau\right) + \frac{1}{2}D_r\partial^2_{\bar{\mathrm{X}}_\tau\bar{\mathrm{X}}_\tau}\varphi\, d\tau\\
&\quad + \partial_{\mathcal{V}_\tau}\varphi\cdot\left(v_r\mathcal{V}_\tau d\tau\right).
\end{aligned} \tag{A.21}$$

Consider the expected (average) rate of change of all possible projections of φ defined by realisations $\gamma_\tau = \mathcal{V}_\tau(\bar{\mathrm{x}}_\tau)$ as:

$$\begin{aligned}\langle\dot{\varphi}_{\mathcal{V}_\tau}\rangle(\tau) &\triangleq \left\langle \frac{d}{d\tau}\int_1^{\gamma_\tau} \varphi(\bar{\mathrm{X}}_\tau,\mathcal{V}_\tau)d\mathcal{V}_\tau \right\rangle \\ &= \left\langle \int_1^{\gamma_\tau} \partial_\tau\varphi(\bar{\mathrm{X}}_\tau,\mathcal{V}_\tau)d\mathcal{V}_\tau \right\rangle \\ &\equiv \int_{\mathbb{R}^{n_x}}\int_1^{\gamma_\tau} \varphi\left(\bar{\mathrm{x}}_\tau,\upsilon_\tau\right)\partial_\tau\tilde{p}\,d\upsilon_\tau d\bar{\mathrm{x}}_\tau. \end{aligned} \tag{A.22}$$

Substituting (A.21) into (A.22), we have

$$\begin{aligned}\langle\dot{\varphi}_{\mathcal{V}_\tau}\rangle &= \left\langle \int_1^{\gamma_\tau} \partial_\tau\varphi(\bar{\mathrm{X}}_\tau,\mathcal{V}_\tau)d\mathcal{V}_\tau \right\rangle \\ &= \left\langle \int_1^{\gamma_\tau} \left[\partial_{\bar{\mathrm{X}}_\tau}\varphi\cdot\mu_r + \frac{1}{2}D_r\partial^2_{\bar{\mathrm{X}}_\tau\bar{\mathrm{X}}_\tau}\varphi\right]d\mathcal{V}_\tau \right\rangle \\ &+ \left\langle \int_1^{\gamma_\tau} \left[\partial_{\mathcal{V}_\tau}\varphi\cdot v_r\mathcal{V}_\tau\right]d\mathcal{V}_\tau \right\rangle \\ &= \int_1^{\bar{\gamma}_\tau}\int_{\mathbb{R}^{n_x}} \left[\partial_{\bar{\mathrm{x}}_\tau}\varphi\cdot\mu_r + \frac{1}{2}D_r\partial^2_{\bar{\mathrm{x}}_\tau\bar{\mathrm{x}}_\tau}\varphi\right]\tilde{p}\,d\bar{\mathrm{x}}_\tau d\upsilon_\tau \\ &+ \int_{\mathbb{R}^{n_x}}\int_1^{\gamma_\tau} \left[\partial_{\upsilon_\tau}\varphi\cdot v_r\upsilon_\tau\right]\tilde{p}\,d\upsilon_\tau d\bar{\mathrm{x}}_\tau. \end{aligned} \tag{A.23}$$

Integrating (A.23) by parts and offsetting the integration constant to cancel out the surface terms, we have

$$\begin{aligned}\langle\dot{\varphi}_{\mathcal{V}_\tau}\rangle &= \int_1^{\bar{\gamma}_\tau}\int_{\mathbb{R}^{n_x}} \varphi\left[-\partial_{\bar{\mathrm{x}}_\tau}(\mu_r\tilde{p}) + \frac{1}{2}D_r\partial^2_{\bar{\mathrm{x}}_\tau\bar{\mathrm{x}}_\tau}\tilde{p}\right]d\bar{\mathrm{x}}_\tau d\upsilon_\tau \\ &+ \int_{\mathbb{R}^{n_x}}\int_1^{\gamma_\tau} \varphi\left[-v_r\partial_{\upsilon_\tau}(\upsilon_\tau\tilde{p})\right]d\upsilon_\tau d\bar{\mathrm{x}}_\tau \\ &= \int_{\mathbb{R}^{n_x}}\int_1^{\gamma_\tau} \varphi\left[-\partial_{\bar{\mathrm{x}}_\tau}(\mu_r\tilde{p}) + \frac{1}{2}D_r\partial^2_{\bar{\mathrm{x}}_\tau\bar{\mathrm{x}}_\tau}\tilde{p}\right]d\upsilon_\tau d\bar{\mathrm{x}}_\tau \\ &+ \int_{\mathbb{R}^{n_x}}\int_1^{\gamma_\tau} \varphi\left[-v_r\tilde{p}\right]d\upsilon_\tau d\bar{\mathrm{x}}_\tau. \end{aligned} \tag{A.24}$$

The proof of the lemma is complete by comparing (A.24) to the definition (A.22) and noting that their integrands must be equal. □

Theorem 8. *Let $(\Omega,\mathcal{F},P)$ to be a complete probability space and let $\{\mathcal{F}_\lambda\}_{\lambda\geq 0}$, $\lambda\in[0,T]$, be an increasing family of sub σ-fields of $\mathcal{F}$. Let $\{\mathrm{X}_\lambda : 0<\lambda\leq T\}$ be an $\mathcal{F}_\lambda$-adapted process, considered to be the signal process with state equation*

$$\begin{aligned} d\mathrm{X}_\lambda &= \mu_f\left(\mathrm{X}_\lambda\right)d\lambda + D_f\left(\lambda\right)^{1/2}dW^P_\lambda, \\ \mathrm{X}_\lambda\left(0\right) &= \mathrm{x}_0,\ 0\leq\lambda\leq T; \end{aligned} \tag{A.25}$$

for a Wiener process $\{W_\lambda\}$ under the probability measure P. Assume $p(\mathrm{x}_\lambda,\lambda)$ defined on $(\Omega,\mathcal{F})$ to be the probability density of the measure P, according to $dP = p(\mathrm{x}_\lambda)d\mathrm{x}_\lambda$, that

(a) is the probabilistic representation of the process $\{\mathrm{X}_\lambda\}$,

(b) is absolutely continuous with respect to the Lesbesque measure,

(c) approaches a stationary distribution by $p(\mathrm{x}_\lambda)\overset{\lambda\to T}{\longrightarrow}\pi\left(\mathrm{x}_\lambda\right)\propto e^{-\Phi(\mathrm{x}_\lambda)}$, for a sufficiently long time horizon T.

Let $\left\{\bar{X}_\tau,\mathcal{V}_\tau : \lambda<\tau\leq T\right\}$ be the reverse process of $\{\mathrm{X}_\lambda\}$, as established in Lemma 4 by the stochastic system (A.12) and (A.13), so that the reverse drift and diffusion coefficients are, respectively,

$$\mu_r\left(\bar{\mathrm{x}}_\tau\right) = -\frac{1}{2} D_r\left(\lambda\right) \nabla_{\mathrm{x}} \log \pi\left(\bar{\mathrm{x}}_\tau\right),$$
$$D_r\left(\tau\right) = \left[-\mathcal{H}_{\mathrm{x}}\left[\log \pi\left(\bar{\mathrm{x}}_\tau\right)\right]\right]^{-1}.$$

Assume $\tilde{p}(\bar{\mathrm{x}}_\tau, \tau)$ defined on $(\Omega, \mathcal{F})$ to be the probability density describing the reverse process $\left\{\bar{X}_\tau, \mathcal{V}_\tau\right\}$, under the same measure P, which must satisfy the Kolmogorov forward equation (provided a known initial condition) according to Lemma 7:

$$\frac{\partial}{\partial \tau}\tilde{p} = -\nabla_{\mathrm{x}} \cdot \left(\mu_r \tilde{p}\right) + \frac{1}{2} D_r \Delta_{\mathrm{x}} \tilde{p} - v_r \cdot \tilde{p},\ \lambda \leq \tau \leq T, \tag{A.26}$$
$$\tilde{p}\left(\bar{\mathrm{x}}_\tau\left(\lambda\right), \tau = \lambda\right) = \tilde{p}_\lambda\left(\bar{\mathrm{x}}_\tau\left(\lambda\right)\right) = \pi\left(\mathrm{x}_T\right), \bar{\mathrm{x}}_\tau \in \Omega;$$

If the stationary density is set to be

$$\pi\left(\mathrm{x}\right) \coloneqq \frac{p\left(\mathrm{y}_k|\mathrm{x}\right) p\left(\mathrm{x}|\mathrm{y}_{1:k-1}\right)}{Z_1} = \frac{p\left(\mathrm{y}_k|\mathrm{x}\right) p_x\left(\mathrm{x}\right)}{Z_1}, \tag{A.27}$$

where the prior density $p_x(\mathrm{x})$ and the likelihood $p(\mathrm{y}_k|\mathrm{x})$ are integrable functions with respect to x, $Z_1 = p(\mathrm{y}_k|\mathrm{y}_{1:k-1})$ is a normalisation constant, and the discrete-time observation process $\{\mathrm{y}_k \in \mathbb{R}^{n_y} : k \in \mathbb{N}\}$ is described as

$$\mathrm{y}_k = h\left(\mathrm{x}_k\right) + R^{1/2}\nu_k, \quad \nu_k \sim \mathcal{N}(\nu_k; 0_{n_y}, \mathrm{I}_{n_y}); \tag{A.28}$$

then the probability density corresponding to the signal process (A.25) is equivalent to the following filtering entity

$$p(\mathrm{x}, \lambda|\mathcal{F}_\lambda) = \frac{\mathbb{E}^P\left[e^{h(\mathrm{x}_T)^T R^{-1}\mathrm{y}_k - \frac{1}{2}h(\mathrm{x}_T)^T R^{-1} h(\mathrm{x}_T)}|\mathrm{x}\right] p\left(\mathrm{x}|\mathrm{y}_{1:k-1}\right)}{Z}. \tag{A.29}$$

In addition, the expression (A.29) can be interpreted as the analogous to the well known result (see [92])

$$p(\mathrm{x}, \lambda|\mathcal{F}_\lambda) = \frac{\mathbb{E}^P\left[e^{\int_0^T h_T(\mathrm{x}_\lambda)^T R^{-1} d\mathrm{y}_\lambda - \frac{1}{2}\int_0^T h_T(\mathrm{x}_\lambda)^T R^{-1} h_T(\mathrm{x}_\lambda) d\lambda}|\mathrm{x}\right]}{Z} p\left(\mathrm{x}|\mathrm{y}_{1:k-1}\right), \tag{A.30}$$

for a discrete-time observation process whose analog continuous-time (interpolated) version has the observation function $h_T(.)$.

Proof. By definition of the stochastic system described by (A.12) and (A.13), and *Lemma 7*, the reverse process $\left\{\bar{X}_\tau, \mathcal{V}_\tau\right\}$ is known to satisfy the Kolmogorov forward equation (A.26) in reverse time $\lambda \leq \tau \leq T$, for which the stationary distribution π is an initial condition (initial value problem). Using the reverse time variable $\tau = T - \lambda$, so that $p\left(\mathrm{x}_\lambda, \lambda\right) \equiv \tilde{p}\left(\bar{\mathrm{x}}_\tau(T-\tau), T-\tau\right)$ and $\partial_\lambda p = -\partial_\tau p$; and applying the relations (A.14), (A.15) and (A.18) from *Lemma 4*; we rewrite the equation (A.26) for $0 \leq \lambda \leq T$ as

$$\begin{aligned}
\frac{\partial}{\partial \tau}\tilde{p} &= -\nabla_{\mathrm{x}} \cdot \left(\mu_r \tilde{p}\right) + \frac{1}{2} D_r \Delta_{\mathrm{x}} \tilde{p} - v_r \cdot \tilde{p},\ \lambda \leq \tau \leq T, \\
\frac{\partial}{\partial \tau}\tilde{p} &= -\left(\nabla_{\mathrm{x}} \cdot \mu_r\right)\tilde{p} - \mu_r^T \nabla_{\mathrm{x}} \tilde{p} + \frac{1}{2} D_r \Delta_{\mathrm{x}} \tilde{p} + \left(\nabla_{\mathrm{x}} \cdot \mu_r\right)\tilde{p}, \\
\frac{\partial}{\partial \tau}\tilde{p} &= -\mu_r^T \nabla_{\mathrm{x}} \tilde{p} + \frac{1}{2} D_r \Delta_{\mathrm{x}} \tilde{p}, \\
-\frac{\partial}{\partial \lambda} p &= +\mu_f^T \nabla_{\mathrm{x}} p + \frac{1}{2} D_f \Delta_{\mathrm{x}} p,\ 0 \leq \lambda \leq T, \\
p\left(\mathrm{x}_\lambda, T\right) &= \pi\left(\mathrm{x}_T\right), \mathrm{x}_\lambda \in \Omega.
\end{aligned} \tag{A.31}$$

Now we have a Kolmogorov backward equation in $p\left(\mathrm{x}_\lambda, \lambda\right)$ with a terminal value problem for the forward process $\{\mathrm{X}_\lambda\}$. Hence, we can apply the Feynman-Kac formula for the terminal condition $p(\mathrm{x}, T) = \pi\left(\mathrm{x}\right)$, with $\mathrm{x}_T = \mathrm{x}_\lambda(T)$, to give

$$\begin{aligned}
p(\mathrm{x}, \lambda) &\triangleq \mathbb{E}^P\left[\pi\left(\mathrm{x}_T\right)|\mathrm{x}_\lambda = \mathrm{x}\right] \\
&= \frac{\mathbb{E}^P\left[p\left(\mathrm{y}_k|\mathrm{x}_T\right)p\left(\mathrm{x}_T|\mathrm{y}_{1:k-1}\right)|\mathrm{x}_\lambda = \mathrm{x}\right]}{Z_1} \\
&= \frac{\mathbb{E}^P\left[e^{-\frac{1}{2}\left(\mathrm{y}_k - h\left(\mathrm{x}_T\right)\right)^T R^{-1}\left(\mathrm{y}_k - h\left(\mathrm{x}_T\right)\right)} p_x\left(\mathrm{x}_T\right)|\mathrm{x}\right]}{Z_1\left(2\pi R\right)^{n_y/2}} \\
&= \frac{\mathbb{E}^P\left[e^{h\left(\mathrm{x}_T\right)^T R^{-1}\mathrm{y}_k - \frac{1}{2}h\left(\mathrm{x}_T\right)^T R^{-1}h\left(\mathrm{x}_T\right)} p_x\left(\mathrm{x}_T\right)|\mathrm{x}\right]}{Z_1\left(2\pi R\right)^{n_y/2} e^{+\frac{1}{2}\mathrm{y}_k^T R^{-1}\mathrm{y}_k}} \\
&= \frac{\mathbb{E}^P\left[e^{h\left(\mathrm{x}_T\right)^T R^{-1}\mathrm{y}_k - \frac{1}{2}h\left(\mathrm{x}_T\right)^T R^{-1}h\left(\mathrm{x}_T\right)} p_x\left(\mathrm{x}_T\right)|\mathcal{F}_\lambda, \mathrm{x}\right]}{Z}.
\end{aligned} \tag{A.32}$$

If we reinterpret the discrete-time observation process as a continuous-time process for which we only obtain a realisation at $\lambda = T$, by linearly interpolating it along the interval $0 < \lambda \leq T$ we can write

$$\begin{aligned}
d\mathrm{y}_\lambda &= \frac{1}{T}h\left(\mathrm{x}_\lambda\right)d\lambda + R^{1/2}\frac{1}{\sqrt{T}}\nu_k d\lambda^{1/2}, \\
d\mathrm{y}_\lambda &= h_T\left(\mathrm{x}_\lambda\right)d\lambda + R^{1/2}d\bar{\nu}_\lambda^Q, \quad 0 < \lambda \leq T;
\end{aligned} \tag{A.33}$$

where $\{\bar{\nu}_\lambda\}$ is an interpolated Wiener process that produces the observation noise ν_k at $\lambda = T$, under a probability measure Q, such that $\mathrm{y}_\lambda(T) = \mathrm{y}_k$. By applying the Girsanov theorem, we know that the Radon-Nykodym derivative assumes the form (see [12] for example)

$$\begin{aligned}
\left.\frac{dQ}{dP}\right|_{\mathcal{F}_T} &= e^{\int_0^T h_T\left(\mathrm{x}_\lambda\right)^T R^{-1}d\mathrm{y}_\lambda - \frac{1}{2}\int_0^T h_T\left(\mathrm{x}_\lambda\right)^T R^{-1}h_T\left(\mathrm{x}_\lambda\right)d\lambda} \\
&\propto e^{h\left(\mathrm{x}_T\right)^T R^{-1}\mathrm{y}_k - \frac{1}{2}h\left(\mathrm{x}_T\right)^T R^{-1}h\left(\mathrm{x}_T\right)}.
\end{aligned} \tag{A.34}$$

Rewritting (A.32) in terms of (A.34) and manipulating it further, we obtain

$$\begin{aligned}
p(\mathrm{x}, \lambda) &\propto \mathbb{E}^P\left[e^{h\left(\mathrm{x}_T\right)^T R^{-1}\mathrm{y}_k - \frac{1}{2}h\left(\mathrm{x}_T\right)^T R^{-1}h\left(\mathrm{x}_T\right)} p_x\left(\mathrm{x}_T\right)|\mathcal{F}_\lambda, \mathrm{x}\right] \\
&\equiv \mathbb{E}^P\left[\frac{dQ}{dP}\left(T\right)\cdot p_x\left(\mathrm{x}_T\right)|\mathcal{F}_\lambda, \mathrm{x}\right] \\
&= \mathbb{E}^P\left[\frac{dQ}{dP}\left(T\right)\cdot \mathbb{E}^Q\left[p_x\left(\mathrm{x}_\lambda\right)|\mathcal{F}_T, \mathrm{x}\right]|\mathcal{F}_\lambda, \mathrm{x}\right] \\
&= \mathbb{E}^P\left[\frac{dQ}{dP}\left(T\right)|\mathcal{F}_\lambda, \mathrm{x}\right]\cdot \mathbb{E}^Q\left[p_x\left(\mathrm{x}_\lambda\right)|\mathcal{F}_T, \mathrm{x}\right] \\
&\equiv \mathbb{E}^P\left[e^{h\left(\mathrm{x}_T\right)^T R^{-1}\mathrm{y}_k - \frac{1}{2}h\left(\mathrm{x}_T\right)^T R^{-1}h\left(\mathrm{x}_T\right)}|\mathcal{F}_\lambda, \mathrm{x}\right] p_x\left(\mathrm{x}\right),
\end{aligned} \tag{A.35}$$

where we take into account the smoothing property for conditional expectations as

$$\begin{aligned}
p(\mathrm{x}, \lambda) &\propto \mathbb{E}^P\left[\frac{dQ}{dP}\left(T\right)\cdot p_x\left(\mathrm{x}_T\right)|\mathcal{F}_\lambda, \mathrm{x}_\lambda = \mathrm{x}\right] \\
&= \mathbb{E}^Q\left[p_x\left(\mathrm{x}_T\right)|\mathcal{F}_\lambda, \mathrm{x}\right] \\
&= \mathbb{E}^Q\left[\mathbb{E}^Q\left[p_x\left(\mathrm{x}_\lambda\right)|\mathcal{F}_T, \mathrm{x}\right]|\mathcal{F}_\lambda, \mathrm{x}\right] \\
&= \mathbb{E}^P\left[\frac{dQ}{dP}\left(T\right)\cdot \mathbb{E}^Q\left[p_x\left(\mathrm{x}_\lambda\right)|\mathcal{F}_T, \mathrm{x}\right]|\mathcal{F}_\lambda, \mathrm{x}\right],
\end{aligned}$$

the $\mathcal{F}_\lambda$-measurability of $\mathbb{E}^Q\left[p_x\left(\mathrm{x}_\lambda\right)|\mathcal{F}_T, \mathrm{x}_\lambda = \mathrm{x}\right]$, and

$$\begin{aligned}\mathbb{E}^Q\left[p_x\left(\mathrm{x}_\lambda\right)|\mathcal{F}_T, \mathrm{x}_\lambda = \mathrm{x}\right] &= \int p_x\left(\mathrm{x}\right) dQ(\mathrm{y}_\lambda) \\ &= p_x\left(\mathrm{x}\right) = p\left(\mathrm{x}|\mathrm{y}_{1:k-1}\right).\end{aligned}$$

As a result, the expression (A.35) can be written in the normalised form (A.29), proving the theorem statement. The proof is complete by inserting the continuous-time (interpolated) version of (A.34) into (A.35) to verify the analogy with (A.30). □

Remark 9. A result more general than the one presented by *Theorem 8*, in terms of McKean-Vlasov diffusions, can be found in [18].

Corollary 10. *The signal process with state equation (A.25), under the hypotheses of Theorem 8, filters its associated (unnormalised) probability density in accordance with the Zakai equation*

$$dp_u = \mathcal{L}\left[p_u\right] d\lambda + p_u \cdot h\left(\mathrm{x}_\lambda\right)^T R^{-1} d\mathrm{y}_\lambda, \quad 0 < \lambda \leq T; \tag{A.36}$$

where $\mathcal{L}\left[.\right] = -\nabla_{\mathrm{x}} \cdot (\mu \cdot) + {}^1\!/_2 \Delta_{\mathrm{x}}\left(D.\right)$ *is the forward Kolmogorov operator, and* $\{\mathrm{y}_\lambda : 0 < \lambda \leq T\}$ *is the continuous, linearly interpolated observation process defined by (A.33) for which the realisation is only taken at* $\lambda = T$.

Proof. Define

$$\begin{aligned}d\zeta_\lambda &= h_T\left(\mathrm{x}_\lambda\right)^T R^{-1} d\mathrm{y}_\lambda - \frac{1}{2} h_T\left(\mathrm{x}_\lambda\right)^T R^{-1} h_T\left(\mathrm{x}_\lambda\right) d\lambda \\ &= \frac{1}{2} h_T\left(\mathrm{x}_\lambda\right)^T R^{-1} h_T\left(\mathrm{x}_\lambda\right) d\lambda + h_T\left(\mathrm{x}_\lambda\right)^T R^{-{}^1\!/_2} d\bar{\nu}_\lambda^Q,\end{aligned} \tag{A.37}$$

and recognise the unnormalised probability density to be the numerator of (A.30):

$$p_u = \mathbb{E}^P\left[e^{\zeta_T}|\mathrm{x}\right] p_x\left(\mathrm{x}\right). \tag{A.38}$$

Applying the Îto's Lemma to p_u we get

$$\begin{aligned}dp_u &= \partial_\lambda p_u d\lambda + \partial_\zeta p_u d\zeta_\lambda \\ &\quad + \frac{1}{2}\left[h_T\left(\mathrm{x}_\lambda\right)^T R^{-{}^1\!/_2}\right]\left[R^{-{}^1\!/_2} h_T\left(\mathrm{x}_\lambda\right)\right] \partial^2_{\zeta\zeta} p_u d\lambda \\ &= \partial_\lambda p_u d\lambda + \partial_\zeta p_u d\zeta_\lambda \\ &\quad + \frac{1}{2} h_T\left(\mathrm{x}_\lambda\right)^T R^{-1} h_T\left(\mathrm{x}_\lambda\right) \partial^2_{\zeta\zeta} p_u d\lambda.\end{aligned} \tag{A.39}$$

Because

$$\begin{aligned}\partial_\zeta p_u &= \partial^2_{\zeta\zeta} p_u = p_u, \\ \partial_\lambda p_u &= \mathbb{E}^P\left[e^{-\int_0^T d\zeta_\lambda}|\mathrm{x}\right] \partial_\lambda p_x\left(\mathrm{x}\right) = \mathcal{L}\left[p_u\right];\end{aligned}$$

the expression (A.39) becomes the Zakai equation as

$$
\begin{aligned}
dp_u &= \mathcal{L}\left[p_u\right] d\lambda \\
&\quad + p_u \cdot \left[\frac{1}{2} h_T\left(\mathrm{x}_\lambda\right)^T R^{-1} h_T\left(\mathrm{x}_\lambda\right) d\lambda + h_T\left(\mathrm{x}_\lambda\right)^T R^{-1/2} d\bar{\nu}_\lambda^Q\right] \\
&\quad + p_u \cdot \frac{1}{2} h_T\left(\mathrm{x}_\lambda\right)^T R^{-1} h_T\left(\mathrm{x}_\lambda\right) d\lambda \\
&= \mathcal{L}\left[p_u\right] d\lambda \\
&\quad + p_u \cdot \left[h_T\left(\mathrm{x}_\lambda\right)^T R^{-1} h_T\left(\mathrm{x}_\lambda\right) d\lambda + h_T\left(\mathrm{x}_\lambda\right)^T R^{-1/2} d\bar{\nu}_\lambda^Q\right] \\
&= \mathcal{L}\left[p_u\right] d\lambda + p_u \cdot h_T\left(\mathrm{x}_\lambda\right)^T R^{-1} \left[h_T\left(\mathrm{x}_\lambda\right) d\lambda + R^{1/2} d\bar{\nu}_\lambda^Q\right] \\
&= \mathcal{L}\left[p_u\right] d\lambda + p_u \cdot h_T\left(\mathrm{x}_\lambda\right)^T R^{-1} d\mathrm{y}_\lambda.
\end{aligned}
$$

□

B Derivation of the integration rule

We intend to approximate the integration of the following equation with respect to λ:

$$
d\mathrm{x} = \frac{1}{2} D\left(\lambda\right) \cdot \nabla_{\mathrm{x}} \log \pi\left(\mathrm{x}\right) d\lambda + D\left(\lambda\right)^{1/2} d\mathrm{w}_\lambda. \tag{B.1}
$$

Linearising equation (B.1) w.r.t. x around the current state x_{n-1}, we have

$$
d\mathrm{x} = A \cdot \mathrm{x}\, d\lambda + B\, d\lambda + D^{1/2} d\mathrm{w}_\lambda, \tag{B.2}
$$

where

$$
\begin{aligned}
A\left(\mathrm{x}_{n-1}\right) &= {}^1\!/_2 D\left(\lambda_{n-1}\right) \cdot \mathcal{H}_{\mathrm{x}} \left[\log \pi\left(\mathrm{x}\right)\right]_{\mathrm{x}_{n-1}}, \\
B\left(\mathrm{x}_{n-1}\right) &= a\left(\mathrm{x}_{n-1}\right) - A \cdot \mathrm{x}_{n-1}, \\
a\left(\mathrm{x}_{n-1}\right) &= {}^1\!/_2 D\left(\lambda_{n-1}\right) \cdot \nabla_{\mathrm{x}} \log \pi\left(\mathrm{x}\right)\big|_{\mathrm{x}_{n-1}}.
\end{aligned} \tag{B.3}
$$

If we apply the definition $D\left(\lambda_{n-1}\right) = -\mathcal{H}_{\mathrm{x}} \left[\log \pi\left(\mathrm{x}\right)\right]^{-1}_{\mathrm{x}_{n-1}}$, where $\mathcal{H}_{\mathrm{x}}\left[.\right]$ is the Hessian w.r.t. x, we have

$$
A = -\frac{1}{2} \mathrm{I}_{n_x}, \tag{B.4}
$$

where I_{n_x} is the identity matrix with dimension $n_x \times n_x$. Based on the Laplace transform, we can obtain the solution for a homogeneous version of the equation (B.2) in discrete time by

$$
\begin{aligned}
\mathrm{x}\left(\lambda\right) &= \mathcal{L}^{-1} \left\{\left(s \cdot \mathrm{I}_{n_x} - A\right)^{-1} \mathrm{x}\left(\lambda_{n-1}\right)\right\} \\
&= \int_{\lambda_{n-1}}^{\lambda} \left(s \cdot \mathrm{I}_{n_x} - A\right)^{-1} e^{s \cdot \mathrm{I}_{n_x} \cdot \tau} \mathrm{x}\left(\lambda_{n-1}\right) ds \\
&= e^{A \cdot \left(\lambda - \lambda_{n-1}\right)} \mathrm{x}\left(\lambda_{n-1}\right), \\
\mathrm{x}_n &= e^{A \cdot \Delta\lambda} \mathrm{x}_{n-1}.
\end{aligned} \tag{B.5}
$$

By a similar procedure, and considering the definition of a Wiener integral for the stochastic term, we can obtain the solution of the complete inhomogeneous equation (B.2) as

$$
\begin{aligned}
\mathrm{x}\left(\lambda_n\right) &= e^{A\cdot\Delta\lambda}\mathrm{x}\left(\lambda_{n-1}\right) + \int_{\lambda_{n-1}}^{\lambda_n} e^{-A\cdot(\tau-\Delta\lambda)} B\, d\tau \\
&\quad + \sqrt{\int_{\lambda_{n-1}}^{\lambda_n} e^{-A\cdot(\tau-\Delta\lambda)} D\left(\lambda_{n-1}\right) e^{-A^T\cdot(\tau-\Delta\lambda)} d\tau}\cdot \mathrm{w}_n, \\
\mathrm{x}_n &= e^{A\cdot\Delta\lambda}\mathrm{x}_{n-1} + A^{-1}\left[e^{A\cdot\Delta\lambda} - \mathrm{I}_{n_x}\right]\left[a - A\cdot\mathrm{x}_{n-1}\right] \\
&\quad + \sqrt{\int_0^{\Delta\lambda} e^{A\cdot\nu} D\left(\lambda_{n-1}\right) e^{A^T\cdot\nu} d\nu}\cdot \mathrm{w}_n \\
&= \mathrm{x}_{n-1} + A^{-1}\left[e^{A\cdot\Delta\lambda} - \mathrm{I}_{n_x}\right] a\left(\mathrm{x}_{n-1}\right) \\
&\quad + \sqrt{\int_0^{\Delta\lambda} e^{A\cdot\nu} D\left(\lambda_{n-1}\right) e^{A^T\cdot\nu} d\nu}\cdot \mathrm{w}_n,
\end{aligned} \tag{B.6}
$$

where $\mathrm{w}_n \sim \mathcal{N}(\mathrm{w};\, 0_{n_x}, \mathrm{I}_{n_x})$. Substituting (B.4) into (B.6), we have

$$
\begin{aligned}
\mathrm{x}_n &= \mathrm{x}_{n-1} + \left[-\frac{1}{2}\mathrm{I}_{n_x}\right]^{-1}\left[e^{-\frac{1}{2}\mathrm{I}_{n_x}\cdot\Delta\lambda} - \mathrm{I}_{n_x}\right] a\left(\mathrm{x}_{n-1}\right) \\
&\quad + \sqrt{\int_0^{\Delta\lambda} e^{-\frac{1}{2}\mathrm{I}_{n_x}\cdot\nu} D\left(\lambda_{n-1}\right) e^{-\frac{1}{2}\mathrm{I}_{n_x}^T\cdot\nu} d\nu}\cdot \mathrm{w}_n.
\end{aligned} \tag{B.7}
$$

By noticing that

$$
e^{-\frac{1}{2}\mathrm{I}_{n_x}\Delta\lambda} = e^{-\frac{1}{2}\Delta\lambda}\mathrm{I}_{n_x}, \tag{B.8}
$$

the equation (B.7) can be simplified as

$$
\begin{aligned}
\mathrm{x}_n &= \mathrm{x}_{n-1} - 2\left(e^{-\frac{\Delta\lambda}{2}} - 1\right) a\left(\mathrm{x}_{n-1}\right) \\
&\quad + \sqrt{\int_0^{\Delta\lambda} e^{-\nu/2} e^{-\nu/2} d\nu}\cdot D\left(\lambda_{n-1}\right)^{1/2}\cdot \mathrm{w}_n \\
&= \mathrm{x}_{n-1} + 2\left(1 - e^{-\frac{\Delta\lambda}{2}}\right) a\left(\mathrm{x}_{n-1}\right) \\
&\quad + \sqrt{\int_0^{\Delta\lambda} e^{-\nu} d\nu}\cdot D\left(\lambda_{n-1}\right)^{1/2}\cdot \mathrm{w}_n, \\
\mathrm{x}_n &= \mathrm{x}_{n-1} + \left(1 - e^{-\frac{\Delta\lambda}{2}}\right) D\left(\lambda_{n-1}\right)\cdot\nabla_{\mathrm{x}}\log\pi\left(\mathrm{x}_{n-1}\right) \\
&\quad + \left(1 - e^{-\Delta\lambda}\right)^{1/2} D\left(\lambda_{n-1}\right)^{1/2}\cdot \mathrm{w}_n.
\end{aligned} \tag{B.9}
$$

C Discrete-time stochastic IDM

This section of the appendix presents the resulting discrete-time approximation of the stochastic Intelligent Driver model. Define the state equation for the discrete-time IDM to be

$$
\mathrm{x}_k = A\cdot\mathrm{x}_{k-1} + B + \mathrm{w}_k, \tag{C.1}
$$

where the state vector is represented for α vehicles by

$$\mathrm{x}_k = \begin{bmatrix} p_1 \\ p_2 \\ \vdots \\ p_{\alpha-1} \\ p_\alpha \\ v_1 \\ v_2 \\ \vdots \\ v_{\alpha-1} \\ v_\alpha \end{bmatrix}_k . \tag{C.2}$$

The variables p_i and v_i are the position and velocity of the ith vehicle respectively. The state-transition matrix can be written as

$$A = \begin{bmatrix} A_{1,1} & A_{1,2} & \dots & A_{1,2\alpha} \\ A_{2,1} & A_{2,2} & & \vdots \\ \vdots & & \ddots & \\ A_{2\alpha,1} & \dots & & A_{2\alpha,2\alpha} \end{bmatrix}_{k-1} . \tag{C.3}$$

For $i, j \in \mathbb{N}$, the diagonal elements of the state-transition matrix are given by

$$A_{i,i} = \begin{cases} 1, & i \in [1, \alpha]; \\ 1 + \frac{\partial \dot{v}_{i-\alpha}}{\partial v_{i-\alpha}} \cdot dt, & i \in (\alpha+1, 2\alpha]; \end{cases} \tag{C.4}$$

and the off-diagonal elements given by

$$A_{i,j} = \begin{cases} dt, & i \in [1, \alpha],\ j = i + \alpha; \\ \frac{\partial \dot{v}_{i-\alpha}}{\partial p_\alpha} \cdot dt, & i = \alpha + 1,\ j = \alpha; \\ \frac{\partial \dot{v}_{i-\alpha}}{\partial p_{i-\alpha-1}} \cdot dt, & i \in (\alpha+1, 2\alpha],\ j = i - 1 - \alpha; \\ \frac{\partial \dot{v}_{i-\alpha}}{\partial v_\alpha} \cdot dt, & i = \alpha + 1,\ j = 2\alpha; \\ \frac{\partial \dot{v}_{i-\alpha}}{\partial v_{i-\alpha-1}} \cdot dt, & i \in (\alpha+1, 2\alpha],\ j = i - 1; \\ 0, & \text{otherwise}; \end{cases} \tag{C.5}$$

where

$$\frac{\partial \dot{v}_n}{\partial p_{n-1}} = +2a \left(\frac{s\left(v_n, \Delta v_n\right)^2}{s_n^3} \right), \tag{C.6}$$

$$\frac{\partial \dot{v}_n}{\partial p_n} = -2a \left(\frac{s\left(v_n, \Delta v_n\right)^2}{s_n^3} \right), \tag{C.7}$$

$$\frac{\partial \dot{v}_n}{\partial v_{n-1}} = +2a \left(\frac{s\left(v_n, \Delta v_n\right)}{s_n^2} \right) \left(\frac{v_n}{2\sqrt{a \cdot b}} \right), \tag{C.8}$$

$$\begin{aligned} \frac{\partial \dot{v}_n}{\partial v_n} &= -a \left(\frac{\delta}{v_0} \right) \left(\frac{v_n}{v_0} \right)^{\delta-1} \\ &\quad - 2a \left(\frac{s\left(v_n, \Delta v_n\right)}{s_n^2} \right) \left(T_h + \frac{2v_n - v_{n-1}}{2\sqrt{a \cdot b}} \right). \end{aligned} \tag{C.9}$$

The model takes into account the fact that, on a ring road, the last vehicle in the convoy can be regarded the one potentially in front of the vehicle leading the queue, assuming that the first vehicle can complete the circuit faster and approach the last one from behind. This is represented by the terms $\partial_{p_\alpha} \dot{v}_1 \cdot dt$ and $\partial_{v_\alpha} \dot{v}_1 \cdot dt$ that appear in (C.5) when $i = \alpha + 1$, which shall be calculated

respectively according to expressions analogous to (C.6) and (C.8). The constant term is defined as

$$B = \begin{bmatrix} B_1 \\ B_2 \\ \vdots \\ B_{2\alpha} \end{bmatrix}_k , \tag{C.10}$$

where

$$B_i = \begin{cases} 0, & i \in [1, \alpha]; \\ \langle \dot{v}_i \rangle - \frac{\partial \dot{v}_i}{\partial p_{i-1}} \cdot p_{i-1} - \frac{\partial \dot{v}_i}{\partial p_i} \cdot p_i & \\ \quad - \frac{\partial \dot{v}_i}{\partial v_{i-1}} \cdot v_{i-1} - \frac{\partial \dot{v}_i}{\partial v_i} \cdot v_i, & i \in [\alpha + 1, 2\alpha]; \end{cases} \tag{C.11}$$

and

$$\langle \dot{v}_i \rangle = a \left[1 - \left(\frac{v_i}{v_0} \right)^{\delta} - \left(\frac{s\left(v_i, \Delta v_i\right)}{s_i} \right)^2 \right]. \tag{C.12}$$

The covariance matrix $Q_k = \mathbb{E}\left[\mathrm{w}_k \mathrm{w}_k^T \right]$ is defined as

$$Q_k = \begin{bmatrix} Q_{1,1} & Q_{1,2} & \cdots & Q_{1,2\alpha} \\ Q_{2,1} & Q_{2,2} & & \vdots \\ \vdots & & \ddots & \\ Q_{2\alpha,1} & \cdots & & Q_{2\alpha,2\alpha} \end{bmatrix}_k , \tag{C.13}$$

with diagonal elements

$$Q_{i,i} = \sigma_q^2 \times \begin{cases} Q_{i,i}^{(1)}, & i \in [1, \alpha]; \\ Q_{i,i}^{(2)}, & i = \alpha + 1; \\ Q_{i,i}^{(3)}, & i \in (\alpha + 1, 2\alpha]; \end{cases} \tag{C.14}$$

where

$$\begin{aligned} Q_{i,i}^{(1)} &= \frac{dt^3}{3} + dt, \\ Q_{i,i}^{(2)} &= \left(\frac{\partial \dot{v}_{i-\alpha}}{\partial p_\alpha} + \frac{\partial \dot{v}_{i-\alpha}}{\partial p_{i-\alpha}} + \frac{\partial \dot{v}_{i-\alpha}}{\partial v_\alpha} + \frac{\partial \dot{v}_{i-\alpha}}{\partial v_{i-\alpha}} \right) \cdot \frac{dt^3}{3} \\ &+ \frac{\partial \dot{v}_{i-\alpha}}{\partial v_{i-\alpha}} \cdot dt^2 + dt, \\ Q_{i,i}^{(3)} &= \left(\frac{\partial \dot{v}_{i-\alpha}}{\partial p_{i-\alpha-1}} + \frac{\partial \dot{v}_{i-\alpha}}{\partial p_{i-\alpha}} + \frac{\partial \dot{v}_{i-\alpha}}{\partial v_{i-\alpha-1}} + \frac{\partial \dot{v}_{i-\alpha}}{\partial v_{i-\alpha}} \right) \cdot \frac{dt^3}{3} \\ &+ \frac{\partial \dot{v}_{i-\alpha}}{\partial v_{i-\alpha}} \cdot dt^2 + dt; \end{aligned} \tag{C.15}$$

and off-diagonal elements

$$Q_{j,i} = Q_{i,j} = \sigma_q^2 \times \begin{cases} Q_{i,j}^{(4)}, & i \in [1, \alpha],\ j = i + \alpha; \\ Q_{i,j}^{(5)}, & i = \alpha + 1,\ j = \alpha; \\ Q_{i,j}^{(6)}, & i \in (\alpha + 1, 2\alpha],\ j = i - 1 - \alpha; \\ Q_{i,j}^{(7)}, & i = \alpha + 1,\ j = 2\alpha; \\ Q_{i,j}^{(8)}, & i \in (\alpha + 1, 2\alpha],\ j = i - 1; \\ 0, & \text{otherwise}; \end{cases} \tag{C.16}$$

where

$$
\begin{aligned}
Q_{i,j}^{(4)} &= \frac{\partial \dot{v}_i}{\partial v_i} \cdot \frac{dt^3}{3} + \left(\frac{\partial \dot{v}_i}{\partial p_i} + 1 \right) \cdot \frac{dt^2}{2}, \\
Q_{i,j}^{(5)} &= \frac{\partial \dot{v}_{i-\alpha}}{\partial v_\alpha} \cdot \frac{dt^3}{3} + \frac{\partial \dot{v}_{i-\alpha}}{\partial p_\alpha} \cdot \frac{dt^2}{2}, \\
Q_{i,j}^{(6)} &= \frac{\partial \dot{v}_{i-\alpha}}{\partial v_{i-\alpha-1}} \cdot \frac{dt^3}{3} + \frac{\partial \dot{v}_{i-\alpha}}{\partial p_{i-\alpha-1}} \cdot \frac{dt^2}{2}, \\
Q_{i,j}^{(7)} &= \frac{\partial \dot{v}_{i-\alpha}}{\partial v_\alpha} \cdot \frac{dt^2}{3}, \\
Q_{i,j}^{(8)} &= \frac{\partial \dot{v}_{i-\alpha}}{\partial v_{i-\alpha-1}} \cdot \frac{dt^2}{3}.
\end{aligned} \tag{C.17}
$$

References

[1] A. Gelman and X.-L. Meng, "Simulating normalizing constants: from importance sampling to bridge sampling to path sampling," *Statist. Sci.*, vol. 13, pp. 163–185, 05 1998.

[2] J. Deutscher, A. Blake, and I. Reid, "Articulated body motion capture by annealed particle filtering," in *Computer Vision and Pattern Recognition, 2000. Proceedings. IEEE Conference on*, vol. 2, pp. 126–133 vol.2, 2000.

[3] R. M. Neal, "Annealed importance sampling," *Statistics and Computing*, vol. 11, no. 2, pp. 125–139, 2001.

[4] P. Del Moral, A. Doucet, and A. Jasra, "Sequential Monte Carlo samplers," *Journal of the Royal Statistical Society: Series B (Statistical Methodology)*, vol. 68, no. 3, pp. 411–436, 2006.

[5] P. Bickel, B. Li, and T. Bengtsson, *Sharp failure rates for the bootstrap particle filter in high dimensions*, vol. 3 of *Collections*, pp. 318–329. Beachwood, Ohio, USA: Institute of Mathematical Statistics, 2008.

[6] S. Duane, A. D. Kennedy, B. J. Pendleton, and D. Roweth, "Hybrid Monte Carlo," *Physics Letters B*, vol. 195, no. 2, pp. 216 – 222, 1987.

[7] R. M. Neal, *Bayesian Learning for Neural Networks*. Secaucus, NJ, USA: Springer-Verlag New York, Inc., 1996.

[8] G. O. Roberts and O. Stramer, "Langevin Diffusions and Metropolis-Hastings Algorithms," *Methodology And Computing In Applied Probability*, vol. 4, no. 4, pp. 337–357, 2002.

[9] M. Girolami and B. Calderhead, "Riemann manifold Langevin and Hamiltonian Monte Carlo methods," *Journal of the Royal Statistical Society: Series B (Statistical Methodology)*, vol. 73, no. 2, pp. 123–214, 2011.

[10] R. L. Stratonovich, "Optimum nonlinear systems which bring about a separation of a signal with constant parameters from noise," *Radiofizika*, vol. 2, no. 6, pp. 892–901, 1959.

[11] H. J. Kushner, "On the differential equations satisfied by conditional probability densities of Markov processes, with applications," *J. SIAM Control Ser. A*, vol. 2, no. 1, pp. 106–119, 1964.

[12] M. Zakai, "On the optimal filtering of diffusion processes," *Zeitschrift für Wahrscheinlichkeitstheorie und Verwandte Gebiete*, vol. 11, no. 3, pp. 230–243, 1969.

[13] R. S. Bucy and P. D. Joseph, *Filtering for Stochastic Processes with Applications to Guidance*. John Wiley & Sons, 2nd ed., 1968.

[14] V. E. Beneš, "Exact finite-dimensional filters for certain diffusions with nonlinear drift," *Stochastics*, vol. 5, no. 1-2, pp. 65–92, 1981.

[15] F. E. Daum, "Exact finite-dimensional nonlinear filters," *Automatic Control, IEEE Transactions on*, vol. 31, pp. 616–622, Jul 1986.

[16] D. Crisan and T. Lyons, "A particle approximation of the solution of the Kushner-Stratonovitch equation," *Probability Theory and Related Fields*, vol. 115, no. 4, pp. 549–578, 1999.

[17] D. Crisan, P. D. Moral, and T. J. Lyons, "Interacting Particle Systems Approximations of the Kushner-Stratonovitch Equation," *Advances in Applied Probability*, vol. 31, no. 3, pp. pp. 819–838, 1999.

[18] D. Crisan and J. Xiong, "Approximate McKean-Vlasov representations for a class of SPDEs," *Stochastics-An International Journal of Probability and Stochastic Processes*, vol. 82, pp. 53–68, 2010.

[19] A. Budhiraja and G. Kallianpur, "Approximations to the solution of the Zakai equation using multiple Wiener and Stratonovich integral expansions," *Stochastics and Stochastic Reports*, vol. 56, no. 3-4, pp. 271–315, 1996.

[20] A. Budhiraja and G. Kallianpur, "The Feynman-Stratonovich semigroup and Stratonovich integral expansions in nonlinear filtering," *Applied Mathematics and Optimization*, vol. 35, no. 1, pp. 91–116, 1997.

[21] C. Vergé, C. Dubarry, P. Del Moral, and E. Moulines, "On parallel implementation of sequential Monte Carlo methods: the island particle model," *Statistics and Computing*, vol. 25, no. 2, pp. 243–260, 2015.

[22] P. Rebeschini and R. van Handel, "Can local particle filters beat the curse of dimensionality?," *Ann. Appl. Probab.*, vol. 25, pp. 2809–2866, 10 2015.

[23] U. D. Hanebeck, K. Briechle, and A. Rauh, "Progressive Bayes: a new framework for nonlinear state estimation," 2003.

[24] J. Hagmar, M. Jirstrand, L. Svensson, and M. Morelande, "Optimal parameterization of posterior densities using homotopy," in *Information Fusion (FUSION), 2011 Proceedings of the 14th International Conference on*, pp. 1–8, July 2011.

[25] U. D. Hanebeck and J. Steinbring, "Progressive Gaussian filtering based on Dirac Mixture approximations," in *Information Fusion (FUSION), 2012 15th International Conference on*, pp. 1697–1704, July 2012.

[26] S. Reich, "A dynamical systems framework for intermittent data assimilation," *BIT Numerical Mathematics*, vol. 51, no. 1, pp. 235–249, 2011.

[27] S. Reich, "A Guided Sequential Monte Carlo Method for the Assimilation of Data into Stochastic Dynamical Systems," in *Recent Trends in Dynamical Systems* (A. Johann, H.-P. Kruse, F. Rupp, and S. Schmitz, eds.), vol. 35 of *Springer Proceedings in Mathematics & Statistics*, pp. 205–220, Springer Basel, 2013.

[28] M. Venugopal, R. M. Vasu, and D. Roy, "An Ensemble Kushner-Stratonovich-Poisson Filter for Recursive Estimation in Nonlinear Dynamical Systems," *Automatic Control, IEEE Transactions on*, vol. PP, no. 99, pp. 1–1, 2015.

[29] N. Oudjane and C. Musso, "Progressive correction for regularized particle filters," in *Information Fusion, 2000. FUSION 2000. Proceedings of the Third International Conference on*, vol. 2, pp. THB2/10–THB2/17 vol.2, July 2000.

[30] D. Crisan, "Particle Filters in a Continuous Time Framework," in *Nonlinear Statistical Signal Processing Workshop, 2006 IEEE*, pp. 73–78, Sept 2006.

[31] F. Daum and J. Huang, "Nonlinear filters with log-homotopy," in *Proceedings SPIE of Conference in Signal and Data Processing of Small Targets, 2007*, vol. 6699 of *Signal and Data Processing of Small Targets, 2007*, (USA), p. 18, SPIE, August 26, 2007 2007. id: 1; issn: print.

[32] S. Sarkar, S. R. Chowdhury, M. Venugopal, R. M. Vasu, and D. Roy, "A Kushner-Stratonovich Monte Carlo filter applied to nonlinear dynamical system identification," *Physica D: Nonlinear Phenomena*, vol. 270, pp. 46 – 59, 2014.

[33] D. Crisan and K. Li, "Generalised particle filters with Gaussian mixtures," *Stochastic Processes and their Applications*, vol. 125, no. 7, pp. 2643 – 2673, 2015.

[34] P. Bunch and S. Godsill, "Particle filtering with progressive Gaussian approximations to the optimal importance density," in *Computational Advances in Multi-Sensor Adaptive Processing (CAMSAP), 2013 IEEE 5th International Workshop on*, pp. 360–363, 2013. ID: 1.

[35] M. S. Arulampalam, S. Maskell, N. Gordon, and T. Clapp, "A tutorial on particle filters for online nonlinear/non-Gaussian Bayesian tracking," *Signal Processing, IEEE Transactions on*, vol. 50, pp. 174–188, Feb 2002.

[36] F. Daum and J. Huang, "Curse of dimensionality and particle filters," in *Aerospace Conference, 2003. Proceedings. 2003 IEEE*, vol. 4, pp. 1979–1993, March 2003.

[37] C. Snyder, T. Bengtsson, P. Bickel, and J. Anderson, "Obstacles to High-Dimensional Particle Filtering," *Monthly Weather Review*, vol. 136, pp. 4629–4640, dec 2008.

[38] A. Doucet and A. M. Johansen, *A Tutorial on Particle Filtering and Smoothing: Fifteen Years Later*. Oxford University Press, 2009.

[39] F. Daum and J. Huang, "Particle flow for nonlinear filters with log-homotopy," vol. 6969, pp. 696918–696918–12, 2008. journal: Proc. SPIE.

[40] F. Daum and J. Huang, "Nonlinear filters with particle flow," vol. 7445, pp. 74450R–74450R–9, 2009. journal: Proc. SPIE.

[41] F. Daum and J. Huang, "Nonlinear filters with particle flow induced by log-homotopy," in *Proceedings SPIE of Conference in Signal Processing, Sensor Fusion, and Target Recognition XVIII*, vol. 7336 of *Signal Processing, Sensor Fusion, and Target Recognition XVIII*, (USA), p. 03, SPIE, April 13, 2009 2009. id: 1; issn: print 0277786X.

[42] F. Daum and J. Huang, "A fresh perspective on research for nonlinear filters," vol. 7697, pp. 769705–769705–12, 2010. journal: Proc. SPIE.

[43] F. Daum, J. Huang, and A. Noushin, "Exact particle flow for nonlinear filters," vol. 7697, pp. 769704–769704–19, 2010. journal: Proc. SPIE.

[44] F. Daum and J. Huang, "Generalized particle flow for nonlinear filters," in *Proceedings SPIE of Conference in Signal and Data Processing of Small Targets, 2010*, vol. 7698 of *Signal and Data Processing of Small Targets 2010*, (USA), p. 01, SPIE, April 05, 2010 2010. id: 1; issn: print 0277786X.

[45] F. Daum, J. Huang, and A. Noushin, "Coulomb's law particle flow for nonlinear filters," vol. 8137, pp. 81370B–81370B–10, 2011. journal: Proc. SPIE.

[46] F. Daum and J. Huang, "Fourier transform particle flow for nonlinear filters," vol. 8745, pp. 87450R–87450R–9, 2013. journal: Proc. SPIE.

[47] F. Daum and J. Huang, "Particle flow for nonlinear filters, Bayesian decisions and transport," in *Information Fusion (FUSION), 2013 16th International Conference on*, pp. 1072–1079, 2013. ID: 1.

[48] F. Daum and J. Huang, "Particle flow inspired by Knothe-Rosenblatt transport for nonlinear filters," *Proc. SPIE*, vol. 8745, pp. 87450O–87450O–8, 2013.

[49] F. Daum and J. Huang, "Particle flow with non-zero diffusion for nonlinear filters," vol. 8745, pp. 87450P–87450P–13, 2013. journal: Proc. SPIE.

[50] F. Daum and J. Huang, "Renormalization group flow and other ideas inspired by physics for nonlinear filters, Bayesian decisions, and transport," vol. 9091, pp. 90910–90910–14, 2014. journal: Proc. SPIE.

[51] C. Villani, *Topics in Optimal Transportation*. Graduate studies in mathematics, American Mathematical Society, 2003.

[52] C. E. Gutiérrez, *The Monge-Ampère Equation*. Progress in Nonlinear Differential Equations and Their Applications, Birkhäuser Boston, 2001.

[53] J. Heng, A. Doucet, and Y. Pokern, "Gibbs Flow for Approximate Transport with Applications to Bayesian Computation," *ArXiv e-prints*, Sept. 2015.

[54] S. Choi, P. Willett, F. Daum, and J. Huang, "Discussion and application of the homotopy filter," vol. 8050, pp. 805021–805021–12, 2011. journal: Proc. SPIE.

[55] T. Ding and M. J. Coates, "Implementation of the Daum-Huang exact-flow particle filter," in *Statistical Signal Processing Workshop (SSP), 2012 IEEE*, pp. 257–260, 2012. ID: 1.

[56] M. Khan and M. Ulmke, "Improvements in the implementation of log-homotopy based particle flow filters," in *Information Fusion (Fusion), 2015 18th International Conference on*, pp. 74–81, July 2015.

[57] R. Jordan, D. Kinderlehrer, and F. Otto, "The Variational Formulation of the Fokker–Planck Equation," *SIAM Journal on Mathematical Analysis*, vol. 29, no. 1, pp. 1–17, 1998.

[58] P. Bunch and S. Godsill, "Approximations of the Optimal Importance Density using Gaussian Particle Flow Importance Sampling," *Journal of the American Statistical Association*, vol. 0, no. ja, pp. 0–0, 2015.

[59] L. C. Evans and W. Gangbo, "Differential equations methods for the Monge-Kantorovich mass transfer problem," *Mem. Amer. Math. Soc*, vol. 137, p. 653, 1999.

[60] A. H. Jazwinski, *Stochastic Processes and Filtering Theory*. Academic Press, 1970.

[61] C. W. Gardiner, *Handbook of Stochastic Methods*. Berlin Heidelberg New York: Springer, 2nd enlarged ed., 1985.

[62] H. Risken, *The Fokker-Planck equation: methods of solution and applications*. 2nd, Springer-Verlag, 1989.

[63] R. Jordan and D. Kinderlehrer, "An Extended Variational Principle," in *Partial Differential Equations and Applications: Collected Papers in Honor of Carlo Pucci* (G. Talenti, E. Vesentini, and P. Marcellini, eds.), Lecture Notes in Pure and Applied Mathematics, ch. 18, Taylor & Francis, 1996.

[64] A. S. Dalalyan, "Theoretical guarantees for approximate sampling from smooth and log-concave densities," *ArXiv e-prints*, Dec. 2014.

[65] D. A. Levin, Y. Peres, and E. L. Wilmer, *Markov chains and mixing times*, ch. 4. Providence, R.I. American Mathematical Society, 2009. With a chapter on coupling from the past by James G. Propp and David B. Wilson.

[66] R. C. Rao, "Information and the accuracy attainable in the estimation of statistical parameters," *Bull. Calcutta Math. Soc.*, vol. 37, pp. 81–91, 1945.

[67] N. Higham, "Computing the nearest correlation matrix—a problem from finance," *IMA Journal of Numerical Analysis*, vol. 22, pp. 329–343, 2002.

[68] T. Ozaki, "A bridge between nonlinear time series models and nonlinear stochastic dynamical systems: a local linearization approach," *Statistica Sinica*, vol. 2, no. 1, pp. 113–135, 1992.

[69] B. D. O. Anderson and J. B. Moore, *Optimal Filtering*. Englewood Cliffs, NJ: Prentice-Hall, 1979.

[70] J. H. Kotecha and P. M. Djurić, "Gaussian sum particle filtering," *Signal Processing, IEEE Transactions on*, vol. 51, pp. 2602–2612, Oct 2003.

[71] H. W. Sorenson and D. L. Alspach, "Recursive Bayesian Estimation Using Gaussian Sums," *Automatica*, vol. 7, pp. 465–479, July 1971.

[72] D. L. Alspach and H. W. Sorenson, "Nonlinear Bayesian estimation using Gaussian sum approximations," *Automatic Control, IEEE Transactions on*, vol. 17, pp. 439–448, Aug 1972.

[73] G. Terejanu, P. Singla, T. Singh, and P. D. Scott, "A novel Gaussian Sum Filter Method for accurate solution to the nonlinear filtering problem," in *Information Fusion, 2008 11th International Conference on*, pp. 1–8, June 2008.

[74] M. Klaas, N. de Freitas, and A. Doucet, "Toward Practical N^2 Monte Carlo: the Marginal Particle Filter," *ArXiv e-prints*, July 2012.

[75] R. Graham, "Statistical Theory of Instabilities in Stationary Nonequilibrium Systems with Applications to Lasers and Nonlinear Optics," in *Springer Tracts in Modern Physics* (G. Höhler, ed.), pp. 1–97, Springer Berlin Heidelberg, 1973.

[76] H.-K. Janssen, "On a Lagrangean for classical field dynamics and renormalization group calculations of dynamical critical properties," *Zeitschrift für Physik B Condensed Matter*, vol. 23, no. 4, pp. 377–380, 1976.

[77] Y. Bar-Shalom, P. K. Willett, and X. Tian, *Tracking and Data Fusion: A Handbook of Algorithms*. YBS Publishing, April 2011.

[78] Y. Bar-Shalom, F. Daum, and J. Huang, "The probabilistic data association filter," *Control Systems, IEEE*, vol. 29, pp. 82–100, Dec 2009.

[79] A. Marrs, S. Maskell, and Y. Bar-Shalom, "Expected likelihood for tracking in clutter with particle filters," 2002.

[80] L. Y. Pao, "Multisensor multitarget mixture reduction algorithms for tracking," *Journal of Guidance, Control, and Dynamics*, vol. 17, pp. 1205–1211, 2014/04/27 1994.

[81] H. A. P. Blom and E. A. Bloem, "Probabilistic data association avoiding track coalescence," *Automatic Control, IEEE Transactions on*, vol. 45, pp. 247–259, Feb 2000.

[82] H. A. P. Blom and E. A. Bloem, "Joint Particle Filtering of Multiple Maneuvering Targets From Unassociated Measurements," *Journal of Advances in Information Fusion*, vol. 1, no. 1, pp. 15–34, 2006.

[83] M. Treiber and A. Kesting, *Traffic flow dynamics: Data, Models and Simulation*. Springer-Verlag Berlin Heidelberg, 2013.

[84] C. Villani, *Optimal transport: old and new*. Grundlehren der mathematischen Wissenschaften, Berlin: Springer, 2009.

[85] F. Daum and J. Huang, "Numerical experiments for nonlinear filters with exact particle flow induced by log-homotopy," vol. 7698, pp. 769816–769816–15, 2010. journal: Proc. SPIE.

[86] F. Daum, J. Huang, and A. Noushin, "Numerical experiments for Coulomb's law particle flow for nonlinear filters," vol. 8137, pp. 81370E–81370E–15, 2011. journal: Proc. SPIE.

[87] F. Daum and J. Huang, "How to avoid normalization of particle flow for nonlinear filters, Bayesian decisions, and transport," vol. 9092, pp. 90920B–90920B–9, 2014. journal: Proc. SPIE.

[88] L. Chen and R. K. Mehra, "A study of nonlinear filters with particle flow induced by log-homotopy," vol. 7697, pp. 769706–769706–7, 2010. journal: Proc. SPIE.

[89] M. A. Khan and M. Ulmke, "Non-linear and non-Gaussian state estimation using log-homotopy based particle flow filters," in *Sensor Data Fusion: Trends, Solutions, Applications (SDF), 2014*, pp. 1–6, 2014. ID: 1.

[90] H. Lamb, *Hydrodynamics*. University Press, 1895.

[91] G. N. Milstein, J. G. M. Schoenmakers, and V. Spokoiny, "Transition Density Estimation for Stochastic Differential Equations via Forward-Reverse Representations," *Bernoulli*, vol. 10, no. 2, pp. pp. 281–312, 2004.

[92] R. Bucy, "Nonlinear filtering theory," *Automatic Control, IEEE Transactions on*, vol. 10, pp. 198–198, Apr 1965.